# JET PROPULSION

*Journal of the*
AMERICAN ROCKET SOCIETY
*Rocketry . . . . . Jet Propulsion Sciences . . . . . Astronautics*

VOLUME 26 JANUARY 1956 NUMBER 1





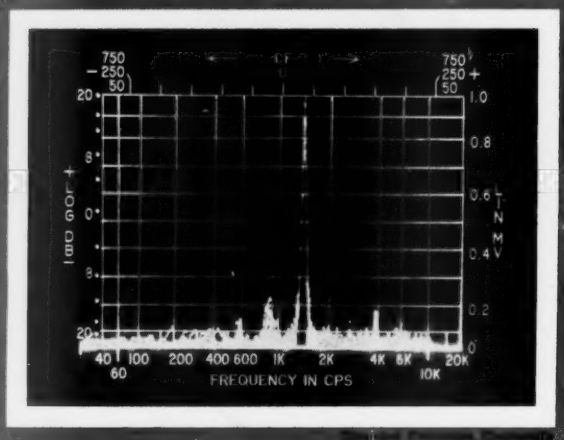


Amplitude of combustion pressure oscillation in liquid rocket engine during screaming operation (fundamental axial mode)



JANUARY 24 ARS-IAS JOINT SESSION (IAS ANNUAL MEETING) SEE PAGE 51

# There goes another one!


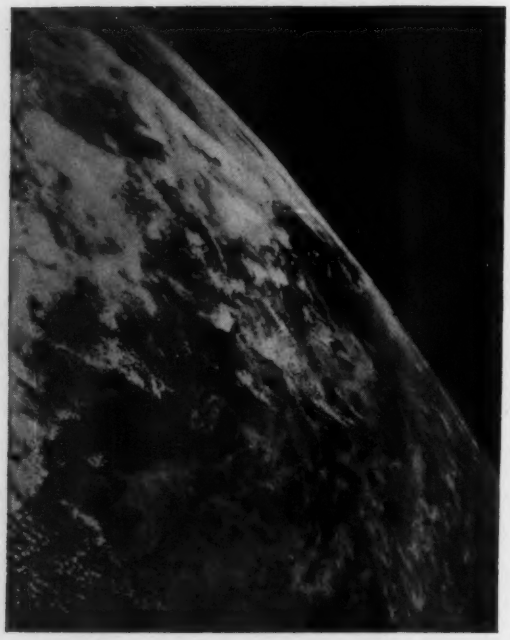

No need for amazement, boys. In the short time since you earned your wings, rocket propulsion has been constantly conquering new frontiers of speed and space.

At RMI, recent major advances in the science of rocket power have made possible the production of new rocket engine designs far superior to the record-holding powerplants of today . . . superiority measured in terms of performance, reliability, economy and producibility.

◀ Photo at left was taken at an altitude of 158 miles from an RMI powered Viking research rocket . . . world speed and altitude record holder for single stage rockets.

*Spearheading Progress through Research*

RMI

Career opportunities available for experienced mechanical, aeronautical, electrical and chemical engineers, physicists, chemists. Send complete resume to employment manager.

REACTION MOTORS, INC.
Denville, New Jersey
Affiliated with OLIN MATHIESON CHEMICAL CORP.

## Scope of JET PROPULSION

JET PROPULSION, the Journal of the American Rocket Society, is devoted to the advancement of the field of jet propulsion through the publication of original papers disclosing new knowledge and new developments. The term "jet propulsion" as used herein is understood to embrace all engines that develop thrust by rearward discharge of a jet through a nozzle or duct; and thus it includes systems utilizing atmospheric air and underwater systems, as well as rocket engines. JET PROPULSION is open to contributions, either fundamental or applied, dealing with specialized aspects of jet and rocket propulsion, such as fuels and propellants, combustion, heat transfer, high temperature materials, mechanical design analyses, flight mechanics of jet-propelled vehicles, astronautics, and so forth. JET PROPULSION endeavors, also, to keep its subscribers informed of the affairs of the Society and of outstanding events in the rocket and jet propulsion field.

## Limitation of Responsibility

Statements and opinions expressed in JET PROPULSION are to be understood as the individual expressions of the authors and do not necessarily reflect the views of the Editors or the Society.

## Subscription Rates

| | |
|---|---|
| One year (twelve monthly issues) | $10.00 |
| Foreign countries, additional postage | add .50 |
| Single copies | 1.75 |
| Special issues, single copies | 2.50 |
| Back numbers | 2.00 |

## Change of Address

Notices of change of address should be sent to the Secretary of the Society at least 30 days prior to the date of publication.

## Information for Authors

### *Preparation of Manuscripts*

Manuscripts must be double spaced on one side of paper only with wide margins to allow for instructions to printer. Submit two copies: original and first carbon. Include a 100–200 word abstract of paper. The title of the paper should be brief to simplify indexing. The author's name should be given without title, degree, or honor. A footnote on the first page should indicate the author's position and affiliation. Include only essential illustrations, tables, and mathematics. References should be grouped at the end of the manuscript; footnotes are reserved for comments on the text. Use American Standard symbols and abbreviations published by the American Standards Association. Greek letters should be identified clearly for the printer. References should be given as follows: For Journal Articles: Title, Authors, Journal, Volume, Year, Page Numbers. For Books: Title, Author, Publisher, City, Edition, Year, Page Numbers. Line drawings must be made with India ink on white paper or tracing cloth. Lettering on drawings should be large enough to permit reduction to standard one-column width, except for unusually complex drawings where such reduction would be prohibitive. Photographs should be clear, glossy prints. Legends must accompany each illustration submitted and should be listed in order on a separate sheet of paper.

### *Security Clearance*

Manuscripts must be accompanied by written assurance as to security clearance in the event the subject matter of the manuscript is considered to lie in a classified area. Alternatively, written assurance that clearance is unnecessary should be submitted. Full responsibility for obtaining authoritative clearance rests with the author.

### *Submission of Manuscripts*

Manuscripts should be submitted in duplicate to the Editor-in-Chief, Martin Summerfield, Professor of Aeronautical Engineering, Princeton University, Princeton, N. J.

### *Manuscripts Presented at ARS Meetings*

A manuscript submitted to the ARS Program Chairman and accepted for presentation at a national meeting will automatically be referred to the Editors for consideration for publication in JET PROPULSION, unless a contrary request is made by the author.

### *To Order Reprints*

Prices for reprints will be sent to the author with the galley proof, and orders should accompany the corrected galley when it is returned to the Assistant Editor.


# JET PROPULSION

*Journal of the* AMERICAN ROCKET SOCIETY









JET PROPULSION, the Journal of the American Rocket Society, published monthly by the American Rocket Society at 20th and Northampton Streets, Easton, Pa., U.S.A. The Editorial Office is located at 500 5th Ave., New York 36, N. Y. Price $1.75 per copy, $10.00 per year: Entered as second-class matter at the Post Office at Easton, Pa., under the Act of March 3, 1879.

# PRIVATE EYE FOR THE U. S. NAVY

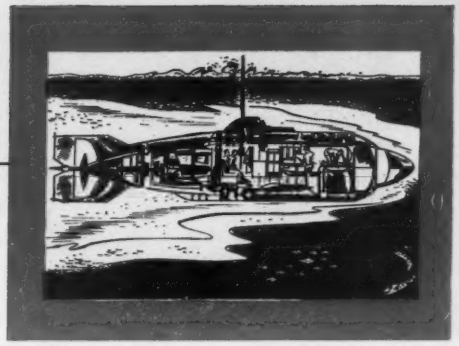

Incorporated in the X-1 are all personnel living essentials of larger subs. Crews are just as safe, just as comfortable, as those in large subs.

MBER 10 OF A SERIES

Because of its maneuverability in shallow water, and its agility in finding secure hiding places, the X-1 is a highly versatile addition to our Navy.

## FAIRCHILD ENGINE DIVISION DESIGNED AND BUILT AMERICA'S FIRST MODERN MIDGET SUBMERSIBLE FOR THE U. S. NAVY

New tactical mobility is brought to many U.S. Navy operations by the Fairchild X-1, a revolutionary underwater weapons system for close-in reconnaissance of harbors and inlets. The X-1 is the first of its kind ever produced in America, and the first naval vessel of any kind to be designed and constructed by a U.S. aircraft manufacturer.

Fairchild designed and built the 25-ton, 50-foot X-1 with an unconventional underwater propulsion system, and with airplane-like controls. The new "pocket" sub has a four-man crew—operates quietly and stealthily, performing missions that large craft could never do.

Once again, Fairchild design and engineering ingenuity has produced a vital new instrument of defense for our armed forces.

*A Division of Fairchild Engine and Airplane Corporation*

**FAIRCHILD**

ENGINE DIVISION • DEER PARK, L. I., N. Y.

...WHERE THE FUTURE IS MEASURED IN LIGHT-YEARS!

**Multiple Mitchell Cameras on Mobile Turret at U. S. Naval Air Missile Test Center, Point Mugu, Calif. Seventeen 35mm and five 16mm Mitchells are used here.**

# CAMERA BECOMES BASIC RESEARCH TOOL

Official U. S. Army Photograph

**200 Mitchell Cameras,** mostly high-speed models, are in use here at White Sands Proving Ground, New Mexico.

Official U. S. Navy Photograph

**Powered Tracking Mount** has Mitchell Cameras; over 50 Mitchells are used at U.S. Naval Ordnance Test Station, Inyokern, Calif.

**Mitchell Telephoto Tracking Camera** in use at Air Force Missile Test Center, Cape Canaveral, Florida.

Official U. S. Air Force Photograph

**One of 12 Mitchell cameras** used to track missiles at Holloman Air Development Center, Alamogordo, New Mexico.

Official U. S. Air Force Photograph

**Vital Projects Now Heavy Users of Motion Picture Cameras With Flexible Performance Range**

Accelerated project work has today put increased demands upon motion picture equipment. Because of the need for a camera which can perform under a broad range of research and development requirements, the Mitchell Camera has today become the standard *basic* motion picture camera used in projects in this country and abroad.

No other single camera can be used so flexibly, under such extreme filming conditions, and for such a broad range of cinematography as can a Mitchell Camera. In one location, alone, 200 Mitchell 35mm and 16mm cameras are now in use at White Sands Proving Ground.

Write today on your letterhead for information on the Mitchell Camera line.

**Mitchell Camera**
**CORPORATION**
666 WEST HARVARD STREET
GLENDALE 4, CALIFORNIA
Cable Address: "MITCAMCO"

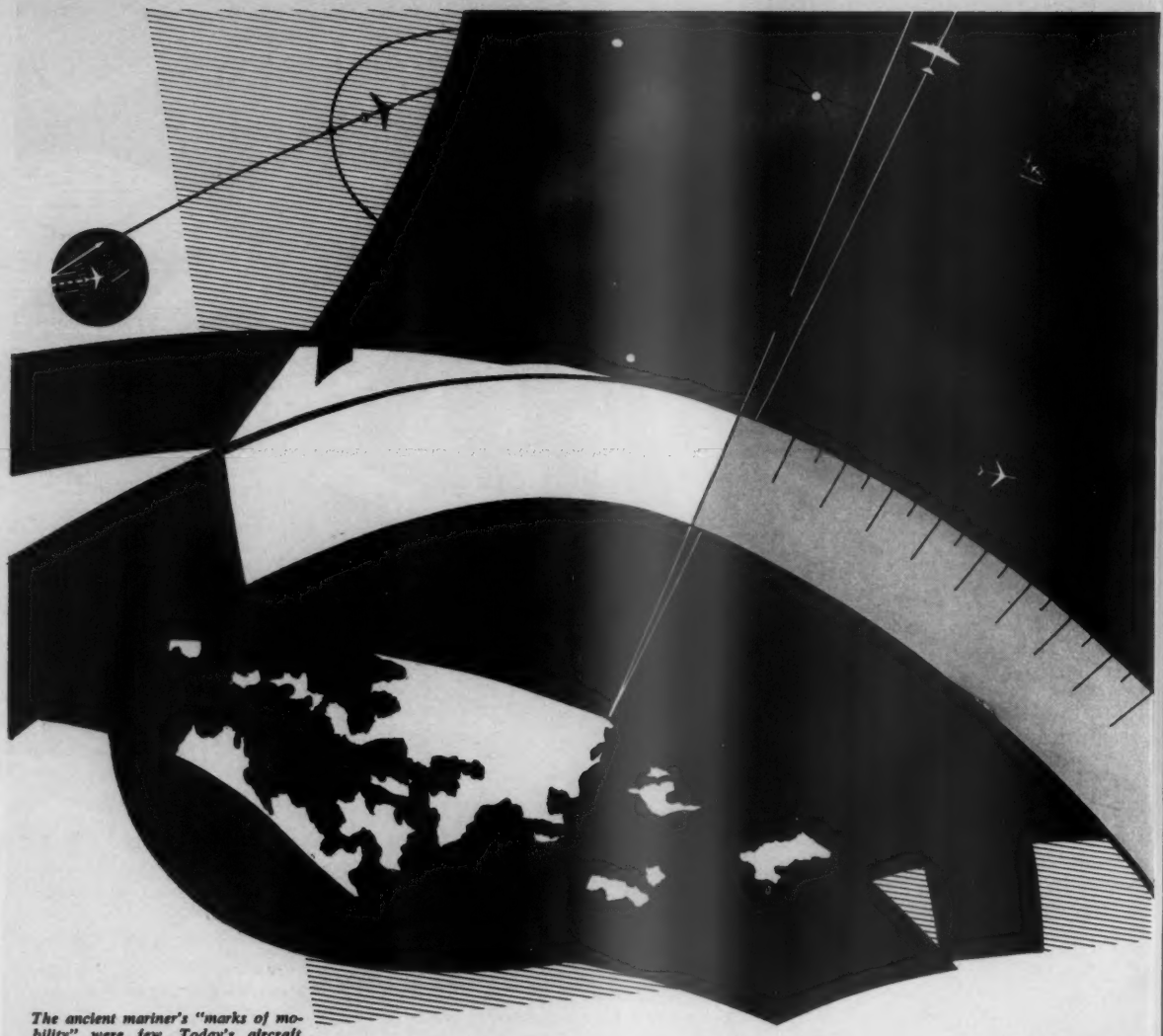

*The ancient mariner's "marks of mobility" were few. Today's aircraft navigate the celestial sphere with confidence — thanks to Kollsman's scientific instruments and controls.*

## the marks of mobility

In an aircraft, instruments and controls are the very marks of its mobility . . . for accurate measurement and observation are the only guides to safe, predictable flight. There are no "marks of mobility" more accurate and dependable than Kollsman in the seven fields of . . .

**AIRCRAFT INSTRUMENTS**
**PRECISION CONTROLS**
**PRECISION COMPUTERS AND COMPONENTS**
**OPTICAL COMPONENTS AND SYSTEMS**
**RADIO COMMUNICATIONS AND NAVIGATION EQUIPMENT**
**MOTORS AND SYNCHROS**
**INSTRUMENTS FOR SIMULATED FLIGHT TRAINERS**

Our manufacturing and research facilities . . . our skills and talents, are available to those seeking solutions to instrumentation and control problems.

**kollsman INSTRUMENT CORPORATION**

**80-08 45th AVE., ELMHURST, N. Y. • GLENDALE, CALIF. • SUBSIDIARY OF *Standard* COIL PRODUCTS CO. INC.**

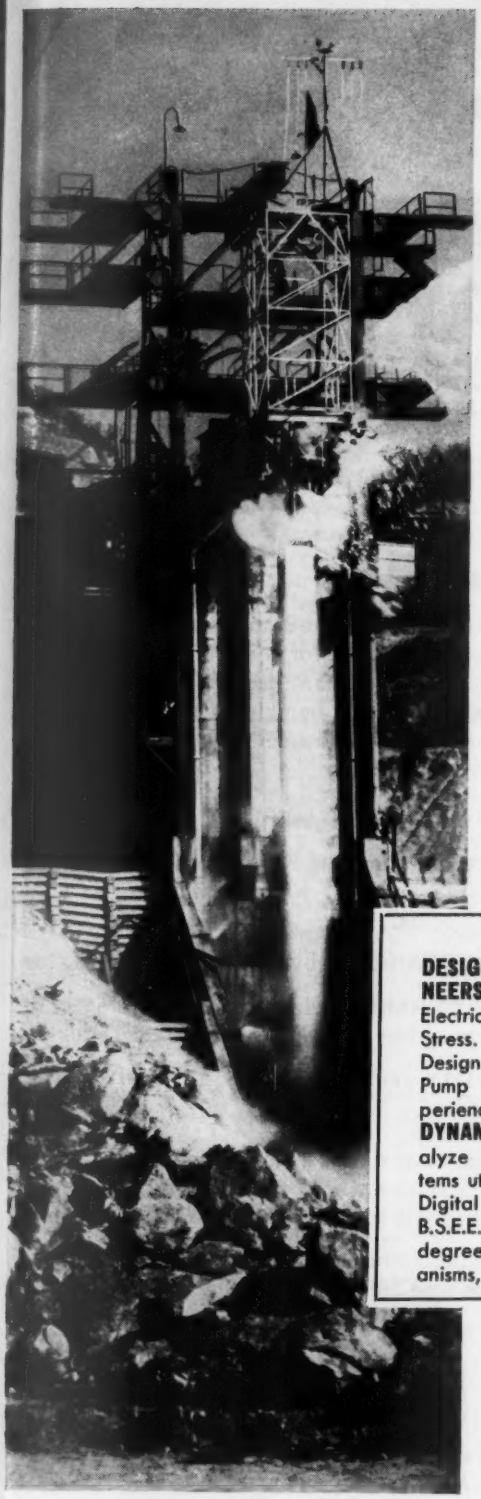

**PIONEER AND LEADER IN ROCKET ENGINE DESIGN AND DEVELOPMENT**

*Rocketdyne Offers*

# CAREERS FOR ENGINEERS IN ROCKET ENGINES

**NOW,** you can check on positions in the engine industry with an assured future—rocket engine design and development. North American . . . the company that has built more airplanes than any other company in the world. . . is also a pioneer in rocket engine design and development. Today, North American is the acknowledged leader in large liquid rocket engines.

**YOU** can be part of this success. . . team up with the top engineers in rocket engine design and development. Your ideas and work are given unusual recognition at North American . . . our liberal Patent and Suggestion Award Programs prove this. A fine Retirement Plan and other personal benefits are yours also at North American.

Assure your future now. You can work at Rocketdyne's Propulsion Test Laboratory in the Santa Susana Mountains or at Rocketdyne Headquarters—in the new multi-million-dollar plant now built in beautiful Canoga Park in Southern California's fabulous San Fernando Valley.

**THESE POSITIONS NOW OPEN AT ROCKETDYNE:**

**DESIGN & DEVELOPMENT ENGINEERS** — Mechanical, Chemical, Electrical, Standards, Structural and Stress. For Rocket Engine Systems Design or Development—Turbine, Pump and Combustion Device experience preferred.

**DYNAMICS ENGINEERS** — To analyze Rocket Engine Control Systems utilizing Electronic Analog and Digital Computers. B.S., M.E., or B.S.E.E. necessary. Prefer graduate degree. Experience in Servomechanisms, Systems Analysis desired.

**COMPUTER APPLICATION ENGINEER** — Application of Automatic Computers to investigate new methods of Numerical Analysis.

**TEST ENGINEERS**—Experienced on engine systems, combustion devices, turbines, pumps and engine instrumentation.

**EQUIPMENT DESIGN ENGINEERS** —Electrical, Mechanical, Structural.

**ELECTRONICS TECHNICIANS, STANDARDS & SPEC. ENGINEERS, ENGINEERING DRAWINGS CHECKERS**

***WRITE TODAY!***

Mr. Harry Malcome, Rocketdyne
Engineering Personnel, Dept. 596JP
6633 Canoga Ave., Canoga Park,
California.

# ROCKETDYNE

**A DIVISION OF NORTH AMERICAN AVIATION, INC.**

# For High Specific Impulse

# NITROGEN TETROXIDE

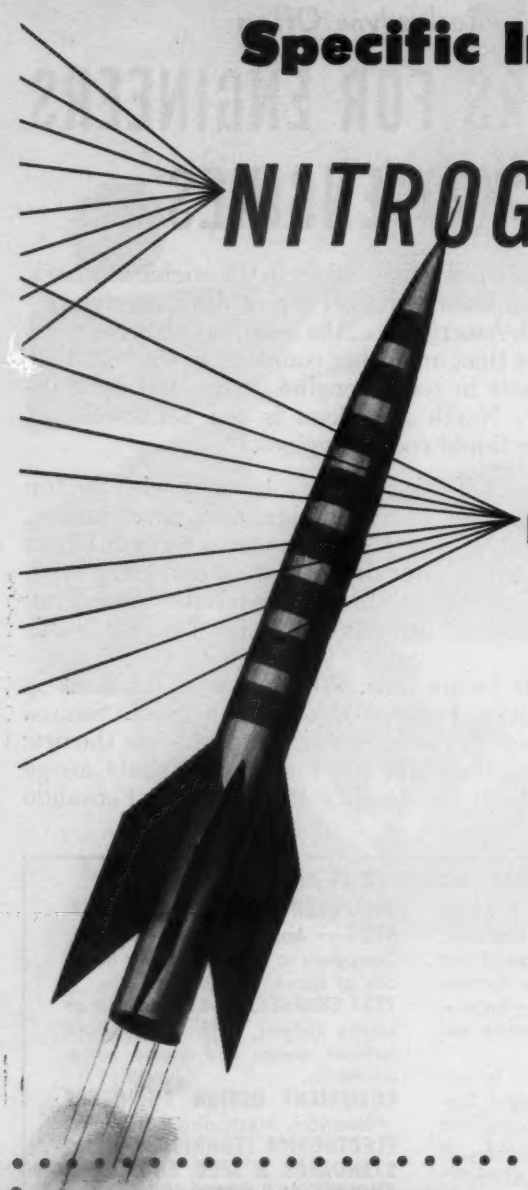

## an outstanding oxidant for liquid propellants

## Read Why!

Nitrogen Tetroxide offers numerous outstanding advantages as an oxidant for liquid rocket propellants. The combination of many factors necessary for efficient operation and handling *makes it uniquely suitable in some applications* and at a cost that is attractive.

**Consider these advantages!**

1. **ENERGY**—performance exceeds that of hydrogen peroxide, red and white fuming nitric acid, mixed acids.
2. **EASILY AVAILABLE**—by the cylinder or by the ton.
3. **EASY TO HANDLE**—shipped, piped, stored in ordinary carbon steel. Has high chemical stability.
4. **DENSITY**—compares favorably with other oxidants.

Under vigorous rocket conditions, ALL the oxygen is used. This means that the Nitrogen Tetroxide is used completely with no waste products to eliminate.

Write today for full details. Available in 125-lb. steel cylinders, and 2000-lb. containers.

## MIXED OXIDES OF NITROGEN

For applications that demand service at extremely low temperatures, mixtures of nitrogen tetroxide and nitric oxide are available in tonnage quantities. The addition of 25% by weight of nitric oxide, for instance, depresses the freezing point of nitrogen tetroxide from 12°F. to –60°F.

*This mixture boils at 14°F. and has a vapor pressure of approximately 8 atmospheres at 100°F.*

NITROGEN DIVISION ALLIED CHEMICAL

Allied Chemical

## NITROGEN DIVISION

**ALLIED CHEMICAL & DYE CORPORATION**

**40 Rector Street, New York 6, N. Y.**

**Hopewell, Va. • Ironton, Ohio • Orange, Tex. • Omaha, Neb.**

Anhydrous Ammonia • Ammonium Sulfate • Sodium Nitrate • Methanol
Ammonia Liquor • Urea • Ethanolamines • Ethylene Oxide • Ethylene Glycol
Diethylene Glycol • Formaldehyde • Nitrogen Tetroxide • Nitrogen Solutions
U.F. Concentrate—85 • Fertilizers & Feed Supplements

JANUARY 1956

VOLUME 26 NUMBER 1

JET PROPULSION
Journal of the
AMERICAN ROCKET SOCIETY

Editor-in-Chief
MARTIN SUMMERFIELD

# Low-Frequency Combustion Instability in Bipropellant Rocket Motors—Experimental Study

M. BARRÈRE[1] and A. MOUTET[2]

Office National d'Études Recherches Aéronautiques, Paris, France

**After a description of the phenomena observed in low-frequency instabilities, this study presents the experimental methods selected for research purposes, and especially the short-time response measurement devices as well as the two types of rockets used: one circular chamber, and one rectangular section chamber. The first experimental results obtained with these two types of chamber are described. These are rather in confirmation of the theory, as long as pressure remains the same, though all other parameters of the rocket may vary. However, important divergencies appear as soon as pressure undergoes alterations.**

## 1 Introduction

COMBUSTION instabilities inherent in rocket chambers have always hindered and still hinder development of these modern engines. Application of a few empiric rules, which led to a choice of convenient propellants, a satisfactory location of the orifices through which propellant is injected into the chamber bottom, a particular shape of the chamber and nozzle, resulted in an improved stability in some particular cases.

Engineers were guided in their research by the nature of sounds emitted by the engine, in confirmation of which, one finds in American literature a profusion of terms qualifying these sounds, such as: "chugging, humming, groaning, motor-boating, screaming, screeching, buzzing, squalling, etc."

In fact, all of these pertain to two kinds of sounds: the low-pitched deep tones appearing in a noisy combustion, which characterize low-frequency instabilities ($N \sim$ 100 $sec^{-1}$) and defective functioning of the chamber; the shrill, high-pitched whistling sounds correspond to high-frequency instabilities ($N \sim 1000$ $sec^{-1}$).

Progress recently achieved in short-time response measuring devices now fitted on modern test stands made it possible to observe the combustion instability phenomena, as expressed by sharp variations in pressure, in temperature and in velocity, in any one point of the chamber, the injection, or the fuel system of an engine.

Instabilities are an important factor in the development of a rocket, as they affect both performance and reliability of the engine(1);[3] unstable combustion modifies at every moment the various factors which characterize the performance of the engine, and, particularly, chamber pressure oscillations can reach amplitudes such that not only performance but even the life of the engine is endangered.

Thermic exchanges between gases and walls are considerably modified and increased, when combustion is unstable. Under such fluctuations, direction and intensity of the thrust may be changed every moment, due to lack of adaptation of the nozzle to low pressures (this phenomenon was evidenced in rectangular section chambers, during low-frequency instabilities). See Fig. 9b.

All this results in such a dispersion of data obtained in tests that it is impossible to foresee the flight performances of an engine. Sharp accelerations hamper the action of airborne measurement devices, and the whole situation entails long and costly test programs which are usually followed by trial and error, with little chance of good results.

For these reasons, the rocket designers now attach steadily growing importance to this phenomenon, which is observed whatever the power of the engine, the nature of the propellant, or the injection and fuel systems may be, but the incidence of which increases with the size of the rocket.

So, the interest attached to the study of the basic mechanism which generates these unstable pressures and violent combustions is easily conceivable. With L. Crocco (4), we made a basic distinction between normal combustion and unstable combustion: in normal combustion, local fluctuations may occur, but they are due entirely to hazard and have no effect on any sufficiently distant point of the chamber, so that there is no correlation between the fluctuations of one given quantity measured in two points of the chamber, sufficiently distant one from the other. But if the fluctuations are coordinated and no longer distributed at random, if there is a certain degree of organization in the phenomena, then there is a correlation between the fluctuations observed in two points of the chamber; the cause for coordination characterizes an unstable combustion. It is this last type we analyze in this study, solely from the experimental point of view.

As a first approximation, two ranges of instability are observed: (a) a range of low frequency, of less than 100 $sec^{-1}$, (b) and one of high frequency, or several hundreds of cycles per sec, which differ from the first by the very nature of the phenomena, i.e., by the coordinating cause (4).

Theoretical study of low-frequency instabilities (2, 3, 4, 5) has shown that these may be ascribed to a difference in phase between the variations of the chamber pressure, and the burnt flow of propellant produced by combustion. This difference in phase results from the time difference between injection and combustion of a given fraction of propellant. Within this time difference, the active pulverized particles mix, are vaporized, and absorb the quantity of energy necessary to start combustion. This ignition delay, which was at

Received July 26, 1955.

[1] Head, Rocket Division.

[2] Research Engineer, Rocket Division.

[3] Numbers in parentheses indicate References at end of paper.

first supposed to be constant (2, 3), was, later on, tied to fluctuations of the pressure in the chamber, according to the law of shape $\tau p^n = C$, a constant (4), where $n$ is index of interaction which characterizes the evolution of the propellant in the chamber.

These theoretical studies defined a criterion of stability and put the accent on certain parameters tied to the engine or to its performance. Though such studies are numerous, one finds few experimental results, and this is due, particularly, to the extremely severe conditions under which such tests take place and under which the measurement instruments have to work (6).

We are presenting, in our study, experimental results obtained in the matter, as well as our own results. Our analysis has two objects: (a) an experimental determination of the influence of various parameters on the engine of low-frequency instabilities; (b) a comparison of theoretical and experimental results, with the object of checking the theories previously formulated.

## 2 Description of the Phenomenon

The typical diagram of a bi-liquid rocket engine is represented in Fig. 1.

It comprises, in the simplest case (pressurized gas): (a) A high pressure tank of some neutral gas (nitrogen) which, through a pressure reducer, distributes a uniform low pressure in the two tanks containing the fuel and the oxidizer. (b) A feed system bringing the fluids into the combustion chamber. To this system are fitted filters, diaphragms, through which are compensated losses of pressure in the connections of the measuring devices which record the flow and the pressure. (c) A combustion chamber with its injection system, the flame tube and the nozzle through which burned gas is rejected.

Combustion instabilities in a liquid propellant rocket are evidenced by variations of pressure in the fuel system and in the combustion chamber, by variations of temperature in the flame tube or at the nozzle outlet as well as in the flow of propellant.

We have endeavored to examine how these three values—pressure, temperature, and flow—vary under low-frequency instability regime.

This regime appears especially in low pressures of the combustion chamber, and low gage injection pressures; it is characterized, as every recurring phenomenon, by frequency, amplitude, and shape of signals obtained.

Fluctuations of pressure in the chamber during low-frequency instabilities are of two types:

1. For high amplitude fluctuations, one observes a very quick increase of the pressure during approximately a millisecond (Fig. 2a), and a damped decrease at exponential rate.

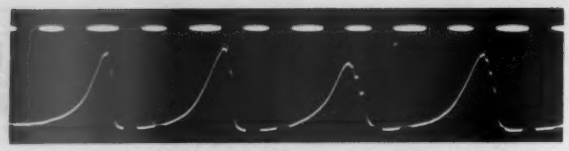

2a Pressure oscillations $p = 9$ kg/cm² $N = 44$ sec$^{-1}$. Time base $10^{-2}$ sec.

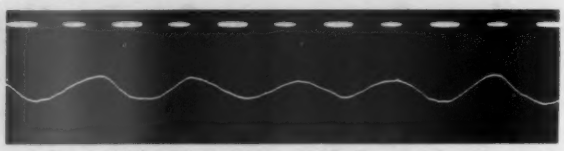

2b Sinusoidal oscillations of pression $N \simeq 53$ sec$^{-1}$. $p = 12$ kg/cm². Time base $10^{-2}$ sec.

2c Fluctuations of chamber pressure $P = 25$ kg/cm². Time base $10^{-2}$ sec.

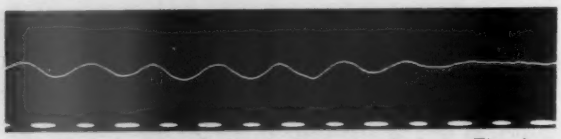

2d Beginning of oscillations in the course of a test. Time base $10^{-2}$ sec.

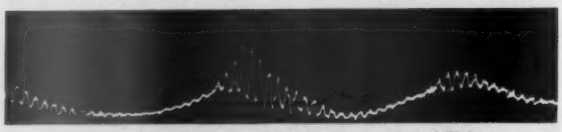

2e Superposition of high- and low-frequency instabilities.

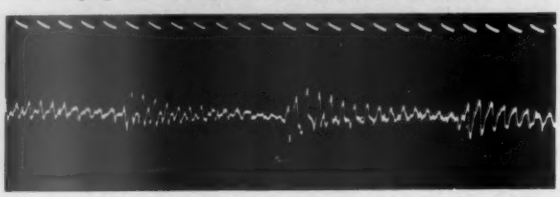

2f Propagation of waves at low frequency in the chamber. Time base $10^{-3}$ sec.

**Fig. 2 Records of chamber pressure fluctuations in chamber. (Propellant: nitric acid-furfurylic alcohol)**

This high pressure practically stops the inflow of propellant and the combustion, and this entails a progressive drop of the

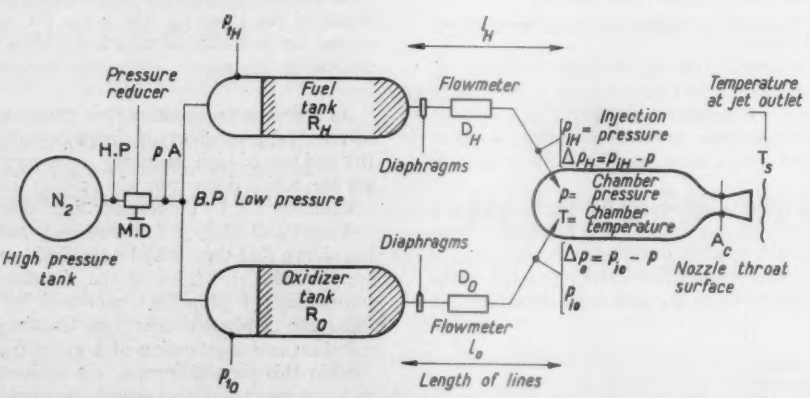


**Fig. 1 Schematic diagram of bipropellant rocket system**

pressure: after which a new injection follows, with a new sharp rise. The chamber empties during the exponential part of the curve, because the newly injected propellant has had no time to ignite. The constant duration of the phenomenon, while the pressure drops, corresponds to the presence of the propellant in the flame body. These phenomena of instability follow a curve rather similar to relaxation oscillations. (These phenomena are characterized by low pressures.)

2. If the mean pressure in the chamber is increased through variation of the inlet pressure, the frequency increases and the amplitude decreases. Pressure is no longer submitted to sharp drops, but rather to modulations. The shape of signals obtained is sinusoidal (Fig. 2b).

Beside these two types of evolution of the chamber pressure, which correspond to a phenomenon of pure low-frequency instability, one observes some not-so-well-defined phenomena, such as those seen in Fig. 2c. Amplitude is no longer constant, and there is a superposition of various frequencies, which are distributed at random, without any correlation cause. (This type of instability was observed at high chamber pressures: $p \geq 25$ kg/cm².) Fig. 2d represents another type of low-frequency instability. During the firing, we observe the birth of oscillations the amplitude of which increases, then stabilizes, and suddenly stops. The frequency is practically constant during this sequence of instabilities. It all happens just as if the ignition delay would, for some reason, increase sharply for a certain time and produce an unstable regime.

We have to point out, however, that these recordings pertain solely to low-frequency pressure fluctuations; pressure curves obtained with shorter response time instruments evidence a superposition of high and low frequencies, as shown in Figs. 2e and 2f.

Analysis of recordings of the temperature in chamber or at outlet of the nozzle shows the same phenomena. In the flame body, low chamber pressures (Fig. 3a) produce oscillations of temperature (2nd method) of high amplitude; when the pressure is progressively increased (Fig. 3b) the amplitude decreases and frequency increases. If the pressure is further increased, the oscillation amplitudes of low frequency are so small that they become perturbed by other phenomena which, though they are of secondary importance in other cases, then become prevailing. A more complex analysis is then necessary, which calls for a diagram of the frequencies spectrum, to determine basic oscillations. Examination of temperatures at the outlet of the nozzle by the first method evidences in a similar way the low-frequency instabilities (Fig. 3d and 3e taken in the chamber and at the outlet of the nozzle).

Instantaneous recordings of the flow disclose important fluctuations in the low-frequency zone. Fig. 4b discloses simultaneous variations of nitric acid flow and of pressure in the chamber, while frequencies observed in pressure and flow are very nearly similar. For higher frequencies (Fig. 4a) there is practically no fluctuation in the flow; this is partly due to low amplitudes of the pressure variations, which cause no perturbation to injection. Moreover, for higher frequencies $N \sim 150$, the flowmeter, which has a response time of $10^{-2}$ sec, damps the fluctuations, and these may pass unnoticed.

Having thus analyzed low-frequency instabilities in a well-defined point of the engine, i.e., the combustion chamber and tubings, it is of interest to know what happens when there are perturbations in the flame body, so as to have complete information on the low-frequency instabilities. In a general way, temperature and pressure recorded in various points of the chamber are in phase. Simultaneous recordings of the injection pressure of acid, of the injection pressure of fuel, and of the two pressures in two points of the chamber, disclose the following facts:

For certain amplitudes of the chamber pressure, there is no repercussion of the fluctuations on injection pressure. This phenomenon corresponds to Fig. 5a. The four recorders have the same sensibility; injection pressures are stable, and oscillations of the chamber pressure are in phase. This confirms the instantaneous measurements of the flow, which give indications for small perturbations of the chamber pressure (Fig. 4a). Oscillations correspond to intrinsic instabilities, which have their source in the combustion zone and are exclusively due to combustion phenomenon.

We have also found that the chamber pressure fluctuations are preceded in some cases by pressure oscillations in the injection header, mainly in the tank containing nitric acid. These frequencies are of about 1600 sec$^{-1}$ and are very likely due to propagation of pressure waves in the propellant inlet system. These oscillations are progressively damped (Fig. 5b). Recordings have shown that low-frequency oscillations

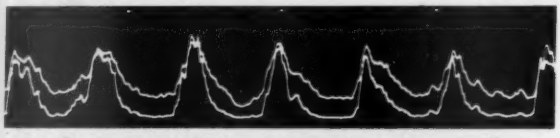

3a Temperature oscillations for a chamber pressure of 4.2 kg/cm². Time base $2.10^{-2}$ sec.

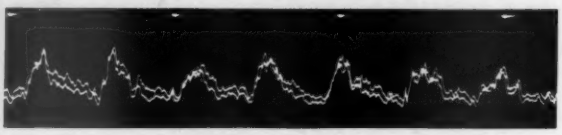

3b Temperature oscillations for a chamber pressure of 9 kg/cm². Time base $2.10^{-2}$ sec.

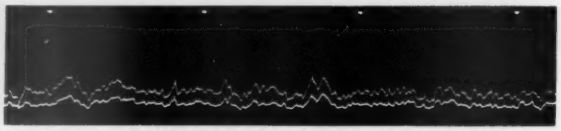

3c Temperature oscillations for a chamber pressure of 15 kg/cm². Time base $2.10^{-2}$ sec.

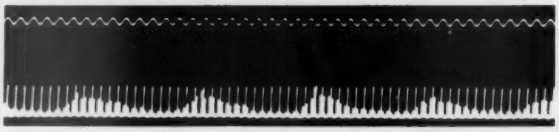

3d Record of temperatures (1st method). (Fluctuations of temperature in a given point of the chamber. Time base $10^{-3}$ sec.)

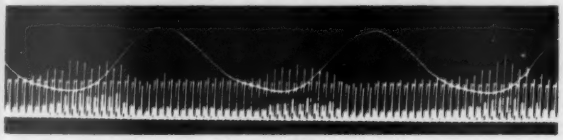

3e Simultaneous record of pressure in the chamber and temperature at the divergent outlet (1st method).

**Fig. 3 Records of temperature variations in a combustion chamber having transparent walls (2nd method)**

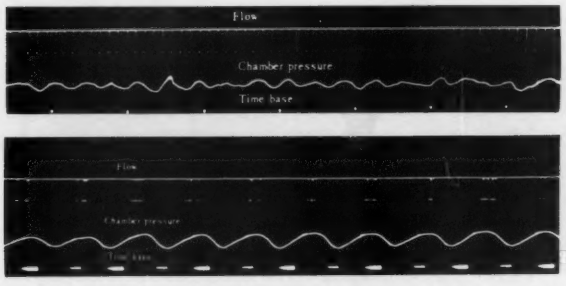


**Fig. 4. (a) Top: Fluctuations of the nitric acid flow, and (b) bottom: of chamber pressure in course of a test**

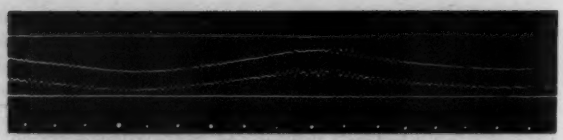

5a Simultaneous records of injection and chamber pressures.

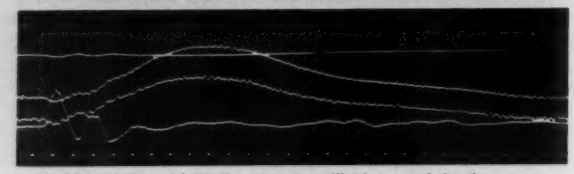

5b Beginning of high-frequency oscillations on injection pressure during low-frequency instabilities. On these two figures are seen from top: fuel injection pressure; chamber pressure near injection area; chamber pressure near area of pressure reduction; pressure of nitric acid injection. Time base $10^{-3}$ sec.

**Fig. 5 Simultaneous records of four pressures (two injection pressures, two chamber pressures)**

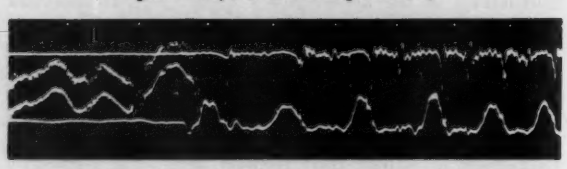

**5c. Simultaneous recording of injection and chamber pressures. Record shows how low-frequency amplitude oscillations become high-amplitude oscillations**

From top: fuel injection pressure; chamber pressure near injection area; chamber pressure near area of pressure reduction; pressure of oxidizer injection. Time base $10^{-2}$ sec.

of high amplitude can start without any apparent reason, from oscillations of the same type but lower amplitude; this can be explained by the sharp and momentary increase of the ignition delay. Fig. 5c shows an aspect of this phenomenon, in a record of four pressures. On the left, low-frequency instabilities are of low amplitudes: then amplitude sharply increases, and becomes such that the spots are outside of the screen of the oscillograph, and there is a repercussion on the injection pressures. However, we found a particularity which had already been noticed by Ross and Datner (6); i.e., that the frequencies observed in the fuel ducts are twice those of the chamber frequencies, and very likely correspond to different impedances of the propellant ducts.

Simultaneous variations of the chamber pressure before the pressure reduction zone and of the temperature (1st method) at the outlet of the nozzle, during low-frequency instabilities, are represented in Fig. 3e. Temperature maxima at the outlet of the nozzle correspond to minima pressures.

## 3 Testing Installation

Experimental study of combustion instabilities of rocket engines necessitated development of new measuring devices as well as new combustion chambers, better fitted for such study.

This led to development of short response time devices, which made it possible to study safely the sharp variations of such factors as pressure, temperature in a definite point of the flame body. Special transparent combustion chambers were built, and special photograph methods developed, for the study of these instability phenomena.

### Measuring Devices

Three basic values had to be measured for the study of performances of a rocket: pressure, temperature, flow. These various factors are interesting at the same time by their mean value and their instantaneous values. Many measuring devices are known for the mean value, but on the contrary, the methods of measurement of instantaneous values are still in full evolution, because shorter and still shorter response times are necessary for the study of these phenomena.

#### *Measure of Pressures*

If measure recording of inlet or injection pressures is rather easy, the problem becomes more complicated when it comes to the measurement of the pressure in the chamber. The temperature of combustion gas is very high, 3000 K, and important fluctuations of this temperature, taking place in the course of the test, bring deep alterations to the characteristics of the wall through which recordings are taken. Advantages and drawbacks of the methods used for the measurement of pressures in rockets have been discussed by Li (7). We have used, for measurement of pressures, three types of recorders, actuated in all three cases through variation of capacity.

The first recorder takes accurately frequencies of 100, and gives the continuous component (Figs. 2a, b, d).

The second recorder also gives the continuous component, and has a passing band from 0 to 5000 $sec^{-1}$.

The third recorder takes only alternative component (band from 50 to 8000 $sec^{-1}$); the diaphragm is directly in contact with the hot gases. Figs. 2e, 2f are an example of the recording obtained. It shows high-frequency oscillations which are superposed to low-frequency oscillations. With this method, the only recordings of interest are those of frequency. However, we tried to figure the value of amplitudes, by rating, through a variable condenser driven by an electric motor, the amplitudes observed in capacity variations, these being marked by a certain sag on the diaphragm, i.e., a certain pressure.

#### *Measure of Temperatures*

Temperatures of the jet at the outlet of the nozzle, or of the gases in the flame body, are measured by optical means; this is, in fact, the only possible way of obtaining very short response times. The main characteristics of methods used and performances of the devices are given further in this study (8, 9), and we shall just sum them up here.

The method of line reversal is based on simultaneous measurement of some given energy (e.g., a bulb filament), of the energy of flame, and of the energy of the filament seen through the flame. These three measurements define the real temperature of the flame, its brilliance temperature, and its absorption coefficient.

For a study of one well-defined point of the combustion chamber, these three measurements cannot be taken simultaneously, but a special rig may be prepared so that the three measurements are taken within a time so short that there is practically no variation of the temperature. With the rigs set up in our Laboratory (8), this time was of about $10^{-4}$ sec, and as much as 4500 temperature recordings inside a second were obtained. On records (Fig. 3e) a series of three impulsions was obtained, the elongations of which represent, respectively, the energy of filament, the energy of the flame, and the energy of filament through flame, increased by the energy of the flame (Fig. 6).

Analysis of the two adjacent zones of the flame gives a determination of the three values. The method is based on the hypothesis that both zones are at the same temperature. This method presents the advantage of working with very short response times ($10^{-5}$ sec). Figs. 3a, b, c give some of the recordings obtained by this method. Energy of the filament (Fig. 6) is recorded at the beginning of the test; further in the course of the test, one of the spots of the oscillograph shows the energy of the flame and the other one the energy of filament through flame increased by energy of the flame.

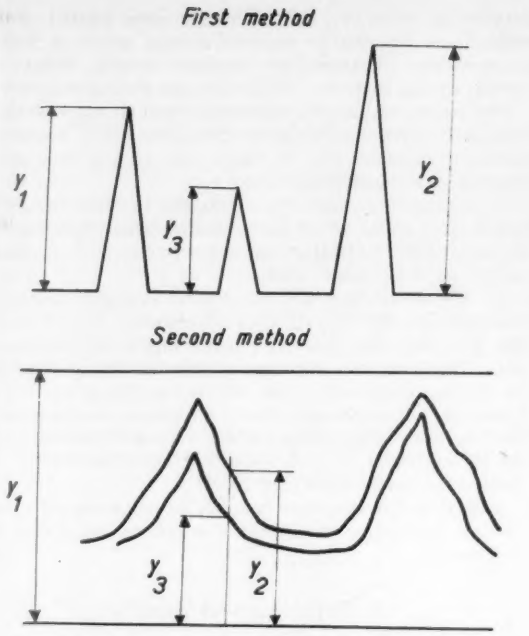


**Fig. 6 Determination of temperatures by optical means**

$y_1$ = filament energy $E$
$y_3$ = flame energy $e$
$y_2 = (1 - \alpha)\, E + e$
$\alpha$ = absorptivity

$$\tau = \frac{y_3}{y_1 + y_3 - y_2}$$

$\tau$ = transmission ratio

$$\text{Colg } \tau = \frac{c_a \log e}{\lambda}\left(\frac{1}{T_L} - \frac{1}{T_F}\right)$$

$T_L$ = brightness temperature
$T_F$ = flame temperature

### *Measure of the Flow*

In the last few years, a great deal of research work was done in connection with measurement of the propellant flows. Recent publications (10) underlined the advantages of short response time flowmeters.

The flowmeter used on our test rig consists of a very light teflon wheel (90 mg) driven by the fluid. Every blade passage delivers a luminous impulsion, expressed in electric impulsion. The frequency of blade passages is in direct relation to the flow.

For the study of dynamic performances, a rig similar to a shock tube is used. At bursting of the diaphragm, the output raises from zero to a constant value. Recording of the blades passages during the bursting of the diaphragm (Fig. 7) discloses that, after a few milliseconds, the constant rate of flow is obtained. The time constant measured by this method is of $2.10^{-3}$ sec.

### Characteristics of Combustion Chambers

Theoretical study of low-frequency instabilities called attention to some of the parameters of the engine; it is therefore of interest to select, for experimental purposes, such installations where these parameters may vary. This is why

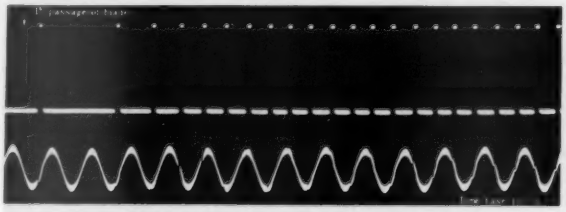

**Fig. 7 Measure of flows (determination of the response time). Recording of passage of the blades at bursting of diaphragm**

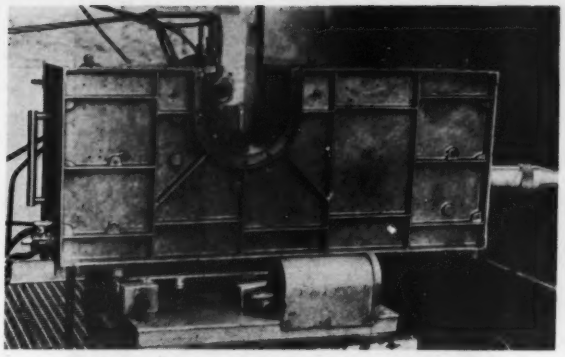

**Fig. 8 External view of a 100-kg thrust test bench**

we used combustion chambers particularly fitted for the study of low-frequency instabilities.

The first engine used for experimental work was a 100-kg thrust engine, shown in Fig. 8. The chamber is of a 9-cm diameter circular shape.

The injection system comprises 9 injectors having crossed jets, each delivering two jets of oxidizer under a 90-degree angle, and a central jet of fuel which is adjusted to strike the point where the two oxidizer jets cross each other. The orifices are interchangeable, so that the mixture and the injection pressures can be varied. The nozzle is conical, the $^1/_2$ angle of the convergent is of 45 degrees, the $^1/_2$ angle of the divergent is of 14 degrees. Combustion chamber and nozzle are cooled by means of a water circuit.

Beside the mixture and the injection pressures, it is also possible to modify the characteristic length by addition of supplemental ducts of various lengths. The tubings are very nearly of the same length for combustor, and for fuel ($l \sim 3$ m) their section is of 1.6 cm$^2$. Calibrated diaphragms, located at the outlet of the tanks, render it possible to modify at will load losses between injection system and the tanks.

In each test we measured medium thrust, chamber pressure, the two injection pressures, feed pressure on each tank, temperature at the outlet of nozzle, and outputs of fuel and oxidizer.

To check influence of the size of the engine on combustion instabilities, a second chamber was tested with a throat diameter which was half of the first one and which had a medium thrust of about 25 kg. The length of tubings remained the same, and their surface was of 0.79 cm$^2$. The various characteristic lengths were similar for both engines, as well as the shape of the nozzle, but the combustion chamber had no cooling system. This chamber, without any cooling, was able to withstand 20-second firings, without damage.

To eliminate as far as possible lateral oscillations, bidimensional chambers were used. These chambers had two Plexiglas walls so that the various phenomena, from injection to combustion of the propellant, could be visualized.

There are two types of chambers now in service:

1. The first type comprises a crossed jets injector. All orifices are interchangeable. Characteristic lengths can be modified by variation of the throat surface. Fig. 9a shows the

**Fig. 9a Combustion chamber of rectangular section having transparent walls**

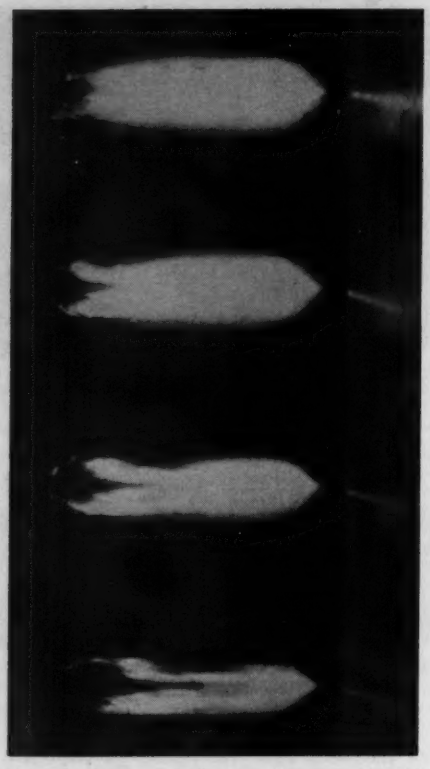

Fig. 9b Jet deviation during low-frequency instability

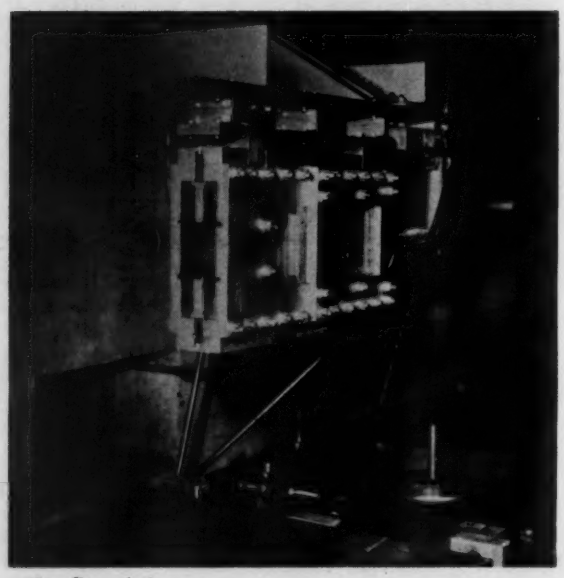

10a General view

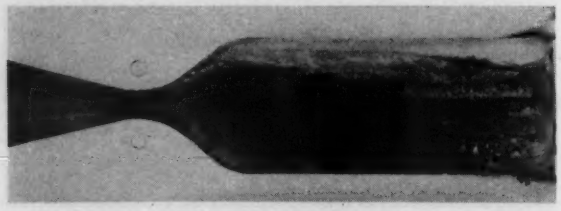

10b Aspect of wall after a 2-second test

Fig. 10 Combustion chamber with transparent walls

chamber in course of a test. Through filters located on the walls, it is possible to observe certain zones of higher temperatures. Measurement devices usually fitted on circular section chambers can be mounted on this chamber.

The major trouble with transparent wall chambers is their very short duration (from about 2 to 3 seconds). However, numerous measures can be taken, due to the very short response time of instruments used.

To improve transparency of Plexiglas in some particular points, silica plates, which have a better surface finishing and are better fitted to temperature measuring by optical means, can be inserted in the Plexiglas.

2. The second type makes it possible to study influence of the injection system on chamber instabilities. Such a chamber (Fig. 10a) comprises five primary injectors with crossed jets. The same measurements as with the former chambers are taken. Longevity of the chamber is also of about 2 to 3 seconds. A rough zone, due to turbulence, is observed in the chamber; a festooned erosion is found in the nozzle throat and traces of shock waves are found engraved in the Plexiglas of the divergent (Fig. 10b).

A study of low-frequency instabilities was made with these various combustion chambers, of which we are giving the first results.

## 4 Experimental Results

The object of an experimental study of low-frequency instabilities is to achieve a complete understanding of the phenomena which produce them, and to define experimentally such conditions as will damp these fluctuations to such an extent that they no longer hamper performances of the rocket.

We have, first of all, studied the variations of frequencies observed in the chamber, in relation to some of the parameters of the engine. A second step allowed us to determine which of the parameters have the greatest influence on amplitude of oscillations. Further, we had to find how combustion efficiency of the flame body was affected by these instabilities.

We examine, below, influence of the length of chamber, of the surface of propellant injection orifices, of chamber pressures, of the mixture ratio, of high injection overpressures $\Delta p_0$ and $\Delta p_H$ of the nature of propellant, of the size of chamber, on the frequencies observed during low-frequency instabilities. We will mention, in some cases, the value of amplitudes, as results of the first study mentioned above. We shall give two series of results, obtained with circular section chambers, and with rectangular section chambers.

### Cylindrical Chambers

We have kept constant, for each test, the diameter of the chamber and the length and section of feeding ducts.

#### *Influence of the Chamber Pressure*

Figs. 11 and 12 show the influence of the chamber pressure upon frequencies observed. As a general rule, and for the two propellants used, frequency increases when chamber pressure increases. Moreover, amplitudes of oscillations decrease when pressure increases. With a chamber pressure of over 16 kg/cm², and with furfurylic alcohol-nitric acid as propellant, amplitudes are very low and never exceed 5 per cent of the mean pressure; with the same pressure, but with nitric acid-octane as propellant, amplitudes are more important and may vary from 20 to 50 per cent. These measures were taken with a constant injection speed, and with different injection orifices surfaces for each mean pressure of the chamber.

#### *Influence of Length of the Chamber*

This parameter, tied to characteristic length $L^* = V/A_c$ = volume of chamber/surface of throat, is of the highest im-

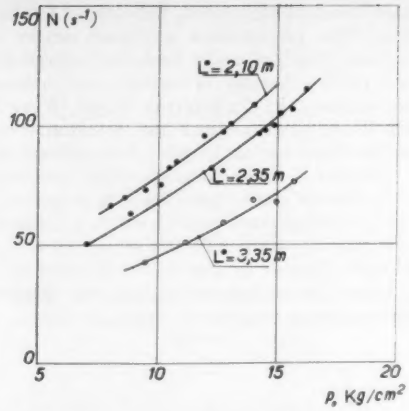


**Fig. 11 Variation of frequency under influence of chamber pressure and characteristic length $L^*$. Propellant: nitric acid-furfurylic alcohol**

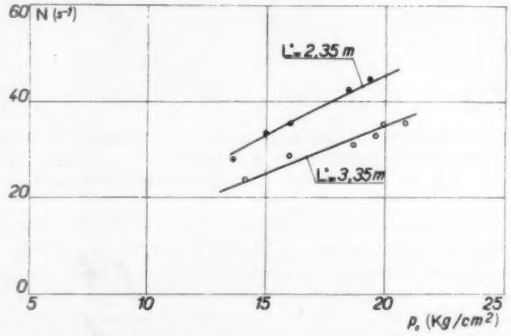


**Fig. 12 Variation of frequency under influence of chamber pressure and characteristic length $L^*$. Propellant: nitric acid-octane**

portance in the study of combustion instabilities because it conditions the time during which active bodies remain in the flame body.

Results obtained for three characteristic lengths

$$L^* = 2.10\ m - 2.35\ m - 3.35\ m$$

are given in Figs. 13 and 14. We find that frequency increases when characteristic length decreases. For the same chamber pressure, amplitudes slightly decrease when the length of the chamber is increased.

### *Influence of Gage Injection Overpressures $\Delta p_0$ and $\Delta p_H$*

These pressures are determined from recorded curves of chamber pressure and injection pressures. They may also be computed from the flow of each of the propellants, but in any case, with both methods, the accuracy is far from perfect, and errors may be, in some cases, of over 10 per cent. It is therefore difficult to give precise values of the variation of frequencies vs. injection overpressure. Fig. 15 shows the direction of frequency variations observed for the two overpressures $\Delta p_0$ and $\Delta p_H$. One sees that frequency varies in the same direction as gage injection pressures.

An accurate study of this parameter can be achieved only by a direct measure of gage injection pressures.

### *Influence of the Nature of Propellant*

Two propellants have been tested: nitric acid-furfurylic alcohol, and nitric acid-octane. Figs. 11 and 12 give the frequencies observed for various chamber pressures and for two characteristic lengths. In a general way, higher frequencies are obtained with lower amplitudes for the same

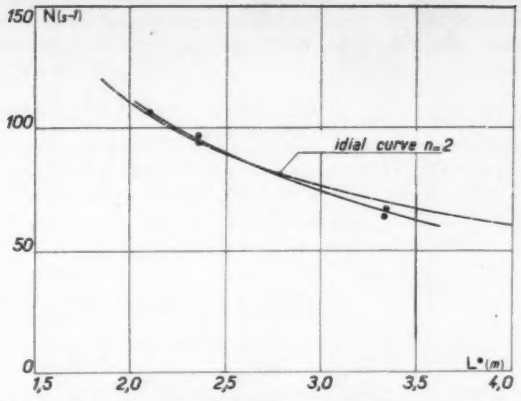


**Fig. 13 Variation of frequency according to characteristic length $L^*$. Chamber pressure: 14 kg/cm². Propellant: nitric acid-furfurylic alcohol**

NOTE: "idial curve" on figure should read "ideal curve."

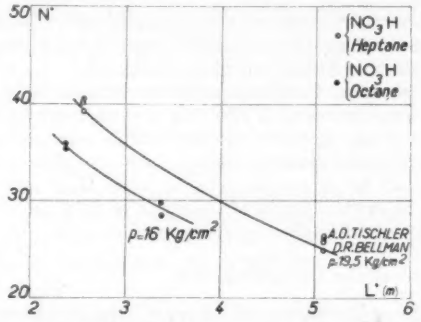


**Fig. 14 Variation of frequency according to characteristic length $L^*$. Chamber pressure: 16 kg/cm². Propellant: nitric acid-octane**

NOTE: Upper left corner should read: $N(s^{-1})$

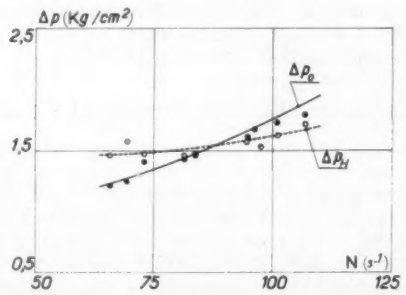


**Fig. 15 Effect of injection pressure drop on the frequencies observed. Propellant: nitric acid-furfurylic alcohol; characteristic length $L^* = 2.10$ m**

chamber pressure, with propellant AN-AF (nitric acid-furfurylic alcohol) than with the mixture AN-O (nitric acid-octane). For a chamber pressure of 15 kg/cm², the frequency observed with propellant AN-AF is of about 100 $sec^{-1}$ and an amplitude of 10 per cent. For the same chamber pressure, frequency is only 35 $sec^{-1}$ with propellant AN-O with amplitude of about 30 per cent. Results obtained (5) with nitric acid-heptane as a propellant show, for the same pressure of 15 kg/cm², frequencies of about 23 $sec^{-1}$.

### *Influence of the Mixture*

Variations in the mixture have only a slight influence on low-frequency instabilities, at least in the field in which we experimented, which corresponds to a variation of $m^* =$

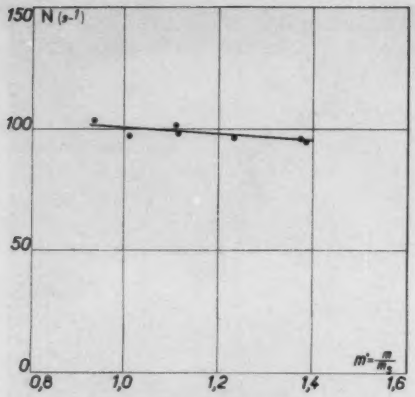


**Fig. 16 Effect of characteristic mixture ratio on frequencies observed. Propellant: nitric acid-furfurylic alcohol. Pressure in chamber 15 kg/cm²**

$m/m_s$, from 0.9 to 1.4 ($m_s$ being the ratio of stoichiometric mixture).

The various mixture ratios are obtained with injection high pressure constant, and modified surface of fuel injection orifices. Results obtained are given in Fig. 16.

It is observed that amplitudes are most important with weak mixtures and with rich mixtures, so that, for a given pressure in the chamber, the most stable combustion is obtained with stoichiometric mixture ratios, rather than with higher and lower ratios. This is what Ross and Datner evidenced in their study of the stability field defined in coordinates $p$, $m$ (chamber pressure, mixture ratio).

### *Influence of the Size of Chamber*

Whatever the object and nature of experiments conducted with this type of engine may be, the relation to size should always be kept in mind. We experimented with two chambers of 25 and 100-kg thrust. A few comparison tests, run with the same characteristic lengths, same injection speed, and same chamber pressure, evidenced very similar frequency oscillations. The only difference was found in the amplitudes of chamber pressures, which are slightly lower for the rocket of 100 kg than for the rocket of 25 kg.

## Transparent Chambers of Rectangular Section

These chambers were, at first, experimented upon for the study of ignition delays at the start, and so the conditions are as close as possible to the real functioning of a rocket engine. It was demonstrated (11) that this delay is tied to the frequency of the first oscillations which appear at the start. A decrease of frequencies (Fig. 17) is obtained when the delay increases, which shows importance of hypergols with short delays. Amplitude of the oscillations increases as the frequency decreases; i.e., the delay increases. In the course of these tests we observed, on temperature recordings and photographs taken at high speed, well-defined low-frequency oscillations. The phenomenon appeared clearer than in circular section chambers, and it seemed of interest to pursue the study, on such a chamber, of low-frequency instabilities.

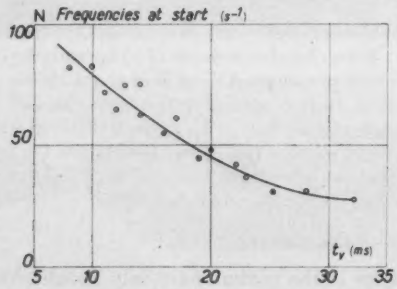


**Fig. 17 Relation between ignition delay and frequency of the first oscillations at start**

We kept constant the characteristic length ($L^* = 2.15$ m). An erosion on the throat of the nozzle, found after each test, decreased the characteristic length by an average of 0.1 to 0.15 m. The life of these chambers being very short, it is necessary to provide a very quick starting propellant feeding so as to obtain a permanent velocity within a few hundredths of a second after the start. The tanks are, for this purpose, U-shaped tubes, located as close to the chamber as possible. We may state that permanent velocity was obtained practically within the first second.

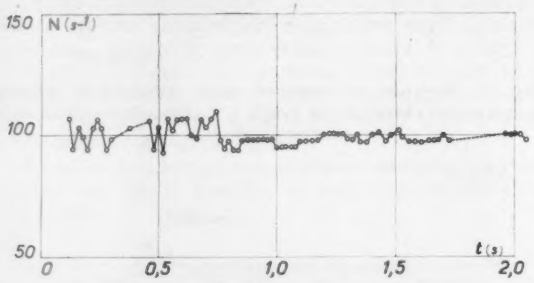


**Fig. 18 Variation of frequency according to the duration of tests. Flat combustion chamber $p = 6$ kg/cm², $p_0 \simeq p_H \simeq 1.5$. $L^* = 2.15$ m. Propellant: nitric acid-furfurylic alcohol**

Test shown in Fig. 18 discloses a stabilization of frequencies with time after 0.8 sec. This figure also shows, during the increase of pressure, frequencies which oscillate around a medium value. This phenomenon is different in chambers of rectangular section, where frequency increases progressively with pressure in the chamber, while amplitudes decrease.

Another fuel system is now under study, with which we expect even more rapid injections at start. This system comprises two small interchangeable tanks, which are located near the chamber. The active liquids are kept, before the test, upon two diaphragms which burst at the start, under a pressure which is near the normal pressure.

In this study, we have varied the chamber pressure, injection overpressure, the mixture ratio, and the nature of propellant.

### *Influence of the Chamber Pressure*

In this series of tests, the surface of injection orifices being constant, we progressively altered the pressure in the chamber by acting upon the feed pressure. We found, as in the case of circular section chambers, an increase of the frequency with that of the chamber pressure, and a decrease of the amplitudes. For a chamber pressure of above 11 kg/cm² (Fig. 19) and with nitric acid-furfurylic alcohol as propellant, low-frequency amplitudes are no longer clear. We observed the appearance of very different frequencies, and instabilities of low frequency were no longer the basic phenomenon. Fig. 19 shows that, for a variation of the chamber pressure from 4 to 9 kg/cm², frequency passed from 86 to 109 $sec^{-1}$.

For the same chamber pressure, the same characteristic length, and the same propellant, frequencies are higher for rectangular section chambers. Recording of temperatures in the flame body gave the following results: (a) Taking into account that the walls were blackened during the test, it is not possible to study the relative variations of temperature. (b) However, the result is important because it makes it possible to figure the amplitude of temperature oscillations. We found that for low pressures ($p \sim 4.2$ kg/cm²) the difference $\Delta T = Tm - T$ (where $Tm$ is the maximum temperature selected as reference, and $T$ is instantaneous temperature) is of over 500 degrees (Fig. 20). (c) For a higher value of the

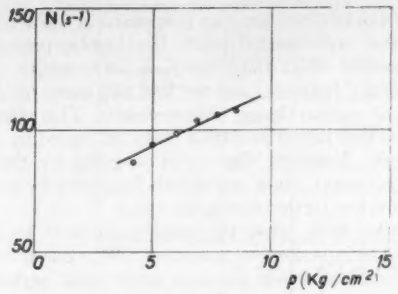


**Fig. 19 Effect of pressure on frequencies observed. Rectangular section chamber. Propellant: nitric acid-furfurylic alcohol**

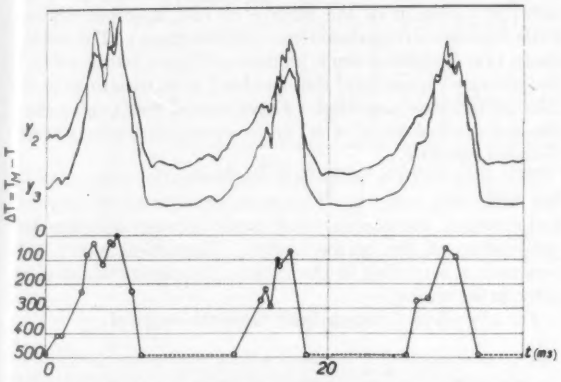


**Fig. 20 Variation vs. time of the difference between maximum temperature $T_M$ and instantaneous temperature of flame, $T$, $\Delta T = T_M - T$ ($p$ = 4.2 kg/cm²)**

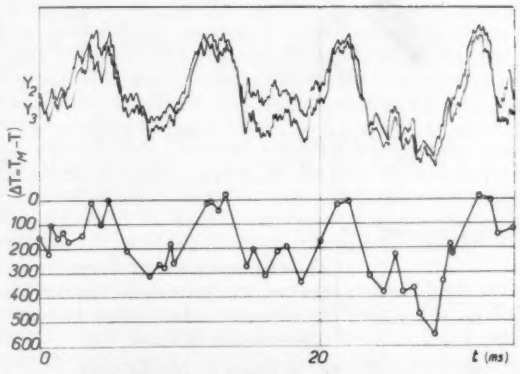


**Fig. 21 Variation vs. time of the difference between maximum temperature $T_M$ and instantaneous temperature of flame, $T$, $\Delta T = T_M - T$($p$ = 9 kg/cm²)**

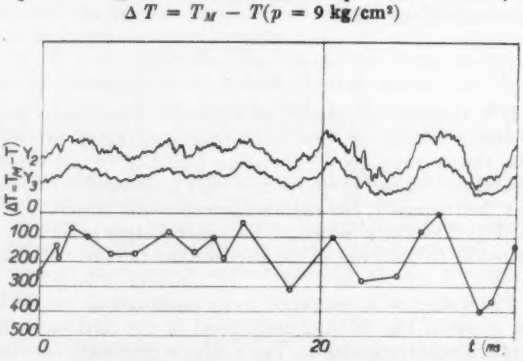


**Fig. 22 Variation vs. time of the difference between maximum temperature $T_M$ and instantaneous temperature of flame, $T$, $\Delta T = T_M - T$($p$ = 15 kg/cm²)**

pressure $p$ = 9 kg/cm², the amplitude decreases (Fig. 21) and its mean value is of about 300 degrees. (d) For chamber pressures of about 11 kg/cm², the mean amplitude is about 200 degrees (Fig. 22).

***Influence of Injection Overpressure***

Constant pressure and variable overpressure were obtained by alteration of the surface of fuel and oxidizer orifices, while the surfaces ratio (oxidizer/fuel) remained constant. Fig. 23

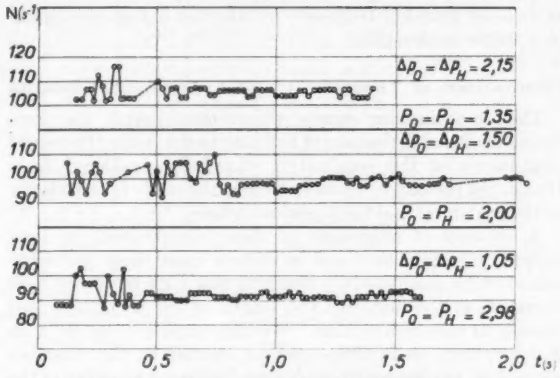


**Fig. 23 Variation of frequency under effect of injection pressure drop. Chamber pressure: 6 kg/cm². Propellant: nitric acid-furfurylic alcohol**

shows the variations of frequencies observed for a pressure of 6 kg/cm² vs. $\Delta p_0$ ($\Delta p_0$ undergoes a variation of 1.05 at 2.16 kg/cm²). As for unidimensional chambers, frequency increases when injection overpressure increases. The amplitudes observed are greater at low overpressures, i.e., at low injection speeds.

***Influence of the Mixture Ratio***

The mixture ratio has very little influence on low-frequency instabilities. As in the case of circular section chambers, we found a decrease of frequency when the mixture ratio increases Amplitudes increase, for a given chamber pressure, when the mixture ratios come near extreme values.

***Influence of the Nature of Propellant***

We have only used, so far, in these chambers, hypergolic mixtures. For the same chamber pressure and the same injection overpressure, we obtained for various propellants, the following frequencies:

—nitric acid-furfurylic alcohol: $N = 106\ \text{sec}^{-1}$
—nitric acid-furfurylic alcohol 75%-xylidine 25%: $N = 117\ \text{sec}^{-1}$
—nitric acid-furfurylic alcohol 50%-xylidine 50%: $N = 128\ \text{sec}^{-1}$

Frequency increases when xylidine is added to furfurylic alcohol.

Under similar conditions, it is possible to find experimentally, for each propellant, a characteristic frequency, and to determine for each case a quality index for low-frequency instabilities.

**Combustion Efficiency**

We have not taken as a comparison basis the combustion efficiency such as it is usually defined, but a quality index $\eta$ which is equal to the ratio of the theoretical output factor to the experimental output.

The output factor $C_G$ is the quotient of weight output of propellant injected $G$ and of the product $pA_c$ ($p$ = chamber pressure; $A_c$ = throat surface).

$$C_G = \frac{G}{pA_c}$$

The experimental output factor ($[C_G]_{exp}$) is determined from the mean total output and the chamber pressure, which is obtained by means of a measuring instrument, the response time of which is long as compared to the duration of phenomenon. The surface of the throat is measured prior to the test.

A second method of obtaining $[C_G]_{exp}$ is to integrate the instantaneous values of outputs and of chamber pressure. We have found that the value of $\eta$ decreases during low-frequency instabilities and the more so that the oscillation amplitudes are the greater. $\eta$ increases from 0.84 to 0.95 as we come from low-frequency instabilities of high amplitude to a stable combustion.

**Comparison of Theoretical and Experimental Results**

The co-ordination causes which characterize the low-frequency instabilities cannot be found in the study of acoustic phenomena of the combustion chamber, considered as a Helmholtz resonator, no more than in the study of impedance of the feed ducts and the injection orifices.

A decrease of impedance of these circuits leads to low-frequency instabilities, and in certain cases these perturbations can be eliminated by changing this impedance, through variation of the diameter and length of the propellant feed circuits or injection orifices. We have shown, however, that low-frequency instabilities can be started in the chamber alone, and we observed in such cases little perturbations of the flow of active bodies, as compared to the important chamber pressure oscillations observed (Fig. 5a). This shows that the combustion phenomenon has a preponderant part in the study of instabilities of this type. For this reason, we believe that the L. Crocco theory (4), though it does not explain everything, is still more plausible than that of Elias and Gordon, used by Ross and Datner (6), for explanation of the low-frequency instabilities phenomena.

We compare, in what follows, the results obtained with the Crocco theory, as against experimental results above described.

With regard to the characteristic length of the chamber, which is the first parameter considered by the experimental study, both theory and experimental results are in agreement. In both cases, frequency increases when characteristic length decreases.

For the two propellants considered—nitric acid-furfurylic alcohol and nitric acid-octane—experimental points are within the theoretical curves, with an interaction index $n = 2$ for the first propellant and $n = 0.3$ for the second propellant, under theoretical conditions nearing the experimental conditions (see Fig. 13).

Chamber pressure and injection overpressures appear in the theoretical study by their ratio. The parameters are defined as

$$P_0 = p/2\Delta p_0$$
$$P_H = p/2\Delta p_H$$

If the mean chamber pressure is known within an error of 2 per cent, it is not so for the injection overpressure. Computation of $P_0$ and $P_H$ from injection and chamber pressures introduces errors of over 10 per cent, mainly for low values of $\Delta p$. An exact comparison of theoretical and experimental variations of $P_0$ and $P_H$ can be obtained solely by a direct measure of injection overpressure. This comparison is further complicated by the fact that the theory provides for an interaction index $n$, low variations of critical frequencies $N$. For large variations of the parameters, computation is made from the theory of small variations of critical frequencies.

If we take, for instance, a propellant having an index of $n = 0.5$ and a characteristic length $L^* = 4$ m, the computed critical frequencies are of 24 and 26.5 $sec^{-1}$ when $P_0$ passes from $P_0 = P_H = 1$ to $P_0 = P_H = 5$. For a propellant having an index of $n = 2$, characteristic frequencies are of 54 $sec^{-1}$ and 50 $sec^{-1}$.

Thus, from the theoretical point of view, there is an inversion of the effects when one propellant is replaced by the other. From experimental results, the chamber pressure has a more important effect than injection overpressure. This is what generally happens, and we find the same result in all chambers of various design that we used. This observation leads to another law of evolution more influenced by pressure fluctuations. However, the variation given by the law of $\tau p^n = C$ is correct, since stability is improved by increasing the pressure, i.e., by decreasing the delay.

Theoretical study gives the same importance to chamber pressure as to injection overpressure; this is due to linearization of equations which assumes some small perturbations around a mean value.

Experimental study shows a greater importance of the chamber pressure as compared with injection overpressure.

Influence of the mixture ratio was determined experimentally by variation of the surface of fuel injection orifices, while injection overpressure was kept constant. Theoretical study (12) foresees a small influence of the mixture ratio, if temperature variations of the chamber due to variations in the mixture ratio are neglected. Experimental results also show the lack of importance of $m^*$ on frequency oscillations of the chamber pressure.

The nature of the propellant, theoretically, intervenes by the interaction index $n$. This index includes all the physical and chemical phenomena which occur between injection and combustion of the active bodies. Theoretical study (12) computes $n$ according to the various parameters which characterize the engine.

For a two-liquid system, the $n$ takes the shape of

$$n = \frac{1-\alpha}{2} + \frac{\omega^{*2}}{2} \cdot \frac{1-\beta^2}{1+\alpha}$$

where $\omega^*$ is the critical frequency reduced $= 2\pi N t_r$ ($t_r$ = time during which gas stays in chamber).

$$\alpha = \frac{P_H(1/2 - M)}{1 + \dfrac{P^2_H F^2_H (1/2 - M)^2 \omega^{*2}}{L^{*2}}} + \frac{P_0(1/2 - M)}{1 + \dfrac{P^2_0 F^2_0 (1/2 + M)^2 \omega^{*2}}{L^{*2}}}$$

and

$$\beta = \frac{P^2_H (1/2 - M)^2 (F_H/L^*)}{1 + \dfrac{P^2_H F^2_H (1/2 - M)^2 \omega^{*2}}{L^{*2}}} + \frac{P^2_0 (1/2 + M)^2 F_0/L^*}{1 + \dfrac{P^2_0 F^2_0 (1/2 + M)^2 \omega^{*2}}{L^{*2}}}$$

in these formulas:

$$F_H = \frac{A_c}{\Gamma(\gamma)} \Sigma_H \frac{l_H}{A_H}$$

$A_c$ = surface of nozzle throat
$\Gamma(\gamma)$ = function of ratio of specific heats
$l_H$ = length of fuel feeding ducts
$A_H$ = surface of ducts

$$F_0 = \frac{A_c}{\Gamma(\gamma)} \Sigma_0 \frac{l_0}{A_0}$$

$l_0$ = length of oxidizer lines
$A_0$ = surface of ducts

$M$ = ratio of mixtures

$$M = \frac{1}{2} \cdot \frac{1-m}{1+m}$$

It is therefore of interest to determine $n$ no longer from arbitrary variations, but from results obtained in tests. The theory then gives correlation formulas for all experimental results, and there remains only to determine for each test the frequency, the chamber pressure, the output factor, the injection overpressure, all the other factors being known according to the shape of the chamber and the size of connections.

The values of $n$ computed from experimental conditions are given in Fig. 24, and correspond to the nitric-acid furfurylic alcohol propellant. The $n$ value is practically constant when the length of the chamber is varied, and when the rectangular section chamber is replaced by a cylindrical one; so, it really defines a characteristic value of the propellant.

| | $L^*_m$ | $N$ | $\omega$ | $M$ | $P_o$ | $P_m$ | $J_o$ | $J_m$ | $n$ | $p$ Kg/cm² |
|---|---|---|---|---|---|---|---|---|---|---|
| Rectangular section chamber | 2,15 | 103 | 2,630 | 0,204 | 1,70 | 1,70 | 0,135 | 0,115 | 1,48 | 8,50 |
| Circular section | 2,10 | 69,5 | 1,812 | 0,239 | 3,27 | 2,60 | 2,88 | 0,807 | 1,39 | 8,20 |
| $L^*$ effect | 2,10 | 107 | 2,350 | 0,223 | 3,90 | 4,10 | 3,35 | 1,350 | 2,63 | 14,00 |
| | 2,35 | 97 | 2,418 | 0,229 | 3,60 | 3,72 | 2,79 | 1,068 | 2,37 | 14,30 |
| | 3,35 | 69 | 2,610 | 0,230 | 3,43 | 3,25 | 1,87 | 0,660 | 2,61 | 14,00 |
| Chamber pressure effect | 2,10 | 69,5 | 1,812 | 0,239 | 3,27 | 2,60 | 2,88 | 0,807 | 1,39 | 8,20 |
| | 2,10 | 73 | 1,811 | 0,212 | 3,35 | 3,20 | 2,84 | 1,100 | 1,39 | 9,50 |
| | 2,10 | 82 | 2,060 | 0,244 | 3,65 | 3,60 | 3,22 | 1,036 | 1,92 | 10,30 |
| | 2,10 | 84 | 2,038 | 0,243 | 3,68 | 3,63 | 3,25 | 1,116 | 1,93 | 10,80 |
| | 2,10 | 95 | 2,282 | 0,229 | 3,70 | 3,77 | 3,20 | 1,213 | 2,44 | 11,90 |
| | 2,10 | 96 | 2,231 | 0,220 | 3,80 | 4,20 | 3,25 | 1,392 | 2,34 | 12,70 |
| | 2,10 | 101 | 2,284 | 0,216 | 3,93 | 4,17 | 3,34 | 1,403 | 2,48 | 13,00 |
| | 2,10 | 107 | 2,350 | 0,223 | 3,90 | 4,10 | 3,35 | 1,350 | 2,63 | 14,00 |

**Fig. 24 Effects of the characteristic length and of the chamber pressure. Interaction index $n$, computed from experimental data**

Results are less conclusive for a variable chamber pressure, as the values of $n$ increase when the chamber pressure is increased.

## Conclusion

Although this study is based only on a first series of experimental results, our work brought out a certain number of important points, which we are summing up hereinafter.

Low-frequency instabilities are, for a given propellant, especially characteristical of low chamber pressures, and for low injection overpressures; all the other types of instability then appearing as secondary phenomena (Fig. 3a). For higher chamber pressures, the amplitude of oscillations decreases, and so they cannot be dissociated from other types of instabilities, which are then preponderant (Fig. 3c). The curves obtained no longer answer to a clear phenomenon, but to a superposition of several frequencies which may vary in the course of a test. In Fig. 3c, we find the low frequency $N = 147$ much weakened, and the further frequencies: $N = 670$ sec$^{-1}$, 1120 sec$^{-1}$, 4250 sec$^{-1}$, which depend rather on the acoustics of the chamber (the basic frequency of the chamber is: $N \simeq a^*/2L, \sim 2200$ sec$^{-1}$).

This study discloses the importance of three basic parameters: nature of propellant, characteristic length of chamber, mean pressure of the flame body; the other parameters—injection overpressure, mixture ratio, length and section of connections—are of a less important nature. In a general way, we may conclude that frequency increases with the chamber pressure, the injection pressure, and decreases with the characteristic length and mixture ratio.

We have demonstrated that the nature of the propellant is a determining factor in the study: under precise conditions, a propellant can be characterized by a frequency experimentally obtained; a quality index is then computed for low-frequency instabilities.

From these first tests, we may admit that experimental results are rather in confirmation of the theory developed by L. Crocco; i.e., as long as the chamber pressure remains constant, all other parameters of the engine can vary; but important divergencies appear as soon as this pressure is varied.

## References


1 "Thermodynamique des Systemes Propulsifs à Réaction et de la Turbine à Gaz," by M. Roy, Dunod, Paris, 1947, pp. 60 et seq.

2 "Stability of Flow in a Rocket Motor," by D. F. Gunder and D. R. Friant, *Journal of Applied Mechanics*, vol. 17, 1950, pp. 327–333.

3 "A Theory of Unstable Combustion in Liquid Propellant Rocket Motors," by M. Summerfield, *Journal of the American Rocket Society*, vol. 21, Sept. 1951, pp. 108–114.

4 "Aspects of Combustion in Liquid Propellant Rocket Motors," Parts 1 and 2, by L. Crocco, *Journal of the American Rocket Society*, vol. 21, Nov. 1951, pp. 163–178; vol. 22, Jan.–Feb. 1952 pp. 7–15.

5 "Combustion Instability in an Acid-Heptane Rocket with a Pressurized-Gas-Propellant Pumping System," by A. O. Tischler and D. R. Bellman, *NACA Rep.* 2936, May 1953.

6 "Combustion Instability in Liquid Propellant Rocket Motors," by C. C. Ross and P. P. Datner, AGARD, Cambridge, England, Dec. 7–11, 1953.

7 "Dynamic Pressure Measuring Systems for Jet Propulsion Research," by Y. T. Li, *Journal of the American Rocket Society*, vol. 23, May–June 1953, p. 124.

8 "Méthode de Mesure et d'Enregistrement Rapide des Températures des Flammes," by A. Moutet, *Recherche Aéronautique*, no. 27, pp. 21–31; no. 28, pp. 21–30.

9 "Determination des Temperatures de Combustion par Voie Optique," by A. Moutet, *Revue Optique*, vol. 33, no. 7, 1954, pp. 313–338.

10 "Debitmetre pour Propergols Liquides," by M. Barrère and A. Moutet, *Recherche Aéronautique*, March–April 1954.

11 "Etude des Délais d'Inflammation des Propergols Liquides," by M. Barrère and A. Moutet, Fifth Symposium on Combustion, Pittsburgh, 1954.

12 "Etude Théorique des Instabilités de Basse Fréquence dans les Moteurs Fusées," by M. Barrère and J. J. Bernard, *ONERA Publ.* 79.


### *Erratum*

Through a misunderstanding, the caption for the cover photo of the 25th Anniversary Issue (November) was incorrect. It should have read:

"Ramjet test vehicle with booster rocket launched at Naval Ordnance Test Station, Inyokern, Calif."

THE EDITORS

# Measurements of the Combustion Time Lag in a Liquid Bipropellant Rocket Motor[1]

LUIGI CROCCO,[2] JERRY GREY,[3] and GEORGE B. MATTHEWS[4]

Guggenheim Jet Propulsion Center, Princeton University, Princeton, N. J.

**Current theories concerning combustion instability in rocket motors involve the concept of a time delay between the instant of injection of a propellant element into the combustion chamber and its final evolution into hot gases. In order to apply these theories to actual design problems, it is first necessary to determine experimentally the time lag and several associated parameters for each class of propellants and chamber configurations. These measurements are now being made on a bipropellant chamber at Princeton as the second phase of a program whose ultimate objective is to provide the information necessary to direct the design or development of rocket engines toward suppression of high-frequency combustion instability. The introductory phase of this program, described in Ref. (2),[5] dealt with the development of an experimental technique and instrumentation capable of providing the necessary data.**

**The current paper presents some preliminary results of the second phase, in which these techniques have been used to determine the combustion chamber transfer function of a particular bipropellant configuration and the deduction therefrom of the time lag and related parameters. A brief recapitulation of the conceptual background is given, together with the methods used to obtain the desired measurements. Some of the limitations of these deduced results are discussed, and current methods for reducing the limitations are described.**

## Introduction

THE problem of combustion instability has been encountered in nearly every case of rocket motor development and has been attacked by many investigators with varying degrees of individual success. Although the blind cut-and-try methods of eliminating combustion instability have eventually proved effective in many cases, it is obviously much more economical and generally desirable to avoid or cure instability by some more rational procedure. The establishment of some analytical outline for the problem and its experimental verification is hence of major importance, since the existence of such a formulation would permit an engineer to make the best possible provisions in the design phase, or to take the most logical steps in development, to obtain stable rocket motor operation.

The experimental program described in part by this paper was set up primarily to establish the validity and limitations of theories outlined in this and earlier papers. Successful measurement of parameters which are of significant importance in the theoretical treatment was the first concern of this program. Preliminary results of the first series of these measurements are described in the ensuing discussion.

## Conceptual Background

The concept of the combustion time lag as a well-defined mathematical quantity which provides a close description of the actual combustion process in a rocket chamber has been dealt with in considerable detail in (1). The primary features of this concept were outlined for the simplest case of the monopropellant rocket in (2), and, for convenience, some of these features will be summarized briefly here.

As discussed in (2), the model which has been proposed to represent combustion in a liquid propellant rocket is characterized by an average combustion time lag $\bar{\tau}_T$, composed of an insensitive portion $\bar{\tau}_0$ and a sensitive portion $\bar{\tau}$. This formulation has been shown to be valid in the first approximation for small sinusoidal oscillations (1, 3, 4), provided the actual spread of time lags around the average value is not excessively large, and also that the transformation of each individual propellant element takes place in a sufficiently short time to allow its representation by a discontinuous transformation.[6] The concept of an average time lag upon which instability behavior depends not only permits application of theories based on a uniform time lag (5–9), but also provides a quantity which can be found experimentally by the technique of introducing small sinusoidal oscillations into the injection flow of propellants.

If the injection rates $\dot{m}_F$ and $\dot{m}_0$ of fuel and oxidizer, respectively, are assumed to undergo sinusoidal variations of angular frequency $\omega$ around their mean values $\bar{\dot{m}}_F$ and $\bar{\dot{m}}_0$, the fractional variations may be written in the conventional complex way:

$$\left.\begin{aligned} \frac{\dot{m}_F - \bar{\dot{m}}_F}{\bar{\dot{m}}_F} &= \mu_F = \tilde{\mu}_F e^{i\omega t} \\ \frac{\dot{m}_0 - \bar{\dot{m}}_0}{\bar{\dot{m}}_0} &= \mu_0 = \tilde{\mu}_0 e^{i(\omega t - \delta)} \end{aligned}\right\} \quad \ldots\ldots\ldots\ldots [1]$$

where for the purpose of generality, the phase lag $\delta$ has been introduced arbitrarily into the oxidizer flow rate.

The chamber pressure $P_c$ will thus oscillate around its mean value $\bar{P}_c$, and the fractional variation will be

$$\frac{P_c - \bar{P}_c}{\bar{P}_c} = \varphi = \tilde{\varphi} e^{i(\omega t - \beta_F)} \quad \ldots\ldots\ldots\ldots [2]$$

where the phase lag $\beta_F$ of chamber pressure behind fuel rate has been introduced.

The fundamental equation expressing the balance of mass within the combustion chamber can be written

$$\frac{dM_g}{dt} + \dot{m}_e = \dot{m}_i \quad \ldots\ldots\ldots\ldots [3]$$

where $M_g$ = mass of gas within the chamber

---

Presented at the ARS Semi-Annual Meeting, Boston, Mass., June 22, 1955.

[1] This investigation was sponsored by the Bureau of Aeronautics, U. S. Navy, Contract NOas 53-817-c, and has been performed under the direction of Dr. Luigi Crocco.

[2] Robert H. Goddard Professor, Dept. of Aeronautical Engineering. Mem. ARS.

[3] Assistant Professor.

[4] Research Assistant. Mem. ARS.

[5] Numbers in parentheses indicate References at end of paper.

[6] This latter assumption is common to several other types of more or less standard treatment in combustion theory.

$\dot{m}_e$ = rate at which gas is exhausted from the nozzle
$\dot{m}_b$ = rate at which hot gases are produced by burning

Introducing now the fractional variations in chamber pressure and propellant flow rates, the time lag model described above, and making the assumption that all burning takes place close to the injector face so that the residence time of all gas particles is the same, the mass balance equation becomes (3)

$$\theta_r \frac{d\varphi}{dt} + \varphi - n[\varphi - \varphi(t - \bar{\tau})] = -K[\mu_0(t - \bar{\tau}_T - \theta_r) - \mu_F(t - \bar{\tau}_T - \theta_r)] + 2K[\mu_0(t - \bar{\tau}_T) - \mu_F(t - \bar{\tau}_T)] + \left(\frac{1}{2} + H\right)\mu_0(t - \bar{\tau}_T) + \left(\frac{1}{2} - H\right)\mu_F(t - \bar{\tau}_T) \quad [4]$$

where

$\bar{\tau}_T$ = average total combustion time lag
$\bar{\tau}$ = average sensitive time lag
$\theta_r$ = modified gas residence time, including effects of phase lead angle introduced by isentropic nozzle impedance (2, 10, 11)
$n$ = interaction index between chamber pressure and sensitive time lag (3)
$H, K$ = mixture ratio parameters (3)

and the notation $\mu_0(t - \bar{\tau}_T)$ refers to the quantity $\mu_0$ evaluated at time $(t - \bar{\tau}_T)$; i.e., if combustion of an element is assumed to take place at time $t$, the propellant particles concerned were injected into the chamber $\bar{\tau}_T$ seconds earlier, or at time $(t - \bar{\tau}_T)$.

Before continuing with further discussion, it might be well to mention some of the limitations involved in Equation [4].

First, combustion has been assumed to take place at the injector face only for want of a more realistic model. If the actual pattern of heat release were known, Equation [4] would take another form, which can be computed from the completely general case treated in (1). (Experiments are about to be initiated at Princeton to determine this pattern empirically for use in subsequent tests.) The assumption of uniform time lag has also been made because of a lack of information concerning the actual time lag distribution. The effect of nonuniformity of the time lag has been introduced in (3) and computed in some detail in (1), and appears to entail only a second-order correction to the uniform time lag assumption.

A far more serious limitation on Equation [4] is that, although the effect of mixture ratio on chamber temperature and pressure variations has been taken into account, the time lag itself has been assumed to be insensitive to variations in mixture ratio. Since these variations produce entropy waves which can have a major effect on chamber conditions (and are, in fact, believed to be responsible for some of the observed cases of instability with characteristic frequencies intermediate between "chugging" and "screaming"), it is quite likely that they will also affect the time lag. The case of mixture ratio variations and their effects on the existing analysis is now being attacked analytically at Princeton, but since these effects are at present unknown, the problem will be by-passed on subsequent tests by maintaining constant instantaneous mixture ratio as will be discussed later in further detail.

Variations in mixture ratio also affect the value of exhaust nozzle impedance which is included in the characteristic time $\theta_r$, since this impedance was computed (11) on the basis of isentropic oscillations. Hence, an additional small error will be included in the present analysis due to the variations in mixture ratio, but this error will disappear when tests at constant mixture ratio are made.

In order to further improve the accuracy of the desired calculations, the high frequency analysis of (1) and (3) is now being extended to the lower frequencies used on the experimental tests. This will eliminate the necessity for the assumption (used in the derivation of Equation [4]) that the period of oscillation is sufficiently larger than the wave propagation time so that a change in pressure can be assumed to occur instantaneously throughout the chamber. Although this assumption is probably quite reasonable for the major portion of the range of modulating frequencies used, the more detailed analysis is expected to provide better precision on the calculated results, particularly at the higher values of modulating frequency where this assumption becomes less valid.

As a result of the limitations described above, the calculated results presented here must still be considered to be of a preliminary nature. However, it is most important to observe that the experimental data themselves are obviously *not affected* by any of these limitations on the method of analysis, and represent in themselves a piece of objective knowledge on the process of combustion, namely, the transfer function of the particular rocket configuration used.

Continuing now with the analytical discussion, if the fractional variations in chamber pressure and propellant flow rates are assumed to be sinusoidal as in Equations [1] and [2], the combustion chamber equation (Eq. 4) can be rewritten in the form suitable for analysis of experimental data. Thus

$$R_F e^{i\beta_F} \equiv \frac{\mu_F}{\varphi} = \frac{e^{i\omega\bar{\tau}_T}\left[i\omega\theta_r + 1 - n(1 - e^{-i\omega\bar{\tau}})\right]}{-Ke^{i\omega\theta_r}\left(\frac{\mu_0}{\mu_F} - 1\right) + \left(\frac{1}{2} + H + 2K\right)\frac{\mu_0}{\mu_F} + \left(\frac{1}{2} - H - 2K\right)} \quad [5]$$

which defines the amplitude $R_F$ and the phase angle $\beta_F$ of the ratio between fuel flow rate and chamber pressure variations. (Note that an equivalent equation may also be written for the oxidizer flow rate, and either of these may be used for the analysis. The selection of fuel flow in this case was purely arbitrary.)

The four unknowns appearing in Equation [5] are $\bar{\tau}_T$, $\theta_r$, $\bar{\tau}$, and $n$, all other quantities being obtained directly from experiment. Since Equation [5] is complex, there are actually two equations which may be used to determine the four unknowns by setting real and imaginary parts of both sides to be respectively equal. Two of the unknowns may be determined directly from these equations by noting that as the modulating frequency is increased, the product $\omega\theta_r$ in the numerator of Equation [5] becomes dominant, since $\theta_r$ is of the order of a few millisec and the index $n$ is likely to be of order unity (1, 2). For the higher modulating frequencies, then, the unknowns $n$ and $\bar{\tau}$ may be eliminated by the approximation that

$$(\omega\theta_r) \gg [1 - n(1 - e^{-i\omega\bar{\tau}})] \quad [6]$$

since the quantity in brackets is at most of order 1.0.

Performing this simplification and setting real and imaginary parts respectively equal as described, the following two equations are obtained for the remaining variables $\theta_r$ and $\bar{\tau}_T$:

$$\left(\frac{\omega\theta_r}{R_F}\right)^2 = (A^2 + B^2)(1 + M^2) + (1 + 2AM) + 2\{[A + M(A^2 + B^2)]\cos\omega\theta_r + B\sin\omega\theta_r\} \quad [7]$$

and

$$\omega\bar{\tau}_T = \beta_F - \tan^{-1}\left\{\frac{A\cos\omega\theta_r + B\sin\omega\theta_r + AM + 1}{B\cos\omega\theta_r - A\sin\omega\theta_r + BM}\right\} \quad [8]$$

where

$A, B, M$ = functions of mixture ratio
$R_F$ = ratio of amplitudes of oscillations of fuel mass flow rate and chamber pressure
$\beta_F$ = phase lead angle between fuel flow and chamber pressure

The unknowns $\theta_r$ and $\bar{\tau}_T$ calculated from Equations [7] and [8] are not the true values of these variables because of the condition of Equation [6], but approach the true values asymptotically at higher frequencies, where Equation [6] is more properly applicable. These asymptotic values may be considered to be the actual magnitudes of $\theta_r$ and $\bar{\tau}_T$, which are physical quantities independent of the frequency of oscillation. The remaining two unknowns, $n$ and $\bar{\tau}$, may be calculated at lower frequencies from the original equation by employing the established values of $\theta_r$ and $\bar{\tau}_T$. This determination will, of course, be more accurate at the lowest values of modulating frequency, where the terms containing $n$ and $\bar{\tau}$ become of magnitude comparable to $\omega\theta_r$.

In order to perform these calculations, a number of quantities must be determined directly from experimental measurements. The steady-state data required are: chamber pressure, oxygen and fuel injector pressures, oxygen and fuel mass flow rates, and thrust. These are employed in the calculations of steady-state mixture ratio, injector pressure drop, characteristic exhaust velocity, and chamber temperature, which determine directly the parameters $H$ and $K$. The transient measurements observed are: amplitudes of chamber and injector pressure oscillations, phase angles between injector pressure and chamber pressure for both propellants, and modulating frequency. The combination of steady-state and transient pressure data, together with calculated corrections for the small inertial phase lags in the injector (12), then determine the fractional oscillations $\mu_F$, $\mu_0$, and $\varphi$, the amplitude ratio $R_F$, and the fuel mass flow lead angle $\beta_F$. This total of six steady-state and six transient measurements is thus sufficient to establish all the parameters necessary for the calculation of the four unknowns.

## Apparatus

The equipment used to obtain experimental data consists basically of gas-pressurized propellant feed systems, a rocket motor, flow and pressure sensing elements, and data recording equipment. The propellants used were 95 per cent ethyl alcohol and liquid oxygen.

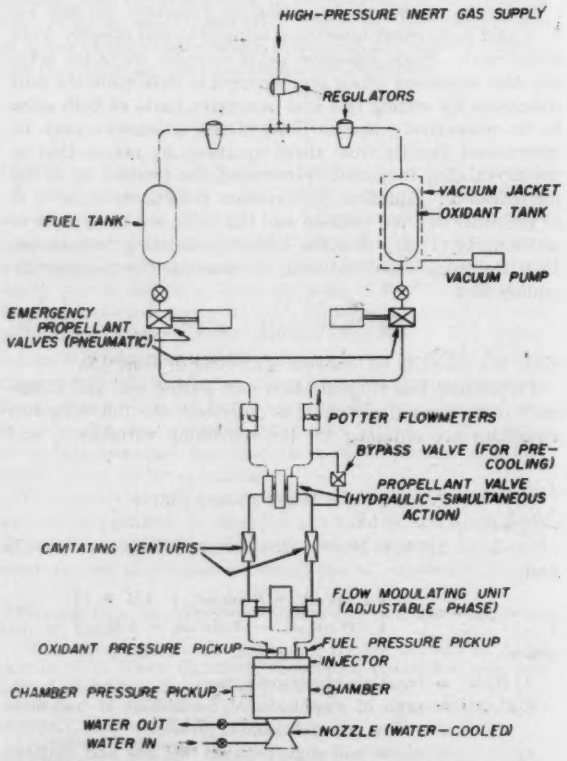


Fig. 1 Bipropellant rocket motor propellant feed system

In the feed system (Fig. 1) inert gas is used to pressurize the propellant tanks, forcing the alcohol and oxygen through flowmeters, cavitating venturis, a flow modulating unit, and into the rocket motor injectors. Fig. 2 is a photograph of the installation, showing the test stand, rocket motor, and flow modulating unit. The motor itself (Fig. 3) is of uncooled copper with a water-cooled nozzle, and uses a ring of 12 pairs of one-on-one impinging jet injector orifices with an impingement distance of zero from the injector face. $L^*$ is approximately 47 inches and the inner chamber diameter is 3 inches. The injector pressure drop is approximately 100 psi in both feed lines, and a nominal chamber pressure of 300 psia was used to obtain the results reported herein. Ignition is accomplished by a solid propellant powder squib.

The flow modulating unit (Fig. 4) is a straightforward crank-piston arrangement with 0.20-in. stroke and two pistons, one for each propellant line. The split shaft is so arranged that the phase angle between the two propellant flow rate oscillations at the injector can be adjusted to zero by rotating the two halves of the flywheel to any desired relative position. (This feature was not used on the first test series, since no foreknowledge of the expected phase difference was available. Settings for subsequent tests can now be made, however, using the phase differences observed on this test series.) Amplitudes of the oscillations can be changed by using interchangeable piston-cylinder assemblies of different cross-section areas. The data presented here were taken with piston diameters of 0.240 inches in the oxygen line and 0.195 inches in the fuel line. The unit is driven by a U. S. Motors 5 hp Varidrive at speeds from 50 to 215 revolutions per second.

The cavitating venturis serve to maintain constant mean propellant flow rates and also to damp out the upstream-traveling disturbances from the flow modulating unit. (Care is taken on all tests to insure that the operating ranges of the venturis are never exceeded, even by the peak pressures of oscillation.) The mean propellant flow rates are measured by Potter turbine-type flowmeters.

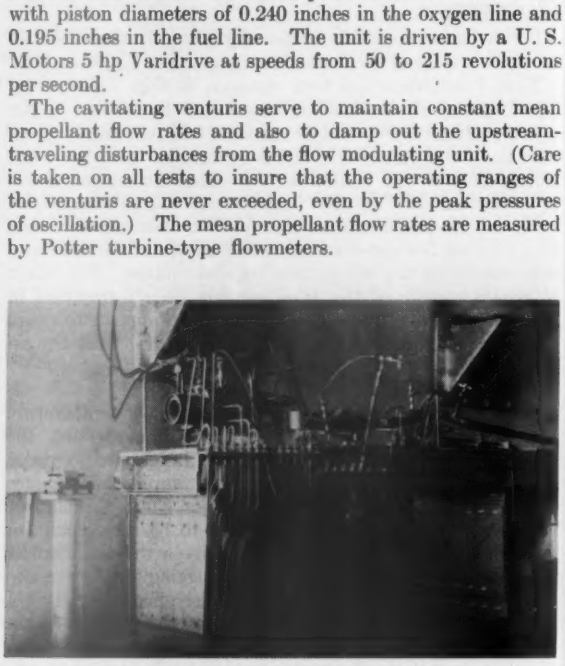

Fig. 2 Thrust stand showing flow modulating unit

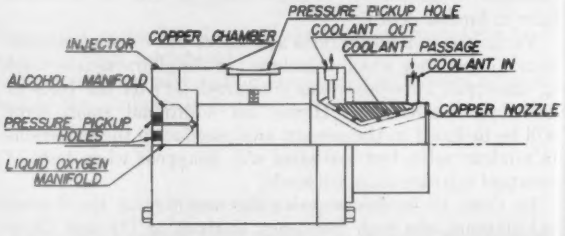


Fig. 3 Bipropellant rocket motor no. 1 (liquid oxygen-alcohol)

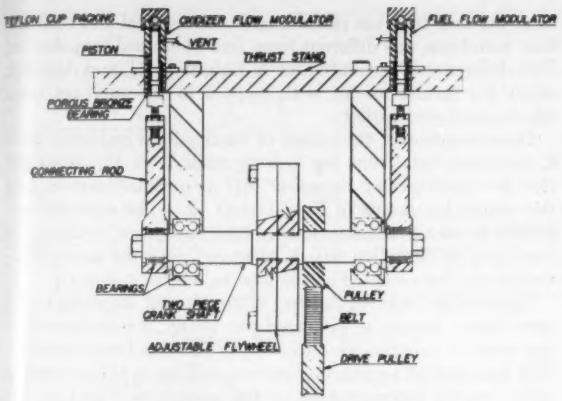


**Fig. 4 Bipropellant flow modulating unit**

Three Li-Liu pressure pickups [described in (13) and (14)] are flush mounted in the chamber and in the two injector manifolds (see Fig. 3). These pickups are used with a reference pressure behind the diaphragms to balance the chamber pressure, so that very sensitive strain tubes may be used regardless of the magnitude of the mean chamber pressure. Only the chamber pickup is supplied with cooling water. The signals from the pickups are recorded simultaneously on recording potentiometers, which provide the mean values of the indicated pressures, and on a 4-channel Ampex magnetic tape recorder, which provides the transient components of the pressures. The complete instrumentation system is diagrammed in Fig. 5, and has been described in detail in (15). Primary features of the transient playback system include a twenty-to-one playback speed reduction on the tape recorder, permitting excellent resolution of the data, a four-channel RC low-pass filter of zero relative phase shift to remove combustion noise from the modulated traces, and a calibrated phase-shift network which permits determination of the phase difference between two pressure signals by nulling their Lissajous pattern on an oscilloscope. Typical transient records are shown in Fig. 6 (unfiltered), Fig. 7 (filtered), and Fig. 8 (method of phase determination).

Data required for determination of the necessary parameters include mean propellant flow rates (obtained from the Potter flowmeters), mean values of injector and chamber pressures (obtained either from potentiometer recordings or, as discussed below, from sequenced pressure-gage photographs), amplitudes of oscillation of injector and chamber pressures (obtained from filtering the taped data and observing the resulting sinusoidal amplitudes on a vacuum-tube voltmeter), and phase differences between the injector and chamber pressures (obtained from the calibrated phase-shift circuit). This method of analysis eliminates the tedious job of manual data reduction of oscillograph records, and, in fact, no oscillograph records are required.

The validity of all steady-state data components was checked by correlating the various parameters with each other; i.e., by plotting thrust vs. mean chamber pressure, mean propellant flow rates vs. mean pressure drops, and total mean propellant flow rate vs. mean chamber pressure. These plots represent thrust coefficient, orifice coefficients, and characteristic velocity, and were used as the criteria for determining the suitability of a particular test run for analysis. If the steady-state data from a given test did not correlate on these plots, the test was discarded. Fig. 9, which is typical of these correlation curves, shows the thrust coefficient computed from 36 separate tests, and includes approximately 70 data points.

Operation of the instrumentation was satisfactory in all respects but one. Some unpredictable zero drift of the Li-Liu pickups in the uncooled motor was observed on several runs, and hence mean values of the three required pressures were taken from sequenced photographs of Heise bourdon-tube gages. In order to check the effect of temperature on the transient pick-up records (which are determined by pick-up sensitivity alone), calibrations of pick-up sensitivity were made during hot runs by introducing different known levels of reference pressure onto the back of the sensing diaphragms Only negligible variations in sensitivity were observed, and hence it was concluded that the effect of temperature was felt only as a zero shift. Subsequent efforts to correct this temperature effect by modification of the pickup have since been successful.

## Discussion of Results

The primary experimental measurements used to determine $\theta_r$ and $\bar{\tau}_T$ from Equation [5] (under the assumption of Equation [6]) are the amplitudes and phase angles of the ratios $\mu_F/\varphi$ and $\mu_0/\varphi$; i.e., the ratios of fractional fuel and oxidizer

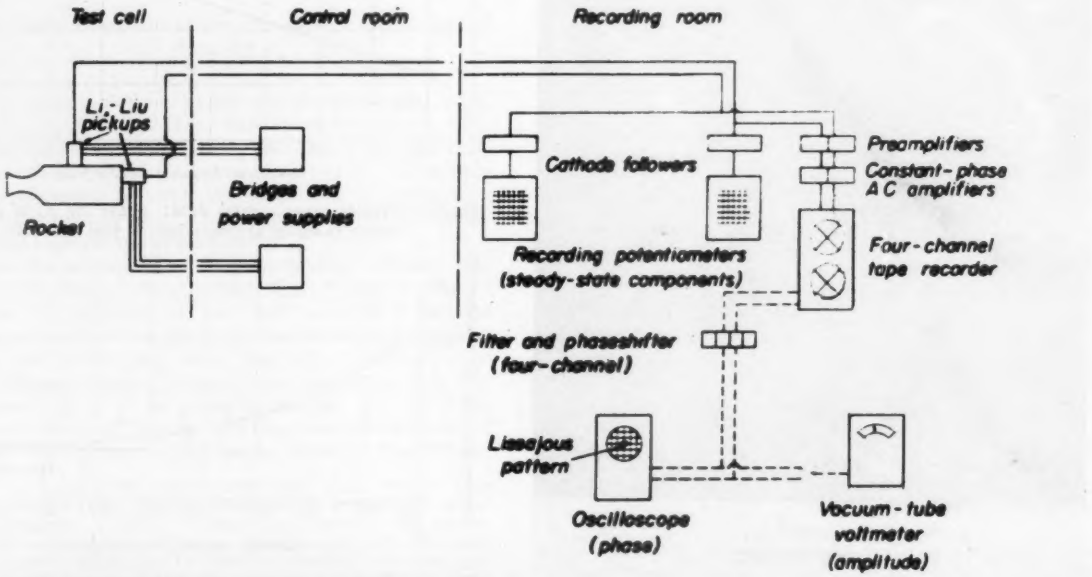


**Fig. 5 Time-lag instrumentation diagram**

flow rate oscillations, respectively, to the fractional chamber pressure oscillation. As mentioned earlier, these ratios are obtained from measurement of the steady-state components of injector and chamber pressures, their amplitudes of oscillation, and the phase differences between them. (The flow rate oscillations are obtained from pressure-drop oscillations by the method of (12), which accounts for inertial effects in the injector passages.)

Fig. 10 shows the phase lead angle $\beta_F$ of the fractional oscillation $\mu_F$ in fuel flow ahead of that of the chamber pressure $\varphi$. Some of the scatter indicated by this figure results

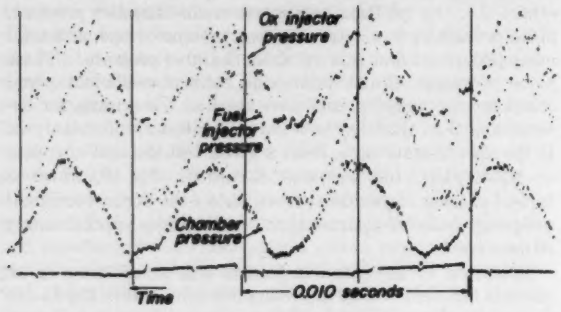


Fig. 6 Typical "raw" data

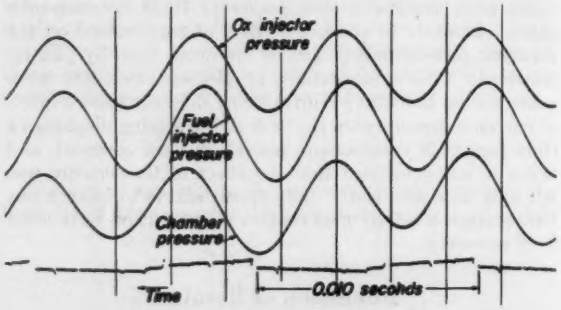


Fig. 7 Data of Fig. 6 after filtering

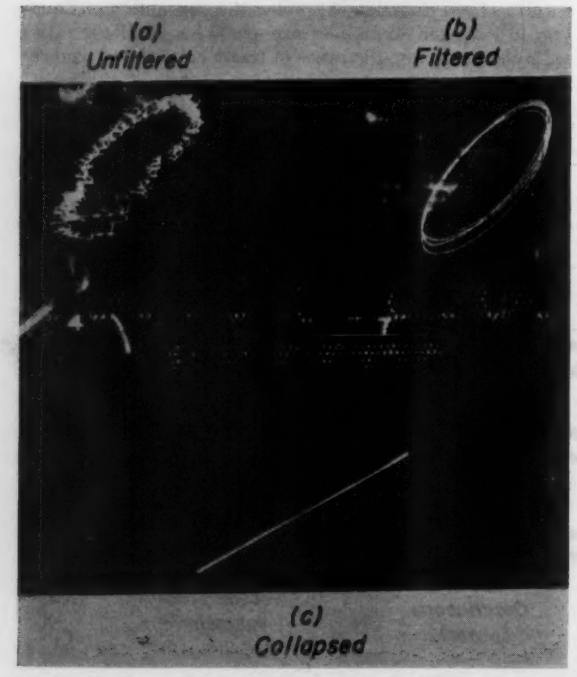


Fig. 8 Method of measuring phase using a Lissajous pattern

from the fact that the phase angle between fuel and oxidizer flow variations was different from zero at several frequencies. This difference is accounted for in Equation [5], and does not affect the results except with respect to the mixture ratio effect mentioned earlier.

Determination of the values of modified gas residence time $\theta_r$ and mean total time lag $\bar{\tau}_T$ were made from Equation [5] (for the condition of Equation [6]) as outlined earlier, and the results are shown in Figs. 11 and 12. The expected approach to an asymptotic value in each case (as a result of the condition of Equation [6]) is observed, and the asymptotic values may be accepted as the true values for $\theta_r$ and $\bar{\tau}_T$.

The results of these figures, although still somewhat of a preliminary nature as discussed previously, are indicative of the order of experimental accuracy which has been obtained. The true test of accuracy, however, will be in the somewhat more refined determination of the quantities $\bar{\tau}$ and $n$, the

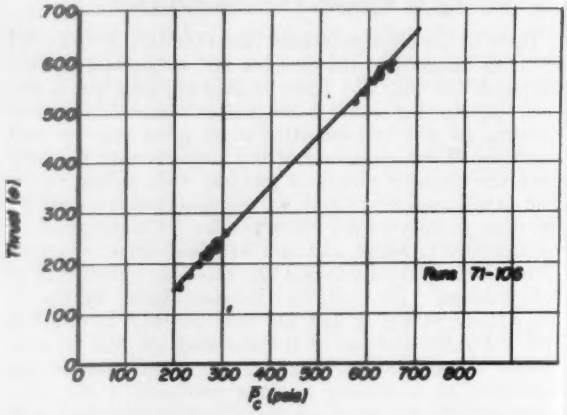


Fig. 9 Steady-state data correlation: bipropellant rocket motor thrust coefficient

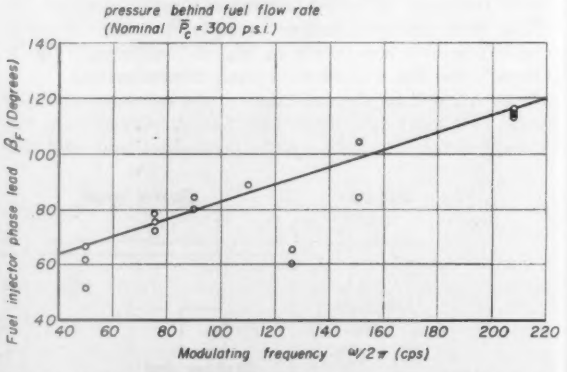


Fig. 10 Typical experimental data: phase lag $\beta_F$ of instantaneous chamber pressure behind fuel flow rate

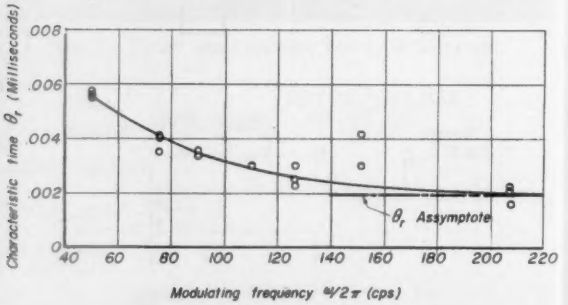


Fig. 11 Modified characteristic gas residence time $\theta_r$ for bipropellant rocket motor no. 1

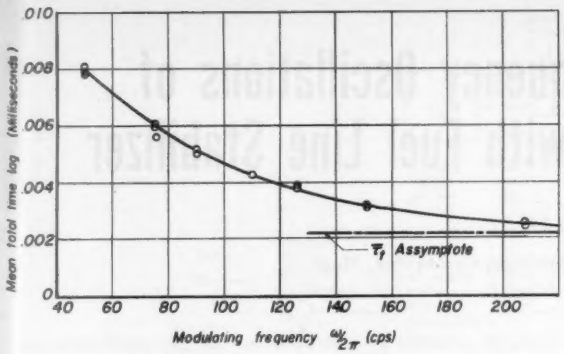


Fig. 12 Mean total time lag $\bar{\tau}_T$ for bipropellant rocket motor no. 1

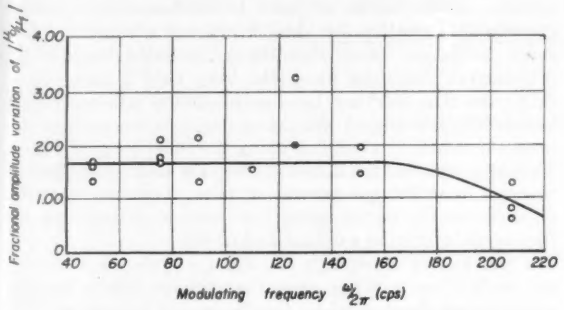


Fig. 13 Amplitude ratio $|\mu_0/\mu_F|$ of fractional variations in oxygen and fuel flow rates

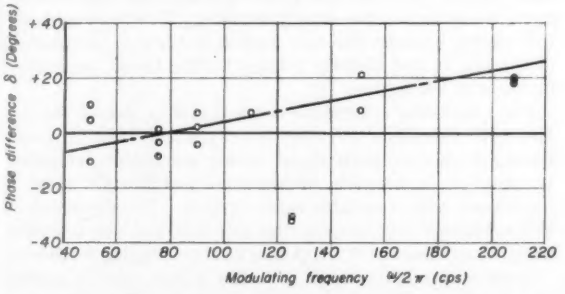


Fig. 14 Phase difference $\delta$ between variations in oxygen and fuel flow rates

sensitive portion of the time lag and the interaction index, respectively. Although these two quantities can be computed from the existing data by the use of Equation [5] (with the now determined values of $\bar{\tau}_T$ and $\theta_r$), it has been deemed preferable to await the attainment of constant instantaneous mixture ratio, which represents the most severe limitation imposed by the analysis.

Some idea of the control of instantaneous mixture ratio which will be required is indicated in Figs. 13 and 14. Fig. 13 presents the amplitude of fractional variation in mixture ratio as a function of frequency for the one set of modulating pistons used on this test series,[7] and Fig. 14 illustrates the phase difference observed between fuel and oxidizer flow rate variations. In order to preserve constant mixture ratio, the amplitude should be unity and the phase difference should be zero. On the basis of the results shown in Figs. 13 and 14, the proper piston diameters and flow modulating unit phase settings have been selected. These values, together with measurements of the combustion pattern which are now being initiated, are expected to eliminate the major limitations imposed by the analysis, and hence to provide more precise determination of the required parameters.

[7] In the absence of quantitative data, these pistons were selected on the basis of total displacement, assuming a "volumetric efficiency" of unity. It was found, however, that cavitation, line capacitance, and other effects apparently decreased the "volumetric efficiency" by different amounts in the two propellant lines, thus producing an amplitude as well as a phase variation in instantaneous mixture ratio.

## Conclusions

Experimental determination of the transfer function of a particular bipropellant rocket chamber configuration has been made with satisfactory accuracy by introducing small sinusoidal oscillations into the flow rates of the propellants. These measurements have been used to determine the combustion time lag and associated parameters. The primary limitation in interpretation of the experimental data is the observed variation in instantaneous mixture ratio. Secondary limitations in deducing the time lag parameters are a lack of knowledge of the exact pattern of heat release in the chamber, and the use of a simplified low-frequency analysis which might introduce some error at the higher flow modulating frequencies.

Forthcoming tests to be made at constant mixture ratio (and at several chamber pressure levels) are expected to provide a substantial improvement in accuracy of deduction of the time lag and associated parameters from experimental data, particularly since the pattern of heat release will also be measured. Further improvement in accuracy of the calculations will be provided by extension of the more general high-frequency analysis of (1) to the ranges of modulating frequency used on these tests.

## References

1 Crocco, L., and Cheng, S. I., "Combustion Instability in Liquid Rockets," Monograph prepared by AGARD, now in process of publication by Buttersworth, Ltd., London, England.

2 Crocco, L., Grey, J., and Matthews, G. B., "Preliminary Measurements of the Combustion Time Lag in a Monopropellant Rocket Motor," Fifth International Symposium on Combustion, September 1954.

3 Crocco, L., "Aspects of Combustion Instability in Liquid Propellant Rocket Systems," *Journal of the American Rocket Society*, vol. 21, 1951, p. 163.

4 Cheng, S. I., "Combustion Instability in Liquid Propellant Rocket Motors," Princeton University Aeronautical Engineering Report 216f, Appendix A (1953).

5 Gunder, D. F., and Friant, D. R., "Stability of Flow in a Rocket Motor," *Journal of Applied Mechanics*, vol. 17, 1950, p. 327.

6 Yachter, M., Discussion of the Paper of Reference 5, *Journal of Applied Mechanics*, vol. 18, 1951, p. 114.

7 Summerfield, M., "A Theory of Unstable Combustion in Liquid Propellant Rocket Systems," *Journal of the American Rocket Society*, vol. 21, 1951, p. 108.

8 Tsien, H. S., "Servo-Stabilization of Combustion in Rocket Motors," *Journal of the American Rocket Society*, vol. 22, 1952, p. 256.

9 Marble, F. E., and Cox, D. W., "Servo-Stabilization of Low-Frequency Oscillations in a Liquid Bipropellant Rocket Motor," *Journal of the American Rocket Society*, vol. 23, 1953, p. 63.

10 Tsien, H. S., "The Transfer Functions of Rocket Nozzles," *Journal of the American Rocket Society*, vol. 22, 1952, p. 139.

11 Crocco, L., "Supercritical Gaseous Discharge with High-Frequency Oscillations," *Aerotecnica*, vol. 33, 1953, p. 46.

12 Matthews, G. B., "Combustion Instability in Liquid Propellant Rocket Motors," Princeton University Aeronautical Engineering Report 216-j, Appendix A (1954).

13 Li, Y. T., "Dynamic Pressure Measuring System for Jet Propulsion Research," *Journal of the American Rocket Society*, vol. 23, 1953, p. 124.

14 Matthews G. B., "Combustion Instability in Liquid-Propellant Rocket Motors," Princeton University Aeronautical Engineering Report 216-f, Appendix C (1953).

15 Jones, H. B., "Combustion Instability in Liquid Propellant Rocket Motors," Princeton University Aeronautical Engineering Report 216-k, Appendix B (1955).

# Stabilization of Low-Frequency Oscillations of Liquid Propellant Rockets with Fuel Line Stabilizer

Y. T. LI[1]

Massachusetts Institute of Technology, Cambridge, Mass.

**Chugging oscillations of a liquid propellant rocket may be explained by using a feedback system principle in which the dynamic characteristics of the fuel supply system play an important role. Suitable modification of the fuel-supply system performance can stabilize the chugging action. In the chugging-frequency range, this dynamic performance approaches those of a first-order system. The use of a high injector restriction factor can give a stabilization effect equivalent to that of a lead-lag network used in a servo system, but it is undesirable because of the large supply pressure required. Two basic types of stabilizer that can modify the dynamic characteristics of the fuel supply system sufficiently to give a stabilization effect without the need of high supply pressure are introduced. The various dynamic and static characteristics of these stabilizers are analyzed. The design problems are also discussed.**

## Nomenclature

$A_i$ = effective area of injector restriction
$A_s$ = effective area of stabilizer valve opening
$C$ = discharge coefficient
$D$ = $d/dt$
$f_f$ = forcing frequency of supply line
$f_n$ = natural frequency
$F$ = flow rate
$FR$ = frequency response function
$g$ = gravitational constant
$k$ = spring constant of valve suspension system
$l$ = effective length of liquid column in valve
$L$ = effective length of fuel supply line
$n$ = stabilizer sensitivity index = $S_i S_s \omega_n$
$P_c$ = combustion chamber pressure
$P_d$ = pressure difference
$\Delta P_d$ = incremental pressure difference
$P_{d_o}$ = operating point pressure difference
$P_s$ = supply source pressure
$PF$ = performance function
$R$ = restriction factor = $dP/dF$
$S$ = flow sensitivity = $dF/dP$
$\tau_l$ = time constant of flow supply system with injector only
$V_s$ = velocity of sound
$\omega$ = angular frequency of oscillation of rocket
$\omega_c$ = angular frequency at chugging condition
$\omega_n$ = natural frequency of valve system
$\zeta$ = damping ratio of valve system
$\rho$ = density of liquid

## Introduction

UNSTABLE combustion oscillations of liquid propellant are generally considered as the result of the coupling behavior of the fuel supply system, the time delay of the combustion process, and the acoustic properties of the chamber (1, 2, 3).[2] The nature of the coupling effect of a longitudinal mode of oscillation can be explained with the use of a simplified block diagram as shown in Fig. 1. In this diagram the chamber pressure is controlled by the gas generation rate, which is controlled by the fuel supply rate which is, in turn, controlled by the pressure difference across the fuel supply system. Three blocks are used to represent the dynamic performances relating the various physical quantities. Unstable oscillation occurs when the accumulated delays of the performance functions along the loop yield a total phase shift more than 360° and have an amplitude ratio more than unity. High-frequency oscillation usually occurs when this unstable criterion is fulfilled along the inner loop of Fig. 1. This loop includes the dashed line which shows the effect of pressure upon the gas generation rate. Low-frequency oscillation usually occurs along the outer loop including the fuel supply system as a dominating factor.

A well-known concept for stabilizing a system is to modify the performance function along the unstable loop so that the accumulated phase shift and amplitude ratio for any realizing frequency would never be larger than 360° and unity, respectively. For the low-frequency oscillation of a rocket the most logical place to apply the performance modification seems to be in the fuel supply system. This is because the fuel supply system dynamic performance is a dominating factor and is not directly related to the thrust generation function of the engine.

One interesting scheme for doing this is to control the fuel flow with a suitable servo system (9), which is in turn controlled by the pressure signal in the combustion chamber. In principle a desirable performance modification may be introduced with a suitable servo system. The drawback to this scheme is the complication involved and the unavailability of an ideal servo to operate at the chugging frequency.

Another possible scheme is to use a high injector restriction together with a high supply pressure. One purpose in using high supply pressure is to atomize the injected fuel and thereby reduce the combustion time delay. But with a proper injector and above a certain minimum pressure required for atomization, an increase of the supply pressure tends to make the system approach a constant flow-rate source and less affected by chamber pressure variation. This method has been found to give effective results in test-stand operation. But for airborne devices, the use of high supply-line pressure means more weight and lower reliability and, therefore, is not desirable.

## Dynamic Performance of the Fuel Supply System

For a small operating range, the static performance or the sensitivity of a fuel supply system is defined as the incremental change of the flow rate divided by the incremental change of pressure difference. In a practical fuel supply system, the dynamic performance is different from the static performance because of the mass of the liquid involved. This is further complicated by the compressibility of the liquid, the deformability of the supply line, and the coupling effect between the fuel supply line and the supply pressure source.

An incompressible fuel supply system, considering the acceleration effect only, is basically a first order system. The polar diagram of the frequency response of this simplified

Presented at the ARS Semi-Annual Meeting, Boston, Mass., June 23, 1955.

[1] Associate Professor, Aeronautical Engineering Department.

[2] Numbers in parentheses indicate References at end of paper.

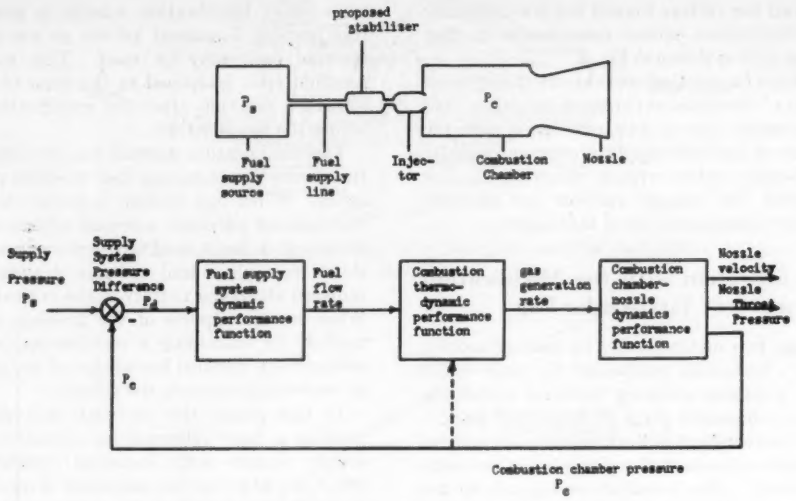


**Fig. 1. Schematic diagram and block diagram for a liquid rocket**

fuel supply system is shown in Fig. 2. In equation form we have

$$(PF)_{FL} = \frac{S_{i_o}}{1 + \tau_i D} \quad \ldots\ldots [1]$$

where

$\tau_i$ = first-order system time constant of fuel supply line with injector

$$= \frac{1}{2} A_i C_i \frac{1}{\sqrt{P_{d_o}}} \frac{L\rho}{g} \quad \ldots\ldots [2]$$

$$= S_i \frac{L\rho}{g} \quad \ldots\ldots [3]$$

$$S_i = \frac{1}{R_i} = \frac{dF}{dP_d} = \frac{1}{2} A_i C_i \frac{1}{\sqrt{P_d}} = \frac{1}{2} \frac{F}{P_d} \quad \ldots\ldots [4]$$

$$S_{i_o} = \frac{1}{2} \frac{F_o}{P_{d_o}} \quad \ldots\ldots [5]$$

where

$S_i$ = flow sensitivity of injector
$R_i$ = flow restriction factor of injector
$S_{i_o}, F_o, P_{d_o} = S_i, F, P_d$, respectively, at a particular operating point
$F$ = volumetric flow rate
$A_i$ = injector area
$C_i$ = injector discharge coefficient
$P_d$ = pressure difference
$L$ = length of supply line
$\rho$ = density of fuel
$g$ = gravitational constant

When the fluid is compressible and the container is deformable, then the performance function becomes a problem of wave propagation. The detail analysis of this performance function is omitted from this paper because of space limitation. A part of the analysis can be represented, however, by the polar diagram as shown in Fig. 3. The frequency response shown in this plot exhibits a circular pattern, with the pressure vector as a diameter. The shape of this curve is independent of the value of the injector restriction factor. Similarly, the frequencies at each end of the pressure vector are fixed values, independent of the injector restriction characteristics. The change in injector characteristics only affects the distribution of the velocity vectors for different frequencies along the circle. A larger pressure drop in the

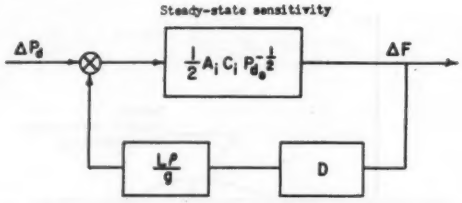


2(a) Block diagram representing the linearized flow characteristics of a rigid fuel supply line at the operating pressure difference $P_{do}$.

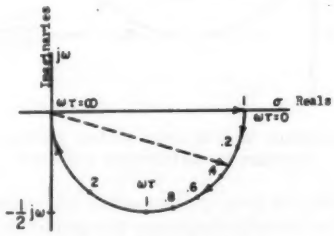


2(b) Performance function and polar diagram for the frequency response function of a rigid fuel supply line.

**Fig. 2 Dynamic properties of a rigid fuel supply line**

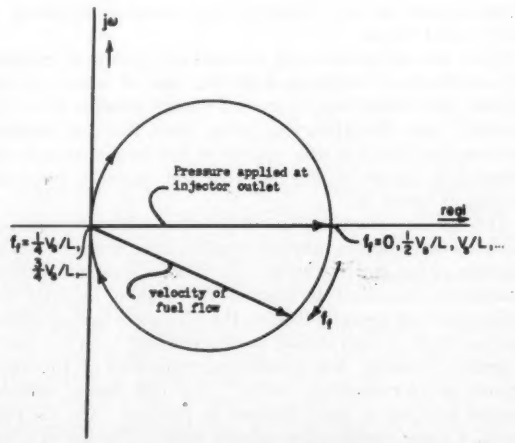


**Fig. 3 Frequency response of a fuel supply system with compressible effect taken into consideration**

injector tends to crowd the vectors toward the low-frequency end and make the distribution pattern more similar to that of a first-order system such as shown in Fig. 2.

When the supply line of a practical rocket is short compared with the wave length of the liquid at chugging frequency, and when the injector pressure drop is relatively large, then the dynamic performance of the fuel supply system can usually be treated as a first-order system without much error. For this reason, first-order fuel supply systems are assumed throughout the rocket system analysis of this paper.

## Stabilization of a System with the Modification of an Important First-Order Lag

Generally speaking, two methods may be used to modify the performance of a first-order component to improve the stability quality of a simple series-lag feedback system in which the first-order component plays an important part.

1. Decrease the time constant of the first-order component so that, at the unstable frequency, the phase lag in the component is much reduced. The situation corresponds to the shift of the operating point at the unstable frequency from "a" to "b" of Fig. 4.

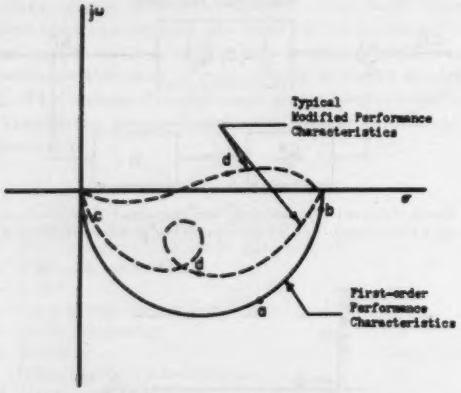


Fig. 4 Modification of first-order system performance characteristics for stabilization purposes

2. Increase the time constant of the first-order component so that at the unstable frequency the amplitude ratio in the component is greatly reduced. This is necessarily accompanied by an undesirable increasing phase lag. Since the lag is limited to 90 degrees and the amplitude reduction goes down rapidly, however, stabilization is possible when the time constant is sufficiently increased. Graphically, this situation is represented by the change of the unstable frequency to point "c" of Fig. 4.

When the performance of a first-order system is modified for stabilization purposes with the use of some suitable scheme, the desired results are not always possible to obtain. Instead, some distortion may occur such that the modified performance function may appear in the form shown by the dotted-line curves of Fig. 4, with the unstable frequency located at point "d."

The stability characteristic of a system with a complicated modified performance function depends upon the performance function of the entire system. To make a complete stability evaluation, standard techniques for system analysis that utilize the root locus method or the Nyquist diagram method for the entire system should be of great help. In the case of a rocket, however, the performance function of the entire system is not completely known. For this reason, complete system analysis is quite difficult to perform. On the other hand, if some modification scheme such as the use of a high injector restriction factor is known to have satisfactory effects, it may be used as a reference for comparison to show whether some other modification scheme is also satisfactory. For this purpose a concept known as the *modified performance function ratio* may be used. This modified performance function ratio is defined as the ratio of the component performance function after the modification, divided by that before the modification.

Two modification schemes may be compared for their relative merits by comparing their modified performance function ratios. When one scheme is known to be satisfactory for stabilization purposes, a second scheme should also be satisfactory if it has a modified performance function ratio that shows more phase lead and gain reduction over a wide range centered about the vicinity of the critical unstable frequency. When certain aspects of the problem are understood, this method for examining a stabilization scheme can be made without any detailed knowledge of the performance function of other components in the system.

In this paper, the modified performance function ratio used as a basic reference for comparison is that of a fuel supply system with increased restriction. The physical effect of a large injector restriction is equivalent to a reduction in the flow sensitivity and a reduction in the time constant of the first-order system, as shown by Equations [5] and [2]. The polar frequency response of a system with a doubled restriction is shown by the heavy solid-line curve of Fig. 5.

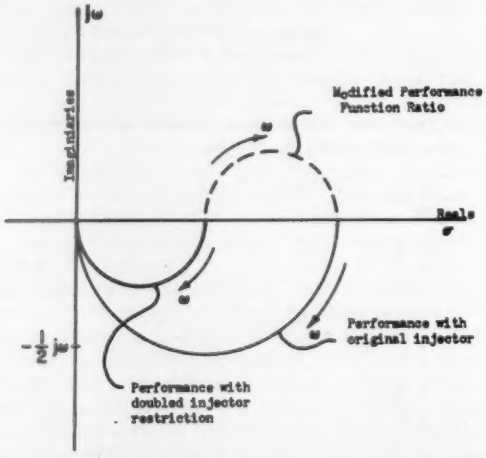


Fig. 5 Modified performance function ratio of a first-order system with doubled injector restriction

The same system with the original restriction is shown by the light solid-line curve, and the corresponding modified performance function ratio is shown by the dashed-line curve.

When the performance function of a component is modified into a new performance function, it is equivalent to the use of an additional component placed in series with the original system and having a performance equal to the modified performance function ratio. For a rocket, the effect of an increased injector restriction as shown in Fig. 5 is equivalent to the use of a lead-lag network in servo systems for stability control, which is a well-known technique.

The shortcoming of the method just described is that it is only qualitative. Also, no conclusion can be made when comparing the modified performance function ratio of one scheme that shows more phase lead with another that shows more gain reduction. Despite this limitation, the concept of the modified performance function ratio serves well in the evaluation of the various schemes discussed in this paper.

## Principle of a Flow Rate Actuated-Type Stabilizer

Generally speaking, a fuel line stabilizer is a device which provides the fuel supply system with a suitable restriction

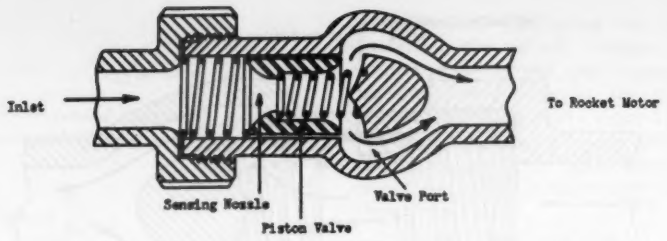


Fig. 6 Typical construction of a flow rate actuated fuel line stabilizer

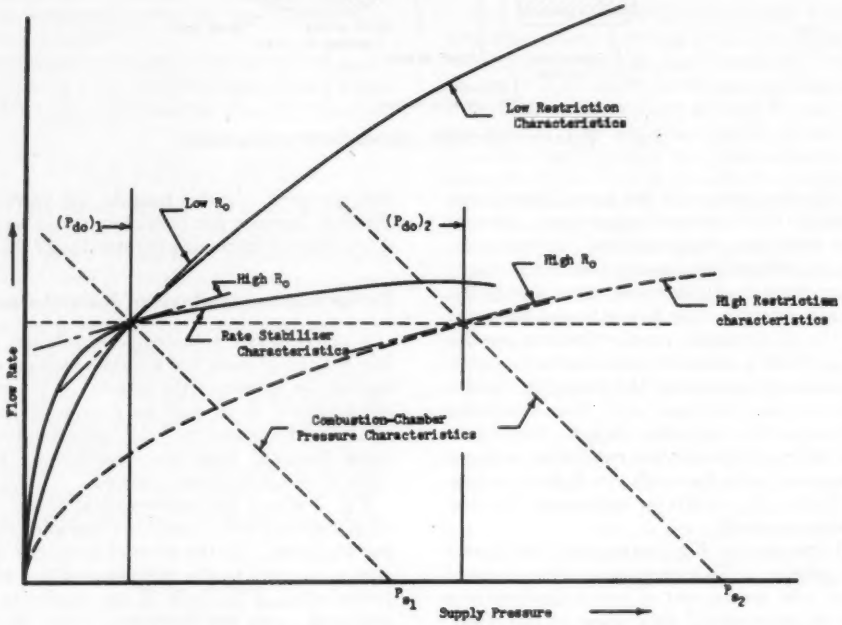


Fig. 7 Pressure flow rate characteristics of injector and rate stabilizer

factor with no need of high supply pressure for a given flow rate. Fig. 6 shows the basic form of a flow rate actuated stabilizer. The arrangement shown in Fig. 8 incorporates further modification to make it frequency dependent. The construction of the stabilizer shown in Fig. 6 uses a spring-loaded piston valve placed immediately ahead of the injector. A flow-rate sensing nozzle is carried by the piston and controlled by the flow rate itself. In operation, the pressure drop of fuel flow through the nozzle would produce a force that would tend to move the piston valve and close the valve port. Under normal operating conditions, the valve of the stabilizer would have a restriction with a characteristic somewhat different from that of a fixed restriction.

The flow discharge characteristics of this type of rate stabilizer valve may be expressed as

$$F = A_v C_v \sqrt{P_d} = \left( A_{v_0} - \frac{FW}{k_v} R_v \right) C_v \sqrt{P_d} \quad \ldots\ldots [6]$$

where

$A_v$ = valve opening area
$C_v$ = valve discharge coefficient
$W$ = port width
$k_v$ = spring constant of valve
$R_v$ = restriction coefficient of valve nozzle
$F$ = force/flow rate

By definition, the flow restriction factor and the flow sensitivity of the stabilizer at an operating point is

$$\frac{1}{R_{s_0}} = S_{s_0} = \left( \frac{dF}{dP} \right)_o = \frac{1}{2} \frac{F_o}{P_{d_0}(1 + \sqrt{P_{d_0}} S_v)} \quad \ldots\ldots [7]$$

where

$S_s$ = stabilizer sensitivity
$S_v$ = valve port sensitivity

$$S_v = \frac{W_v R_v}{k_v} C_v \quad \ldots\ldots [8]$$

when

$$P_{d_0}^{-1/2} S_v > 1$$

$$R_{s_0} = 2 \frac{P_{d_0}^{3/2}}{F_o} S_v \quad \ldots\ldots [9]$$

Equation [9] shows that the stabilizer restriction factor is a function of the valve-port sensitivity. For a given flow rate, a large restriction factor required for stabilization can be obtained by increasing the valve-port sensitivity, $S_v$, without the need of a large value of the pressure difference $P_{d_0}$, at the operating point.

A clearer picture of the relationship between pressure and restriction factor for a fixed restriction and the same relationship for a rate stabilizer is shown in the pressure-flow rate characteristics plot of Fig. 7. In this plot, the light dotted horizontal line represents the condition of a specified flow rate. The light dashed lines represent hypothetical characteristics of mass flow rate versus combustion chamber pres-

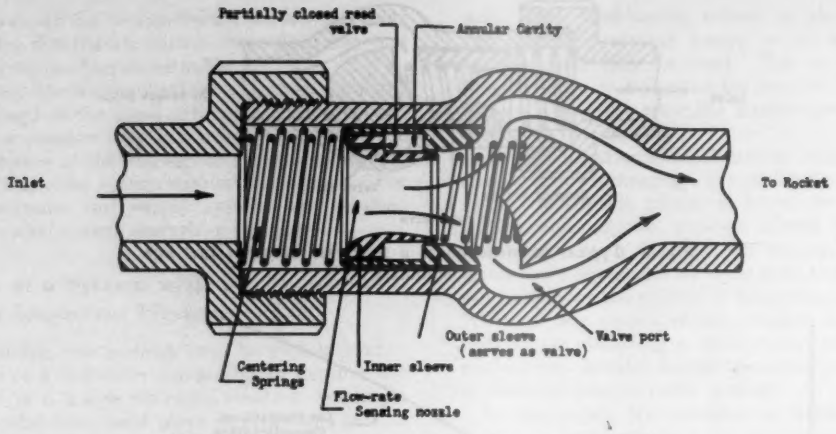


**Fig. 8 Rate stabilizer with a double sleeve arrangement**

sure. The light solid-line curve and the heavy dashed-line curve are two parabolas that represent, respectively, low and high fixed injector restriction characteristics. In principle, the intersection points between the injector restriction curves and the combustion chamber characteristic curve specify the operating points that determine the flow rate and the pressures involved. The total supply pressure determines the location of the combustion chamber characteristic curve. At the operating points the tangents of the restriction characteristic curves specify the operating point flow sensitivity which is the reciprocal of the restriction factor. This figure shows clearly that with a large injector restriction, a larger supply pressure is needed, with the result of a high-operating-point restriction factor, $R_o$, which is responsible for the improved stabilization property.

The heavy solid-line curve of Fig. 7 represents the characteristics of a rate stabilizer. This curve has a sharper bend than the parabolas, with the amount of bent adjustable as a function of the valve sensitivity. As a result of this effect, the rate stabilizer can be made to exhibit a high restriction factor similar to that obtained with high injector restriction but retains the low supply pressure difference, $(P_{d_o})$, and the low total supply pressure, $P_s$.

One limitation of the rate stabilizer is its rather large variation of restriction factor to change flow rate of the system. The situation is clearly shown in Fig. 7. It is apparent that the high restriction factor obtained at a specified flow rate is realized at the sacrifice of the low restriction factor at lower flow rate; i.e., a system stabilized at full-power operation may become unstable at partial power operation. This difficulty can be avoided by using the stabilizer valve as the throttle control so that at partial flow the restriction characteristic curve of Fig. 7 may be shifted downward instead of remaining at a fixed position. Another scheme for achieving the same goal would be to use a frequency sensitive device to make the valve effective near the chugging frequency and ineffective at steady state flow conditions. One possible scheme toward this aim is shown in Fig. 8. In this configuration, the piston valve is made up of two concentric sleeves, each positioned by a separate spring. The outer sleeve serves as the valve and the inner sleeve carries the flow-rate sensing nozzle. Under steady-state flow conditions, the outer sleeve remains stationary because there is not enough shearing force between the two sleeves to operate the valve. When oscillation starts, the cavity between the two sleeves begins to pump fluid so that a force is transmitted from the inner sleeve to the outer sleeve to operate the valve. A small directional-sensitive discharge nozzle with a partially closed reed valve may also be incorporated with the outer sleeve so that, when oscillation starts, a certain pressure may be built in the cavity. This pressure would act upon the outer sleeve in the direction to close the port. In this manner, the valve may be partially closed to increase the restriction factor when the oscillation starts, thereby increasing the stability of the rocket.

## Performance Analysis of Rate-Actuated Stabilizer

A practical rate actuated-type stabilizer always has a certain amount of mass and a certain amount of damping action against the motion of the piston. When mass and damping are involved, there may be a sufficient phase shift in the motion of the piston to void completely the operation principles discussed under ideal conditions. For this reason, a more thorough analysis is needed.

Fig. 9 shows the mathematical block diagram of a fuel supply system with a stabilizer operating near a given operating condition. In the forward loop, the flow sensitivity is shown as equal to the reciprocal of the effective restriction factor which is the sum of the restriction factor of the injector, $R_i$, plus the restriction factor of the stabilizer, $R_s$.

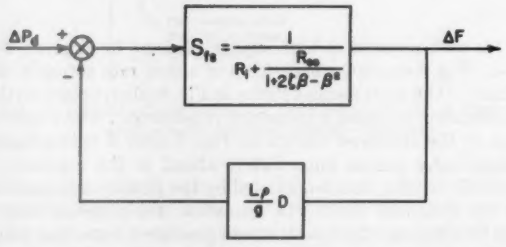


**Fig. 9 Block diagram of a fuel supply system with rate stabilizer**

The restriction factor of a rate stabilizer under steady-state conditions is shown in Equation [9]. Under dynamic conditions, the mass of the valve and the associating damping effect cause the valve to behave like a second-order system; i.e.

$$R_s = \frac{R_{so}}{1 + 2\zeta\beta - \beta^2} \quad \text{[10]}$$

where

$\zeta$ = damping ratio
$\beta$ = $\omega_f/\omega_n$ = frequency ratio
$\omega_f$ = forcing frequency
$\omega_n$ = undamped natural frequency

The complete frequency response function $(FR)_f$ of the fuel supply system is

$$\frac{(FR)_{fs}}{S_i} = \frac{1}{1 + \tau_i\omega_n j\beta + \dfrac{R_{so}S_i}{1 + 2\zeta\, j\beta - \beta^2}} \quad \ldots\ldots [11]$$

Equation [11] is a nondimensional frequency response function that may be determined for a given set of three parameters

$$\tau_i\omega_n; \quad R_{so}S_i = \frac{S_i}{S_{so}}; \quad \zeta$$

The first parameter indicates the relative magnitude of the natural frequency of the stabilizer with respect to the time constant of the original supply system. The second parameter represents the sensitivity ratio of the injector with respect to that of the stabilizer.

As a typical example, the solid-line curve of Fig. 10 shows the frequency response of a fuel supply system having a rate stabilizer with dynamic characteristics as given in Equation [10] in which

$$\tau_i\omega_n = 4; \quad R_{so}S_i = 2; \quad \zeta = 0.5$$

In the same plot, the heavy dotted line shows the modified performance ratio of the stabilized fuel supply system. The light dotted line shows the modified performance ratio of a system stabilized with a doubled injector restriction factor. The comparison between the two dotted line curves shows that for a frequency smaller than $1/\tau_i$, the system with rate stabilizer shows more gain reduction and phase lead than the system with double injector restriction. For a frequency higher than $3/\tau_i$, the system with rate stabilizer shows an increase in gain. If the chugging frequency is in the neighborhood of $1/\tau_i$, then the system with rate stabilizer would be more stable because of greater gain reduction and phase lead. The increase of gain at high frequency usually has no effect on the stability of a system composed of a series of lags, such as the rocket.

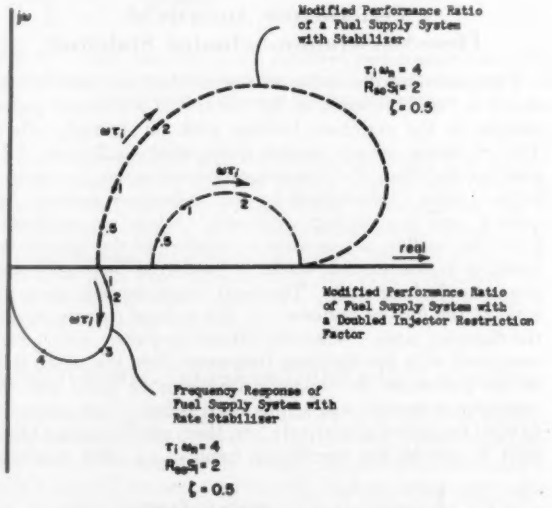


**Fig. 10 Frequency response and modified performance ratio of a fuel supply system with a rate stabilizer**

Since three parameters are involved in the determination of the performance function of Equation [11], a complete survey would be rather complicated. However, some simple guides are available for design purposes. As a general rule, the second-order dynamic effect of the rate stabilizer is to increase the phase lead over the entire frequency range, and to increase the gain at moderately high frequency range. At a low frequency range, it is possible to reduce the gain by increasing the valve sensitivity of the stabilizer but the gain at moderately high range can only be reduced by greatly increasing the natural frequency. This is not necessary, however, because the gain increase at moderately high frequency does not impair the stability quality. For this reason, a stabilizer with a natural frequency two to four times the chugging frequency and with sufficient valve motion sensitivity would be satisfactory. A discussion of valve design to fulfill this requirement is given in the last part of this paper.

## Principle of Flow-Acceleration-Actuated Stabilizer

The discussion of Fig. 3 shows that a system involving a dominating first-order lag may be stabilized by either sufficiently decreasing the time constant of the first-order lag so that it is virtually ineffective as a lag, or sufficiently increasing the time constant of the first-order lag so that other lags become relatively insignificant. Since the inertia effect of a fuel supply system is directly proportional to the time constant of the first-order system, a change of the inertia effect of the fuel supply system would then modify the stability of the entire loop.

For illustration purposes, the effect of the inertia of the mass in a fuel supply system may be considered as a *first-order restriction*. That is, a pressure drop is needed for a first-order derivative of the flow rate. Similarly, an ordinary restriction would be a zero-order restriction factor. To distinguish the first-order restriction factor, the symbol $R'$ will be used instead of $R$, which is the zero-order restriction factor.

The basic principle involved in the design of an acceleration-actuated stabilizer is to incorporate into the fuel supply system a stabilizer that gives a first-order restriction. This first-order restriction can be arranged either to increase the inertia effect to increase the time constant of the fuel supply system or to decrease the inertia effect to decrease the time constant. One possible scheme to get this first-order restriction is shown in Fig. 14.

In the flow-acceleration-actuated stabilizer, as shown in Fig. 14, a spring-loaded piston valve controlling two sets of ports is used. The piston has an annular cavity through which passes the entire quantity of the fuel flow. The inlet and outlet ports are arranged so that the flow is guided to enter and leave the annular cavity in a direction perpendicular to the axial motion of the piston. Under this condition, the inlet and outgoing flow stream does not exert any force upon the piston along its axial direction. The axial force acting upon the piston is then entirely due to the change of momentum of the fluid in the annular cavity which is balanced primarily by the spring.

The force due to momentum change of the fluid is expressed as

$$\dot{V}\, M_f = \frac{\dot{F}}{a}\,\frac{la\rho}{g} = \frac{\dot{F}l\rho}{g} \quad \ldots\ldots [12]$$

where

$M_f$ = mass of fluid in the annular space of valve
$\dot{V}$ = flow velocity in the cavity
$\dot{F}$ = volumetric flow rate
$l$ = length of the cavity
$a$ = sectional area of the cavity
$\rho$ = density of the liquid

Equation [12] shows that a force is produced acting upon the piston proportional to the rate of change of the flow rate. This force may be used to open or close one of the ports depending upon the initial position of the piston. In the arrangement of Fig. 10, the inlet port opening is widened whenever there is an increase in flow rate. The resulting effect is to decrease the pressure drop through the port for an

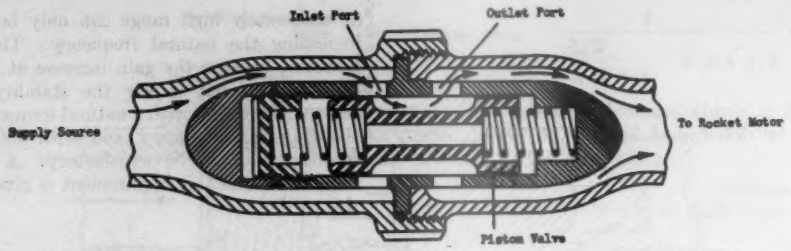


**Fig. 11 Typical construction of a flow-acceleration-actuated fuel line stabilizer**

increase of flow acceleration, and therefore, the system behaves as though it had a negative first-order restriction factor.

When the initial position of the piston of Fig. 11 is pushed one port length toward the upstream end, so as to cover the outlet port and uncover the inlet port, then the action of the stabilizer is reversed. Under this new arrangement, the port opening would be narrowed as the result of positive flow acceleration and the effect upon the pressure drop is that of a positive first-order restriction factor.

Since inertia effect is basically a positive first-order restriction factor, the use of a stabilizer as shown in Fig. 11 in series with the fuel line would either increase or decrease the inertia effect, depending upon the initial setting of the valve as already discussed.

The restriction factor of an acceleration-acutated stabilizer can be obtained by replacing the valve sensitivity, $S_v$, of Equation [7] by $S_v'D$, where the sign depends upon the initial setting of the valve:

$$\left(\frac{dP}{dF}\right)_o = 2\left[\frac{P_{d_o}}{F_o} \mp \frac{\sqrt{P_{d_o}}^3}{F_o} S_v'D\right] \quad \text{[13]}$$

$$= 2\,[R_{s_o} \mp R_{s_o}'\,D] \quad \text{[14]}$$

where

$S_v'$ = valve motion sensitivity
$= l\rho/g\ W/K_v\ C_v$
$R_{s_o}$ = zero-order restriction factor of stabilizer
$R_{s_o}'$ = first-order restriction factor of stabilizer

Equation [14] shows that the restriction factor of the acceleration-actuated stabilizer is made up of two parts: a zero-order restriction factor and a first-order restriction factor. In operation, the zero-order restriction factor would combine with the zero-order restriction factor of the injector, and the first-order restriction factor would combine with the first-order restriction of the inertia effect.

The corresponding block diagram of the fuel supply system is shown in Fig. 12. The performance function for the system is

$$(PF) = \frac{\dfrac{1}{R_i + R_{s_o}}}{1 + \dfrac{l\rho/g \pm R_{s_o}'}{R_i + R_{s_o}} D} \quad \text{[15]}$$

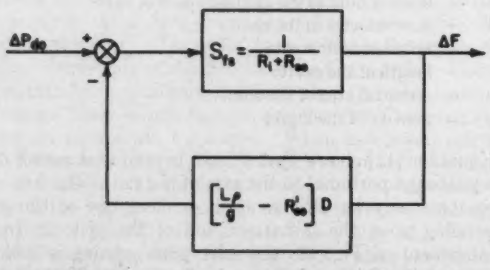


**Fig. 12 Block diagram of an acceleration-stabilized fuel supply system**

With a proper valve design to make $S_v'$ sufficiently large so that $R_v$ becomes much smaller than $R_i$ as shown in Equations [13] and [14], Equation [15] can be simplified to

$$(PF) = \frac{S_i}{1 + (\tau_i \pm S_i\,R_{s_o}')D} \quad \text{[16]}$$

According to this equation the effective time constant of the fuel supply system can be made to approach zero or become very large depending upon the sign and size of the stabilizer sensitivity $R_{s_o}'$. When the value of the valve sensitivity $S_v'$ cannot be made sufficiently large, then it would be desirable to utilize the zero-order restriction factor $R_{s_o}$ of Equation [15] to augment the stabilization effect. This zero-order restriction factor can be made frequency dependent with the use of the double-sleeve arrangement described in Fig. 8. The principle involved in the use of zero-order restriction for stabilization purposes is identical with that discussed under the heading of rate stabilizer and need not be repeated here. It is worth while to note, however, that the value of $R_{s_o}'$ is also proportional to the value of $R_{s_o}$ as shown in the notation definition of Equation [14]. This means that by increasing the value of $R_{s_o}$ with the double-sleeve arrangement, the acceleration stabilization effect is also increased.

## Performance Analysis of Flow-Acceleration-Actuated Stabilizer

The preceding discussion of the acceleration stabilizer as shown in Fig. 11 is based on the function of a massless piston moving in the stabilizer housing with no damping effect. This, of course, is only possible under ideal conditions. In a practical stabilizer, the piston-spring combination is a second-order system characterized by an undamped natural frequency and a damping coefficient. When an oscillatory force due to flow acceleration is applied to the piston, the resulting piston motion would be subjected to considerable amounts of phase shift. The exact value depends upon the ratio of the forcing frequency to the natural frequency, and the damping ratio. When the natural frequency is very high compared with the chugging frequency, then the phase shift of the piston at the chugging frequency is small and the operation is nearly ideal as described before. But when the natural frequency is relatively low, there can be enough phase shift to reverse the operational trend of an ideal stabilizer.

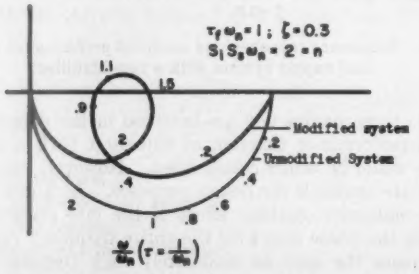


**Fig. 13 Frequency response of an acceleration-stabilized rigid fuel supply system**

The exact performance of the stabilizer should then be examined for each particular stabilizer design.

The performance function of a fuel supply stream with an acceleration stabilizer of finite natural frequency may be obtained by substituting in Equation [16] the second-order function characteristic of the first-order restriction $R_{s_0}'$. In frequency response form, this becomes

$$(FR)_{fs} = \frac{1}{1 + \tau_i\omega_n j\beta + \dfrac{\omega_n R_{s_0}' S_i j\beta}{1 + 2\zeta j\beta - \beta^2}} \quad \ldots\ldots [17]$$

The nondimensional characteristic parameters of this equation are

$$\tau_i\omega_n; \quad \zeta; \quad \omega_n R_{s_0}' S_i = \eta$$

Fig. 13 shows the polar diagram of a typical frequency response function of a stabilized system with the three constants

$$\tau_i\omega_n = 1; \quad \zeta = 0.3; \quad \omega_n R_{s_0}' S_i = 2$$

In this figure, the light line and the associated numbers represent the frequency response of an unmodified fuel supply system. The general phase lead and gain reduction of the modified system as compared with the unmodified system is quite apparent. Fig. 14 compares the modified

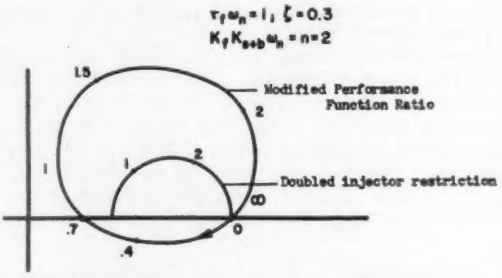


**Fig. 14 Polar diagrams of the modified performance ratio of a typical acceleration stabilized fuel supply system and that of a typical high restriction fuel supply system**

performance ratio of the acceleration-stabilized fuel supply system and that of the fuel supply system with doubled injector restriction. From this figure, it is apparent that if the natural frequency of the stabilizer is chosen to be equal to the chugging frequency of the rocket, then the phase lead and gain reduction introduced by the system utilizing the acceleration stabilizer should be better than the system utilizing the double restriction.

## Typical Design Consideration of a Flow Stabilizer

From an analysis of Figs. 10 and 14, it is apparent that in order to make either a rate or an acceleration type of stabilizer effective, it is necessary to design the piston-spring system with a natural frequency sufficiently high in comparison with the chugging frequency, which is in the neighborhood of a few hundred cycles per second. On the other hand, the piston valve should have enough travel to produce sufficient control valve sensitivity. A design that can fulfill both of these requirements is the key to the success of an effective stabilizer.

In the case of an acceleration actuating stabilizer such as shown in Fig. 11, the valve travel is proportional to the driving force. As shown by Equation [12], this force is proportional to the length of the liquid column in the valve, and inversely proportional to the stiffness of the spring. On the other hand, the length of the liquid column also determines the mass of the oscillating valve system, which, together with the spring constant, determines the natural frequency. To increase the natural frequency by increasing the spring constant or shortening the liquid column length of the piston would cause a decrease in the stabilizer sensitivity. All this means that the natural frequency of the system shown in Fig. 11 is tied closely to the stabilizer sensitivity.

A design which would give large stabilizer sensitivity without lowering the natural frequency is shown in Fig. 15.

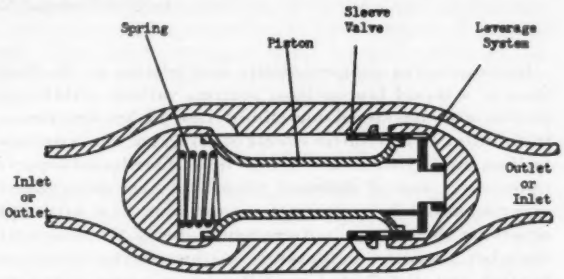


**Fig. 15 Schematic diagram showing the use of a lightweight sleeve valve and leverage system to increase the sensitivity of the control valve**

In this scheme the valve is made up of a series of parallel ports so that the effective opening area per unit valve travel is increased proportionally to the number of ports. Another feature shown in this scheme is to have the valve actuated by the piston through motion magnifying linkage. This arrangement would reduce the effective mass of the piston and of the fluid that travels with the piston. A stabilizer designed with this kind of valve arrangement would give sufficient sensitivity and have a natural frequency in the hundreds of cps range.

## Conclusions

The purpose of using the feedback principle in connection with the chugging oscillation of a liquid rocket is to associate the familiar techniques for the stabilization of a feedback system with rocket operation. From this type of analysis, it can be proved that stabilization of the chugging oscillation can be achieved by modifying the dynamic performance of the fuel supply system. One effective method is to use large injector restriction; this is undesirable, however, because of the large supply pressure needed. Two stabilizers designed to provide necessary performance modification without the need of high supply pressure are then introduced. The first type is called the rate-type stabilizer and provides a large restriction for stabilization without the associated high supply pressure. The second type introduces a positive or negative inertia effect to modify the fuel supply system performance. Dynamic performance analyses for these systems have shown that their stabilization effects compare favorably with those of a fuel supply system with increased injector restriction. This advantage is obtained in addition to the lower supply pressure needed.

In comparison with other feedback schemes for chugging stabilization, the suggested fuel line stabilizers would be rugged, simple, and free of elaborate electronics.

Of the two types of stabilizers, the acceleration type seems to be slightly superior to the rate type because it requires a relatively lower natural frequency for the valve system. Also, the actuating force is more easily controlled. On the other hand, however, the valve of the rate stabilizer can be restrained with a stronger spring to get a high natural frequency. This is because a larger valve actuating force can be realized in this type of valve arrangement.

Clearly, the principle so far introduced needs to be verified with experimental research. An experimental stabilizer with a wide-range adjustment should be most desirable for this purpose.

*(Continued on page 39)*

# Experimental Aspects of Rocket System Stability[1]

Y. C. LEE,[2] A. M. PICKLES,[3] and C. C. MIESSE[4]

Aerojet-General Corporation, Azusa, Calif.

**By considering compressibility and friction in the feed lines of a liquid bipropellant system, various stabilizing devices are considered for elimination of low-frequency instability. The relative effects of several of these devices (orifice, inductive venturi, flexible hose, distributed capacitance core) and of different propellants are determined experimentally by pulsing the propellant flow rate and observing the change in decrement rates of the resultant chamber pressure oscillations. Although the inductive venturi and distributed capacitance core were found to have an appreciable stabilizing effect, the greatest stabilizing effect was achieved by using a more reactive fuel. Both Fourier and Mirragraph analyses of the chamber pressure oscillations indicate the presence of several predominant frequencies.**

## Introduction

OSCILLATORY combustion has long been a major problem for the designers of the liquid propellant rocket, and, as such, has been the object of many experimental programs and theoretical analyses. The basic idea underlying the analyses of low-frequency oscillations is that the rocket system can be represented by a closed feedback loop containing a time lag between the injection of the propellants and their conversion to combustion products.

This concept corresponds to that advanced by Minorsky (1)[5] and applied to the problem of combustion stability by numerous investigators (2–6) in the field of rocketry. Outstanding among these have been the analyses of Summerfield (2), who considered the propellant feed system as a lumped impedance, and Crocco (3), whose best known analysis of intrinsic instability isolated the chamber from the feed system.

By considering the transmission of pressure waves in the propellant lines, as analyzed by Thomson (7), Sabersky showed that the compressibility of the liquid can have appreciable effect on system stability, particularly for the long line lengths in practical use (8). These lines are thus represented by a system of distributed impedances, in the language of electrical engineers, and can be analyzed in accordance with transmission line theory, in which capacitance is analogous to the compressibility of the fluid and elasticity of the line, inductance analogous to the inertance of the fluid, and resistance analogous to friction losses. Application of this theory to the problem at hand suggests the advisability of inserting any of several stabilizing devices into the propellant lines in order to stabilize the rocket system in so far as low frequencies are concerned.

In order to investigate these stabilizing devices, the relative stability of various systems having these devices may be determined by comparing the logarithmic decrement rates of pressure oscillation which result from a given disturbance imposed on each of the systems under consideration. Accordingly, this gives rise to the technique of determining the relative effectiveness of various stabilizing devices and various fuels by pulsing the propellant mass flow and observing the resultant decrement rate of combustion chamber pressure oscillations.

Presented at ARS Fall Meeting, Los Angeles, Calif., Sept. 19, 1955.

[1] The work discussed herein was sponsored by the Wright Air Development Center, United States Air Force.

[2] Department Head, Liquid Engine Division.

[3] Senior Engineer, Liquid Engine Division.

[4] Physicist, Liquid Engine Division.

[5] Numbers in parentheses indicate References at end of paper.

## Stabilizing Devices

It is generally agreed that the occurrence of low-frequency oscillations in a rocket system could result from the interaction of oscillations in the combustion chamber pressure and the oscillations in propellant flow rate. In general the stability of such a nonlinear system is a function of the amplitude and phase of these oscillations. The propellant line impedance possesses resonant peaks as a function of frequency, these resonant peaks corresponding to the low impedance points or high admittance points. These peaks occur ideally with no resistance at frequencies equal to $(n\pi L)/c$, where $n = 1, 2, \ldots$, $c$ the effective acoustical velocity of the propellant line, and $L$ the line length.

In the light of the transmission line theory, any stabilizing device falls into two categories. One is a resistive device and the other a phase-shifting device. It can be shown that the combustion time lag $\tau$ as analyzed in (2) to (6) introduces phase shift of the dynamic system and has no effect on the amplitude. Therefore, any design of the stabilizing device which introduces phase shift must take into consideration the combustion time lag. Unfortunately, the precise value of

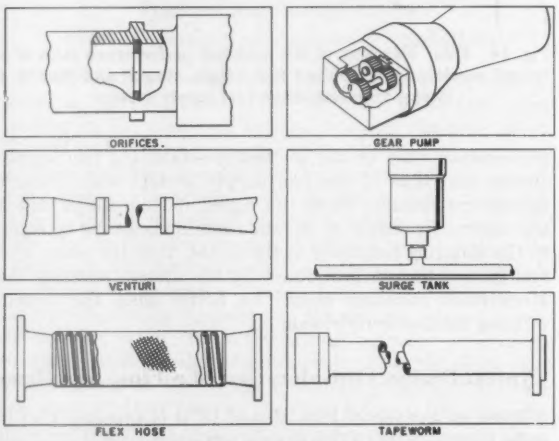


**Fig. 1 Stability devices**

the time lag for a given propellant combination and a given rocket system is not known. Therefore, the rocket designer is confronted with the problems of estimating the value of this time lag if he is to design a successful phase-shifting stabilizing device. In view of these considerations, the following devices, shown schematically in Fig. 1, have been considered. Some of these devices have been tested, and the experimental results will be discussed later.

### *Stability Orifices*

In transmission lines (9), the impedance of an element includes both resistive and reactive components. Since the resistive component impedes the steady-state d-c flow as well

as the a-c oscillations, and hence requires additional pressure and weight to maintain the specified flow rate, it is desirable that the resistive component be small with respect to the reactive component. Stability orifices, which are the most easily installed of the several devices considered, do not possess this desirable characteristic. The impedance of an orifice includes a large resistive component and a small reactive component so that stability can be achieved only at the expense of high system pressure drops. The effect of adding system pressure drop is to suppress the high admittance resonance peaks of the propellant lines so that interaction between line and chamber is reduced.

### *Inductive Venturis*

The venturi section, which combines a relatively high coefficient of discharge with a long section of tube, appears to be the ideal flow stabilizing device. By designing the venturi such that its throat section is long and its divergent section has a small included angle, both a high inductance and a low resistive component of impedance will be attained. Since the length thus prescribed becomes somewhat prohibitive, a compromise over-all length may be chosen, thus reducing the reactive component. An ideal inductive venturi has no resistance to flow, so that it is primarily a stabilizing device to introduce phase shift into the system.

### *Flexible Hose*

The conflicting requirements of a long throat and a relatively short over-all length may be satisfied approximately by using a flexible hose for the throat. This would also aid greatly in decoupling the propellant lines from the structural vibration of the thrust chamber since it would tend to "soften" or decrease the bulk modulus of the line. One great disadvantage inherent in this device, however, is the flexibility of the walls of the hose, in that it adds capacitance to the line, and, as such, may be destabilizing. In general the case of a flexible hose also results in added pressure drop of the system.

### *Idling Gear Pump*

Another inductive device which provides more effective isolation than the venturi section is the idling gear pump. In this positive displacement device of high volumetric efficiency, the inductance is directly proportional to the inertia of the rotating parts, inversely proportional to the square of the flow area through the pump, and inversely proportional to the square of the gear pitch line radius. Of advantage is the possibility of mechanically coupling the moving elements of both fuel and oxidizer idling gear pump, thus permitting the maintenance of both propellant flow rate and mixture ratio. However, plans to test this device were discarded when it was realized that the serious disadvantages of excessive weight, complexity of design and fabrication, and disproportionate space requirements far outweighed the advantages listed above.

### *Surge Tanks*

Use of a surge tank with a short inductive section, which has proved highly successful in the suppression of water hammer phenomena by absorbing energy from the pressure waves, suggested itself as a possible stability device. However, the difficulty in determining the proper frequency for maximum effectiveness of this narrow band filter, and the possibility of a coupling of surge tank cavity oscillations with the pressure oscillations in the chamber, thus providing a positive feedback mechanism, led to the elimination of this device from further consideration.

### *Acoustically Damped Feed Line ("Tapeworm")*

Because the unmodified propellant lines permit the transfer of hydroacoustic energy from one end of the line to the other with negligible energy loss, the stabilizing potentialities of an energy-absorbing device immediately present themselves. Such a device is found in a small-diameter, gas-filled, compliant tube ("tapeworm") inserted axially within the propellant line. The relatively high compliance of the deformable gas-filled tube will enable it to absorb energy much more readily than either the fluid or the wall of the line. Insertion of such a capacitance device in the propellant line eliminates both the modulation of flow produced by tank vibrations and the surging mode of line vibrations, at the same time adding only a negligible resistive component to the impedance of the system. The added compliance of the tapeworm tends also to suppress or even flatten the resonant peaks of the propellant line.

## Pulsing Technique

In order to compare the logarithmic decrement rates in chamber pressure oscillations which result from a given disturbance in various systems, it is necessary to devise some mechanism for imposing a pressure pulse of prescribed magnitude and duration on the rocket system. Several methods suggest themselves: The most direct method would be the pulsing of the chamber, either by means of a solid charge installation, the injection of a given amount of excess fuel through an auxiliary injector, or the firing of a small solid propellant charge into the chamber through the exit nozzle.

An alternative method of exciting the system is to pulse the propellant flow. Ideally, the fuel and oxidizer lines would be pulsed simultaneously in such a manner that the mixture ratio would remain unchanged. Since the control and sequencing of such a dual pulsing device presented considerable difficulty, several devices for pulsing just one of the lines were designed in the hope that the resultant instantaneous variation in mixture ratio would not be too severe.

The first device tested was a positive displacement piston which pumps additional propellant into the propellant line. Fig. 2 is a schematic drawing of this device. Inspection of

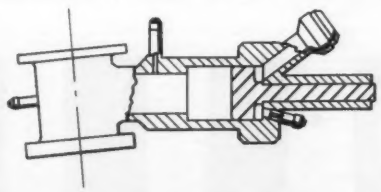

**Fig. 2 Positive displacement flow modulator**

this figure reveals that the piston is driven by compressed air supplied from $1^1/_4$ in. connecting lines and controlled by a pilot-operated line valve. The piston is held in cocked position by means of a shear pin, and internal spacers provide for a variation in the length of the chamber. Allowance is thus made for adjustment of both duration and amplitude of the pulse, since the actuation pressure can also be adjusted.

A second device was designed which would produce a negative pulse in the propellant line. This unit, shown schematically in Fig. 3, consists basically of a $1^1/_8$ in.-diam piston installed in a housing which permits a maximum stroke of $1^1/_2$ in. When the piston is installed in a propellant line, the pressure

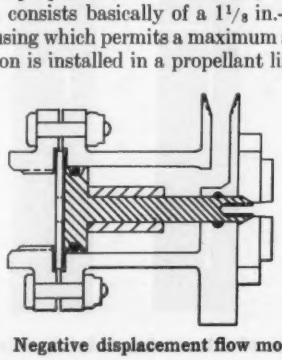

**Fig. 3 Negative displacement flow modulator**

on one face is that of the liquid, and, on the other, atmospheric. The piston is held in place by a tension bolt which is released by electrical heating, allowing the piston to move away from the propellant line so that a quantity of propellant equal to the net volume of the cavity is suddenly removed from the line. Both the length of stroke and the actuating pressure can be varied by internal spacers and shunt-line orifices, respectively.

In order to facilitate the pulsing of a system several times during a single test run, the opposed piston repeater-type pulsing unit was designed. As shown in Fig. 4, air pressure

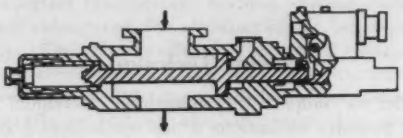

**Fig. 4 Repeater-type flow modulator**

is applied both to one side of the main actuating piston and to a trigger release mechanism. Actuation of the main piston results in application of force to the hydraulic cylinder directly opposite, leading to a buildup of pressure in the hydraulic cylinder. This drives a secondary piston simultaneously with the travel of the main piston, thus injecting two pockets of fuel into the propellant line. Release of the actuating air pressure permits the propellant line pressure to force the pistons back to their original positions, and the triggering mechanism is relatched and ready for subsequent operation.

## Experimental Results

The effects of an oscillatory propellant flow rate on the combustion phenomena in a liquid propellant rocket can be determined in any of several ways. A magnetic tape could record the audible sound of the oscillating pressures, an oscillograph could record the oscillating chamber pressure itself, or a motion picture could capture the variations in exhaust flame intensity. The last-mentioned method is by far the most spectacular, and a series of frames from a typical test is shown in Fig. 5. In this figure, the shock cones are clearly visible, and an irregular oscillation of the flame boundaries is noted during "steady-state" operation. The effect of the pulse in the fuel line is unmistakably apparent, as the large dark clouds of unburned propellants replace the luminous flame at equal intervals after the first disturbance, and with decreasing severity. Inasmuch as the maximum amplitude of chamber pressure oscillations for this run was greater than the steady-state pressure drop across the injector, it is readily conceivable that a momentary cessation of fuel flow occurred whenever the chamber pressure passed through a maximum, thus resulting in periodic flameouts.

Quantitatively, however, the best method for determining the effect of a propellant line pulse on the combustion phenomena is the sensing of the oscillating chamber pressures with a pressure pickup, and the recording of these data on an oscillograph. The variations with time of gas exciter cylinder,

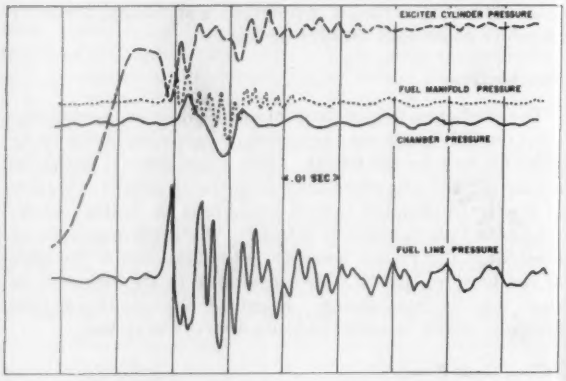


**Fig. 6 Pressure variations for typical pulsing test**

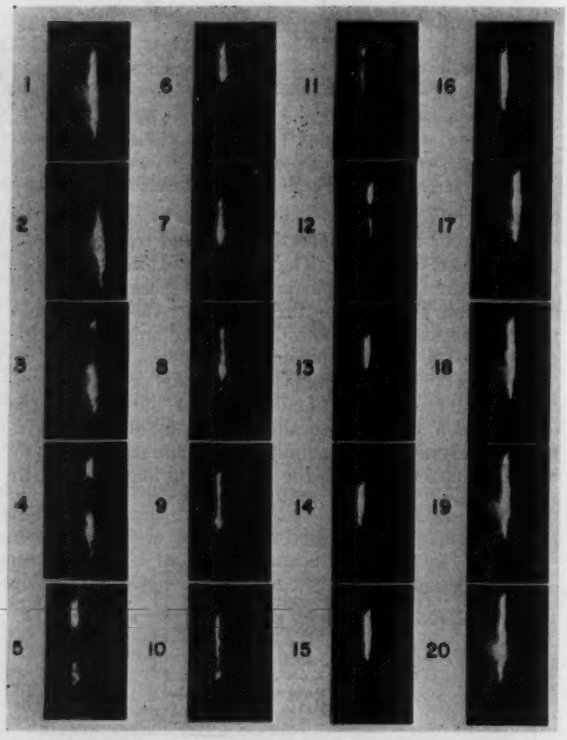


**Fig. 5 Variation of exhaust flame due to pulsing of fuel line**

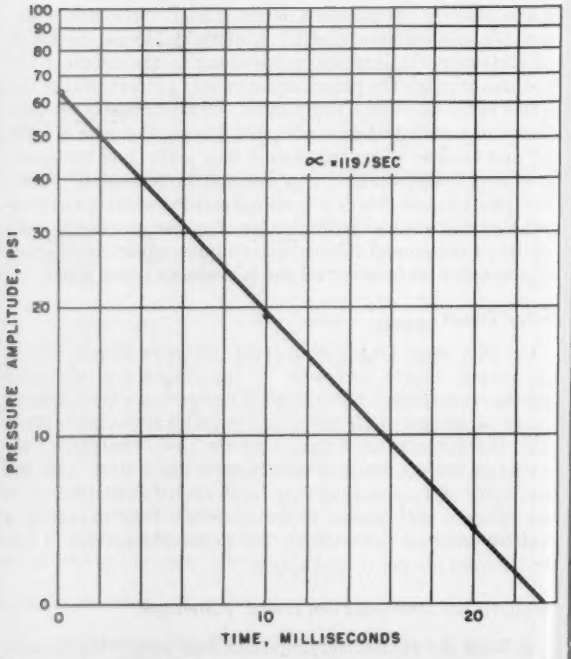


**Fig. 7 Logarithmic plot of variation in chamber pressure amplitude**

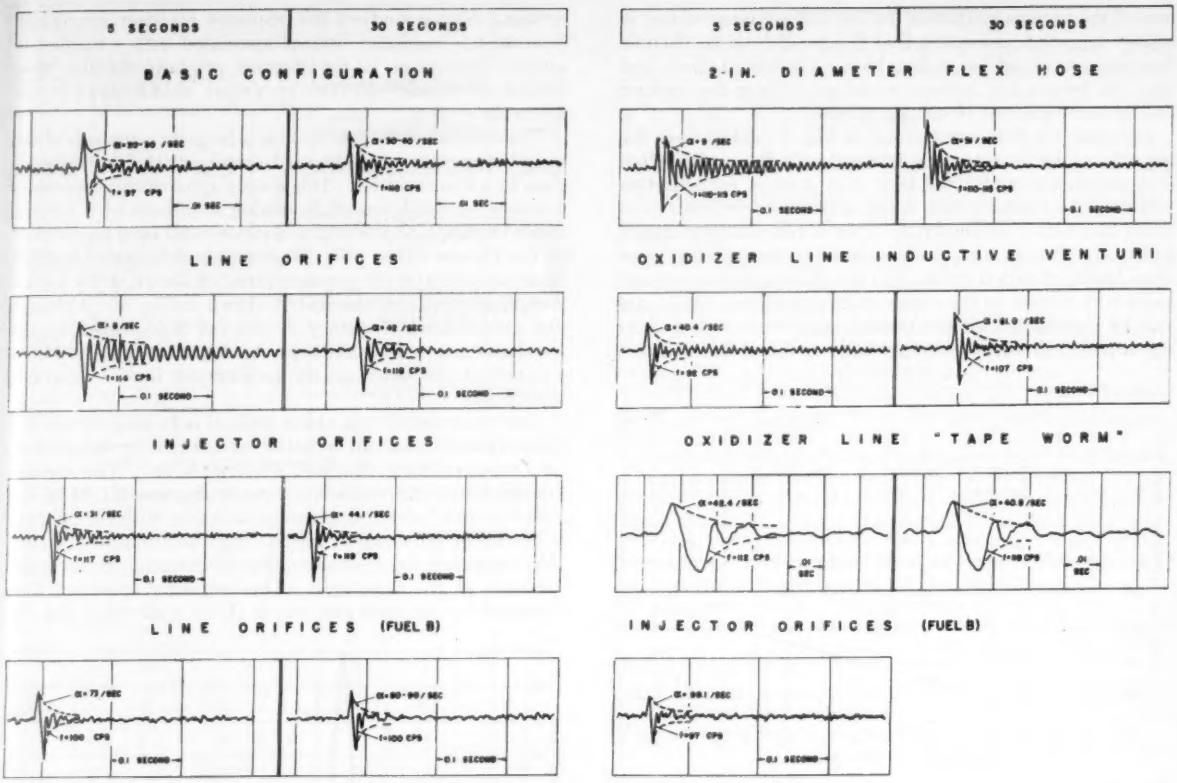


**Fig. 8 Chamber pressure response with various stability devices**

fuel line, fuel manifold, and chamber pressure for the test run depicted in Fig. 5 are shown in Fig. 6. All pickups were Aerojet diaphragm-reluctance pressure gages, mounted on the ends of short $^1/_4$ in. ID tubes. For this run, the single-shot positive displacement piston was used, with a stroke of 0.5 in., an actuation pressure of 1600 psi, and a 14SO aluminum shear pin. From this figure, it is apparent that the peaks in the propellant line and manifold pressures both occurred subsequent to the piston actuation, and that the chamber-pressure oscillations are almost directly out of phase with injector pressure, thus causing maximum chamber pressures to coincide with minimum injector pressures. This out-of-phase relation provides ample justification for the flameout concept proposed above. Also noted is the rapid decline of the amplitude of chamber pressures, resulting in the decreasing severity of luminous flame discontinuities observed in the preceding figure. Plotting of the logarithm of pressure amplitude (difference from steady-state chamber pressure) vs. time yields a logarithmic decrement rate of 119 per sec, as shown by the linear variation in Fig. 7.

A series of tests were made on a basic rocket configuration with a stroke length of 1.75 in. and an actuation pressure of 1350 psig, using various stability devices and two different fuels. Because of the high cost of full-scale test firings, only a limited number of tests (average of 3) were made for each condition. A matrix of representative chamber pressure variations is shown in Fig. 8. From this figure, it is apparent that the chamber pressure oscillations decayed much more rapidly at the end of the test run than at the beginning, thus indicating the presence of structural coupling. Furthermore, the rates of decline for Fuel (B) are greater than those for Fuel (A), regardless of the stability device used, thus indicating a probable difference in the combustion time lags for the two fuels. Also of interest is the increase of predominant frequency, which is effected either by the addition of stability devices or by the increase in time of pulse from FIRE switch.

A graphical summary of the logarithmic decrement rate data obtained from Fig. 8 is shown in Fig. 9. The relative effective-

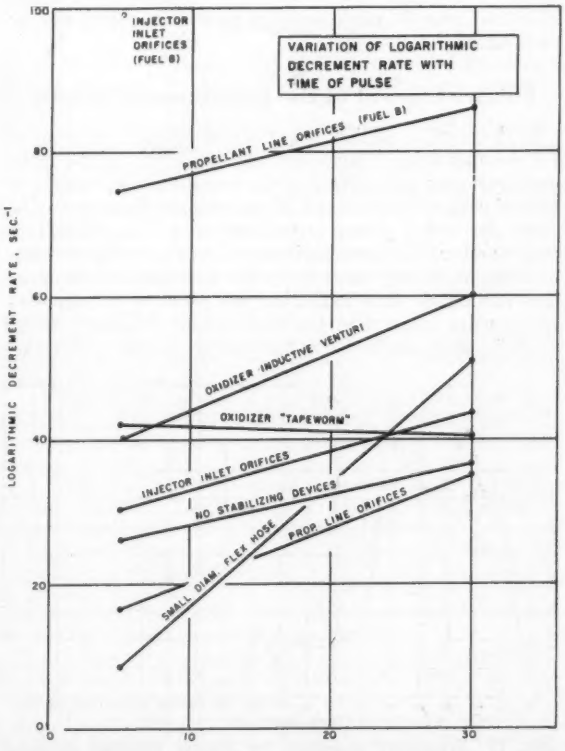


**Fig. 9 Variation of logarithmic decrement rate with time of pulse**

ness of the various stabilizing devices and a change of fuel is readily apparent, indicating that the small-diameter flexible hose and propellant line orifices have no beneficial effect, and that the venturi and internal compliant tube in the oxidizer line have the greatest stabilizing effects.

Although the data summarized in Fig. 8 indicate that the logarithmic decrement rate is determined by the configuration and propellants, additional tests with a given configuration and propellant combination reveal that the decrement rate is also a function of the amplitude of the initial pulse in chamber pressure. This, in turn, is determined by the actuation pressure, length of piston stroke, and the phasing of the imposed pulse with respect to the steady-state oscillations, which cannot be regulated with the present relatively crude pulsing apparatus. However, the amplitude of the initial chamber

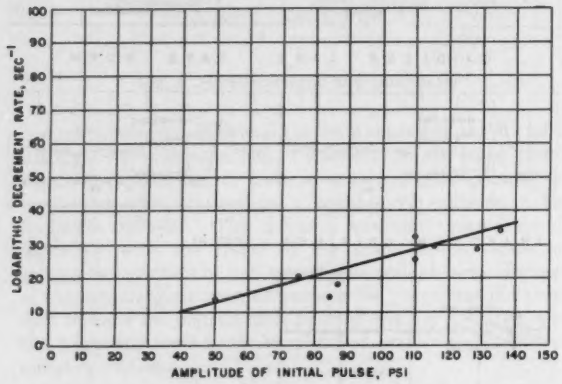


**Fig. 10 Variation of logarithmic decrement rate with amplitude of initial pulse**

pressure pulse can be readily determined from the oscillographs, and a plot of logarithmic decrement rate vs. amplitude of initial pulse is shown in Fig. 10. Inspection of this figure reveals that this variation is approximately linear, which indicates the nonlinearity of the rocket system, as may be expected.

## Fourier Content of the Experimental Results

In the previous section, only the predominant frequency of the chamber pressure oscillation was considered, and the decrement rate was determined as the variation with respect to time of peak amplitudes at this predominant frequency. Because the rocket system is expected to be responsive to a large number of frequencies, it should prove of value to determine the frequency spectrum of the recorded chamber pressure oscillation, thus indicating the presence of frequency components, other than the predominant frequency, which might be associated with some particular element of the rocket

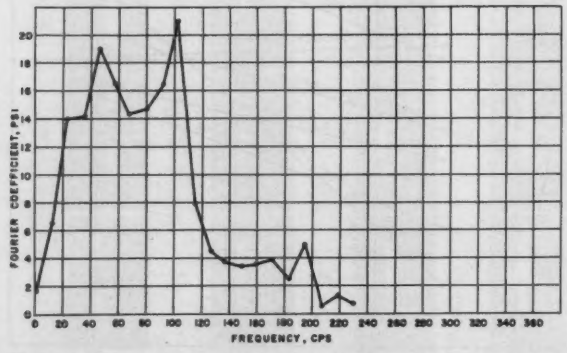


**Fig. 11 Frequency spectrum for typical chamber pressure oscillation**

system. Such a study of the frequency spectrum might well indicate the hydraulic element associated with a major frequency component in the chamber pressure response, thus leading to greater stability by proper modification of the hydraulic system.

The simplest method of making a frequency analysis of the chamber pressure oscillation is to represent the experimental data by a Fourier series. It is readily apparent that representation of an oscillation of decreasing amplitude by a Fourier series implies that the negative exponential term is absorbed in the Fourier series. Fig. 11 shows the frequency spectrum thus computed for the pressure variation shown in the second row, first column of the matrix shown in Fig. 8. Although the predominant frequency of 114 cps is indicated by the maximum amplitude at 104 cps, it is apparent that the 47-cps component not noted on the oscillograph is of comparable amplitude.

One refinement of the above method is to assume that the pressure oscillation can be better represented by the product of a negative exponential and a Fourier series. This method implies the existence of a Fourier series representation for the "steady-state" chamber pressure variation, with the effect of a decreasing pulse merely introducing a multiplicative factor. Also present is the implication that all frequency components decrease at the same rate. The frequency spectrum thus obtained for the same test run as above is shown in Fig. 12,

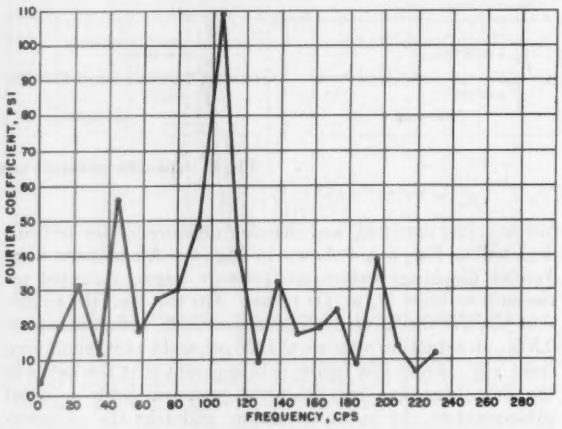


**Fig. 12 Modified frequency spectrum**

which reveals that the relative importance of the various modes is essentially unchanged by this modification, except for a general decrease in the amplitude of low-frequency components.

A further refinement of the frequency spectrum analyses is to determine a separate decrement rate for each of the various frequencies present. Since no readily applicable theoretical method for obtaining this information from experimental data is available, it becomes necessary to use special instrumentation designed for this purpose. One such instrument is the Mirragraph, which photographs the pressure trace and scans the photograph for pressure components in each frequency interval, thus making possible the determination of a separate decrement rate for each frequency range.

Fig. 13 shows a series of pressure traces obtained from the Mirragraph record of a test in which the propellant line orifices were the stabilizing devices. From this figure it is apparent that both the maximum amplitude and decrement rate are different for each frequency band. For the present series of tests, the decrement rate for each frequency range was determined by applying the method of least squares to the peaks from the time at which the maximum amplitude was reached on the pressure trace to the time at which noise level was reached on the individual frequency band trace. Since Fig. 10 indicated that the decrement rate varied

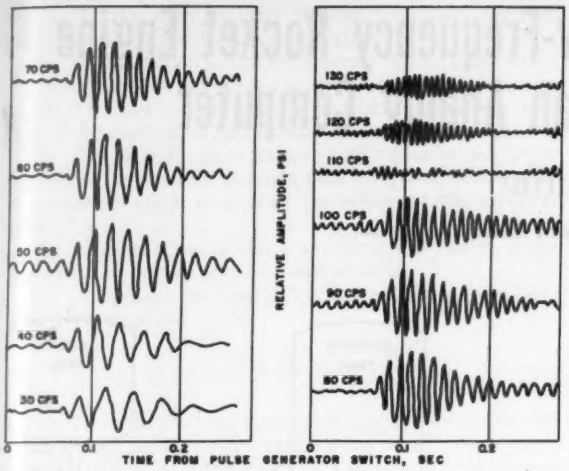


Fig. 13 Mirragraph record of typical pressure oscillation

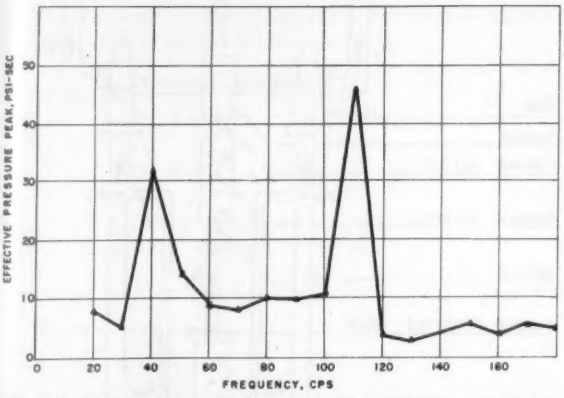


Fig. 14 Mirragraph analysis of typical pressure oscillation

linearly with amplitude of the initial pressure pulse, it was postulated that the variation of the ratio of initial pulse to decrement rate with frequency should give an indication of relative importance of the various frequencies. Fig. 14 shows this variation for the data given in Fig. 13. This initial test indicates predominant frequencies of 40 cps and 110 cps, which compare favorably with the resonant peaks at 47 cps and 104 cps in Fig. 11, which is the Fourier analysis for a similar configuration.

## Conclusions

As a result of this experimental investigation of combustion stability, the following conclusions can be drawn:

1. The transmission of pressure waves in the propellant lines of a liquid propellant combustor is an important factor in the stability of the rocket system.
2. The technique of pulsing the propellant flow, combined with the theoretical concept of the decrement rate of chamber pressure oscillations, is an effective means of determining the relative stability of various rocket systems.
3. The stability of a given rocket system can be increased either by inserting devices in the lines which will increase the inductance or suppress the resonant peaks, or by using a propellant with a shorter combustion time lag.
4. The decrement rate for a given configuration varies linearly with the amplitude of the pressure pulse.
5. There appears to exist in a rocket system a coupling of structural vibration and hydraulic oscillation. Thus, early testing of the rocket system with the flight structural configuration would be desirable.

## Acknowledgment

The invaluable assistance of the following members of the Liquid Engine Division of the Aerojet-General Corporation is gratefully acknowledged: D. M. Tenenbaum, L. Shenfil, W. A. Murray, and M. B. Cooley.

## References

1 Minorsky, N., "Self-Excited Oscillations in Systems Possessing Retarded Actions," *Journal of Applied Mechanics*, vol. 9, 1942, p. 65.

2 Summerfield, M., "A Theory of Unstable Combustion in Liquid Propellant Rocket Systems," *Journal of the American Rocket Society*, vol. 21, 1951, p. 108.

3 Crocco, L., "Aspects of Combustion Stability in Liquid Propellant Rockets," *Journal of the American Rocket Society*, vol. 21, 1951, p. 163; vol. 22, 1952, p. 7.

4 Tsien, H. S., "Servo-Stabilization of Combustion in Rocket Motors," *Journal of the American Rocket Society*, vol. 22, 1952, p. 256.

5 Marble, F. D. and Cox, D. W., Jr., "Servo-Stabilization of Low-Frequency Oscillations in a Liquid Bipropellant Rocket System," *Journal of the American Rocket Society*, vol. 22, 1952, p. 78.

6 Lee, Y. C., Gore, M. R., and Ross, C. C., "Stability and Control of Liquid-Propellant Rocket Systems," *Journal of the American Rocket Society*, vol. 23, 1953, p. 75.

7 Thomson, W. T., "Transmission of Pressure Waves in Liquid Filled Tubes," *Proceedings of the First U. S. National Congress of Applied Mechanics*, J. W. Edwards, Ann Arbor, Michigan, 1952, p. 927.

8 Sabersky, R. H., "Effect of Wave Propagation in Feed Lines on Low Frequency Rocket Instability," *Journal of the American Rocket Society*, vol. 24, 1954, p. 172.

9 Olson, H. F., "Dynamical Analogies," D. Van Nostrand Co., Inc., New York, 1943.

---

## Stabilization of Low-Frequency Oscillations of Liquid Propellant Rockets with Fuel Line Stabilizer

(*Continued from page 33*)

## References

1 "Aspects of Combustion Stability in Liquid Propellant Rocket Motors," by Luigi Crocco, *Journal of the American Rocket Society*, vol. 21, Nov. 1951, p. 163.

2 "Low Frequency Combustion Instability in Liquid Rockets with Different Nozzles," by Sin-I Cheng, presented at Annual Meeting of the American Rocket Society, Dec. 1953.

3 "Servo-Stabilization of Combustion in Rocket Motors," by H. S. Tsien, *Journal of the American Rocket Society*, vol. 22, Sept. 1952.

4 "Stability of Flow in Rocket Motor," by D. R. Gunder and D. R. Friant, *Journal of Applied Mechanics*, vol. 17, 1950.

5 Discussion of the paper of Reference 4, by M. Yachter, *Journal of Applied Mechanics*, vol. 18, 1951.

6 "A Theory of Unstable Combustion in Liquid Rocket Systems," by M. Summerfield, *Journal of the American Rocket Society*, vol. 21, Sept. 1951, p. 108.

7 "Servo-Stabilization of Low Frequency Oscillations in a Liquid Bipropellant Rocket Motor," by F. Marble and D. W. Cox, Jr., *Journal of the American Rocket Society*, vol. 23, Mar. 1953.

8 "Stability and Control of Liquid Propellant Rocket Systems," by Y. C. Lee, M. R. Gore, and C. C. Ross, *Journal of the American Rocket Society*, vol. 23, Mar. 1953.

9 "Servo-Stabilization of Low Frequency Oscillations in Liquid Propellant Rocket Motors," by F. E. Marble, presented at Brooklyn Symposium on Combustion Instability in Liquid Rocket Engines, Oct. 1953. (This paper is unclassified, but the Proceedings of the Symposium is confidential.)

10 "Theory of Combustion Instability in Liquid Rockets," by Luigi Crocco and Sin-I Cheng, Monograph, AGARD, NATO, chap. 2, sec. 7, to be published soon.

11 "Unconditional Stability of Low-Frequency Oscillation in Liquid Rockets," by Sin-I Cheng, *Journal of the American Rocket Society*, vol. 24, Sept.-Oct. 1954.

ness of the various stabilizing devices and a change of fuel is readily apparent, indicating that the small-diameter flexible hose and propellant line orifices have no beneficial effect, and that the venturi and internal compliant tube in the oxidizer line have the greatest stabilizing effects.

Although the data summarized in Fig. 8 indicate that the logarithmic decrement rate is determined by the configuration and propellants, additional tests with a given configuration and propellant combination reveal that the decrement rate is also a function of the amplitude of the initial pulse in chamber pressure. This, in turn, is determined by the actuation pressure, length of piston stroke, and the phasing of the imposed pulse with respect to the steady-state oscillations, which cannot be regulated with the present relatively crude pulsing apparatus. However, the amplitude of the initial chamber

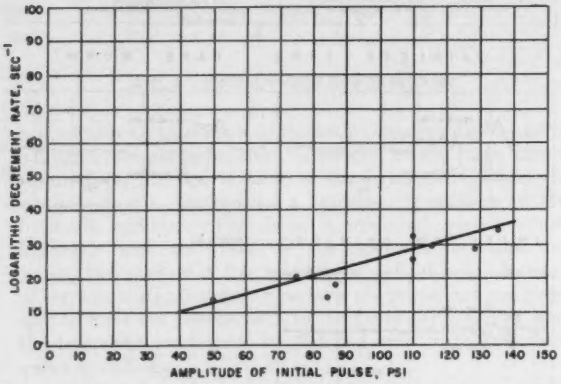


**Fig. 10 Variation of logarithmic decrement rate with amplitude of initial pulse**

pressure pulse can be readily determined from the oscillographs, and a plot of logarithmic decrement rate vs. amplitude of initial pulse is shown in Fig. 10. Inspection of this figure reveals that this variation is approximately linear, which indicates the nonlinearity of the rocket system, as may be expected.

## Fourier Content of the Experimental Results

In the previous section, only the predominant frequency of the chamber pressure oscillation was considered, and the decrement rate was determined as the variation with respect to time of peak amplitudes at this predominant frequency. Because the rocket system is expected to be responsive to a large number of frequencies, it should prove of value to determine the frequency spectrum of the recorded chamber pressure oscillation, thus indicating the presence of frequency components, other than the predominant frequency, which might be associated with some particular element of the rocket

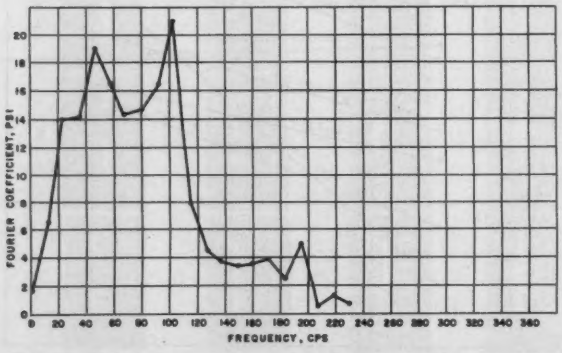


**Fig. 11 Frequency spectrum for typical chamber pressure oscillation**

system. Such a study of the frequency spectrum might well indicate the hydraulic element associated with a major frequency component in the chamber pressure response, thus leading to greater stability by proper modification of the hydraulic system.

The simplest method of making a frequency analysis of the chamber pressure oscillation is to represent the experimental data by a Fourier series. It is readily apparent that representation of an oscillation of decreasing amplitude by a Fourier series implies that the negative exponential term is absorbed in the Fourier series. Fig. 11 shows the frequency spectrum thus computed for the pressure variation shown in the second row, first column of the matrix shown in Fig. 8. Although the predominant frequency of 114 cps is indicated by the maximum amplitude at 104 cps, it is apparent that the 47-cps component not noted on the oscillograph is of comparable amplitude.

One refinement of the above method is to assume that the pressure oscillation can be better represented by the product of a negative exponential and a Fourier series. This method implies the existence of a Fourier series representation for the "steady-state" chamber pressure variation, with the effect of a decreasing pulse merely introducing a multiplicative factor. Also present is the implication that all frequency components decrease at the same rate. The frequency spectrum thus obtained for the same test run as above is shown in Fig. 12,

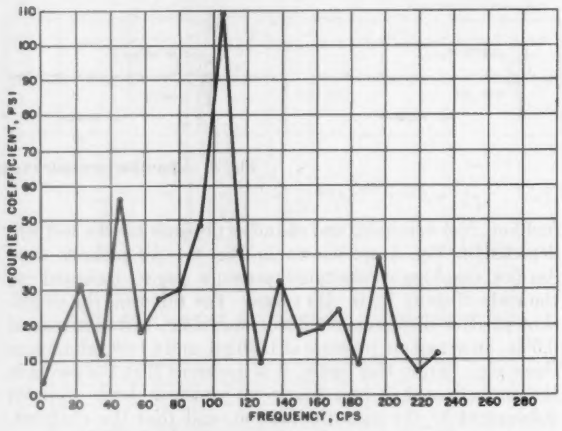


**Fig. 12 Modified frequency spectrum**

which reveals that the relative importance of the various modes is essentially unchanged by this modification, except for a general decrease in the amplitude of low-frequency components.

A further refinement of the frequency spectrum analyses is to determine a separate decrement rate for each of the various frequencies present. Since no readily applicable theoretical method for obtaining this information from experimental data is available, it becomes necessary to use special instrumentation designed for this purpose. One such instrument is the Mirragraph, which photographs the pressure trace and scans the photograph for pressure components in each frequency interval, thus making possible the determination of a separate decrement rate for each frequency range.

Fig. 13 shows a series of pressure traces obtained from the Mirragraph record of a test in which the propellant line orifices were the stabilizing devices. From this figure it is apparent that both the maximum amplitude and decrement rate are different for each frequency band. For the present series of tests, the decrement rate for each frequency range was determined by applying the method of least squares to the peaks from the time at which the maximum amplitude was reached on the pressure trace to the time at which noise level was reached on the individual frequency band trace. Since Fig. 10 indicated that the decrement rate varied

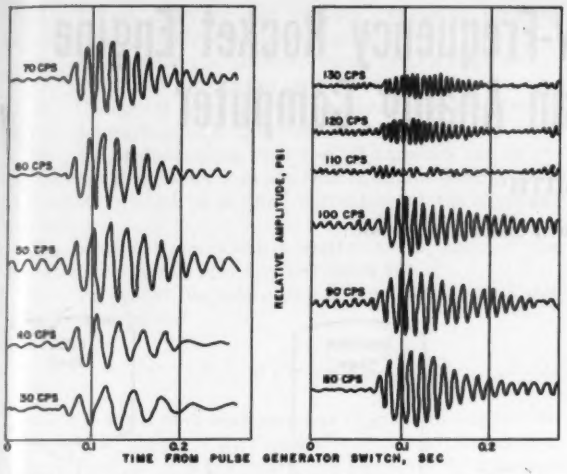


Fig. 13 Mirragraph record of typical pressure oscillation

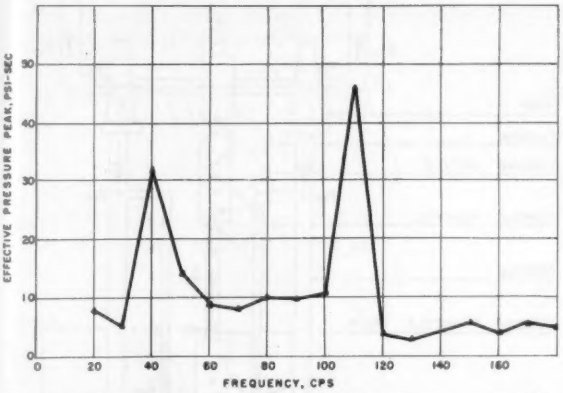


Fig. 14 Mirragraph analysis of typical pressure oscillation

linearly with amplitude of the initial pressure pulse, it was postulated that the variation of the ratio of initial pulse to decrement rate with frequency should give an indication of relative importance of the various frequencies. Fig. 14 shows this variation for the data given in Fig. 13. This initial test indicates predominant frequencies of 40 cps and 110 cps, which compare favorably with the resonant peaks at 47 cps and 104 cps in Fig. 11, which is the Fourier analysis for a similar configuration.

## Conclusions

As a result of this experimental investigation of combustion stability, the following conclusions can be drawn:

1. The transmission of pressure waves in the propellant lines of a liquid propellant combustor is an important factor in the stability of the rocket system.
2. The technique of pulsing the propellant flow, combined with the theoretical concept of the decrement rate of chamber pressure oscillations, is an effective means of determining the relative stability of various rocket systems.
3. The stability of a given rocket system can be increased either by inserting devices in the lines which will increase the inductance or suppress the resonant peaks, or by using a propellant with a shorter combustion time lag.
4. The decrement rate for a given configuration varies linearly with the amplitude of the pressure pulse.
5. There appears to exist in a rocket system a coupling of structural vibration and hydraulic oscillation. Thus, early testing of the rocket system with the flight structural configuration would be desirable.

## Acknowledgment

The invaluable assistance of the following members of the Liquid Engine Division of the Aerojet-General Corporation is gratefully acknowledged: D. M. Tenenbaum, L. Shenfil, W. A. Murray, and M. B. Cooley.

## References

1 Minorsky, N., "Self-Excited Oscillations in Systems Possessing Retarded Actions," *Journal of Applied Mechanics*, vol. 9, 1942, p. 65.

2 Summerfield, M., "A Theory of Unstable Combustion in Liquid Propellant Rocket Systems," *Journal of the American Rocket Society*, vol. 21, 1951, p. 108.

3 Crocco, L., "Aspects of Combustion Stability in Liquid Propellant Rockets," *Journal of the American Rocket Society*, vol. 21, 1951, p. 163; vol. 22, 1952, p. 7.

4 Tsien, H. S., "Servo-Stabilization of Combustion in Rocket Motors," *Journal of the American Rocket Society*, vol. 22, 1952, p. 256.

5 Marble, F. D. and Cox, D. W., Jr., "Servo-Stabilization of Low-Frequency Oscillations in a Liquid Bipropellant Rocket System," *Journal of the American Rocket Society*, vol. 22, 1952, p. 78.

6 Lee, Y. C., Gore, M. R., and Ross, C. C., "Stability and Control of Liquid-Propellant Rocket Systems," *Journal of the American Rocket Society*, vol. 23, 1953, p. 75.

7 Thomson, W. T., "Transmission of Pressure Waves in Liquid Filled Tubes," *Proceedings of the First U. S. National Congress of Applied Mechanics*, J. W. Edwards, Ann Arbor, Michigan, 1952, p. 927.

8 Sabersky, R. H., "Effect of Wave Propagation in Feed Lines on Low Frequency Rocket Instability," *Journal of the American Rocket Society*, vol. 24, 1954, p. 172.

9 Olson, H. F., "Dynamical Analogies," D. Van Nostrand Co., Inc., New York, 1943.

---

## Stabilization of Low-Frequency Oscillations of Liquid Propellant Rockets with Fuel Line Stabilizer

(*Continued from page 33*)

## References

1 "Aspects of Combustion Stability in Liquid Propellant Rocket Motors," by Luigi Crocco, *Journal of the American Rocket Society*, vol. 21, Nov. 1951, p. 163.

2 "Low Frequency Combustion Instability in Liquid Rockets with Different Nozzles," by Sin-I Cheng, presented at Annual Meeting of the American Rocket Society, Dec. 1953.

3 "Servo-Stabilization of Combustion in Rocket Motors," by H. S. Tsien, *Journal of the American Rocket Society*, vol. 22, Sept. 1952.

4 "Stability of Flow in Rocket Motor," by D. R. Gunder and D. R. Friant, *Journal of Applied Mechanics*, vol. 17, 1950.

5 Discussion of the paper of Reference 4, by M. Yachter, *Journal of Applied Mechanics*, vol. 18, 1951.

6 "A Theory of Unstable Combustion in Liquid Rocket Systems," by M. Summerfield, *Journal of the American Rocket Society*, vol. 21, Sept. 1951, p. 108.

7 "Servo-Stabilization of Low Frequency Oscillations in a Liquid Bipropellant Rocket Motor," by F. Marble and D. W. Cox, Jr., *Journal of the American Rocket Society*, vol. 23, Mar. 1953.

8 "Stability and Control of Liquid Propellant Rocket Systems," by Y. C. Lee, M. R. Gore, and C. C. Ross, *Journal of the American Rocket Society*, vol. 23, Mar. 1953.

9 "Servo-Stabilization of Low Frequency Oscillations in Liquid Propellant Rocket Motors," by F. E. Marble, presented at Brooklyn Symposium on Combustion Instability in Liquid Rocket Engines, Oct. 1953. (This paper is unclassified, but the Proceedings of the Symposium is confidential.)

10 "Theory of Combustion Instability in Liquid Rockets," by Luigi Crocco and Sin-I Cheng, Monograph, AGARD, NATO, chap. 2, sec. 7, to be published soon.

11 "Unconditional Stability of Low-Frequency Oscillation in Liquid Rockets," by Sin-I Cheng, *Journal of the American Rocket Society*, vol. 24, Sept.-Oct. 1954.

# Perturbation Analysis of Low-Frequency Rocket Engine System Dynamics on an Analog Computer

B. N. SMITH[1]

North American Aviation, Inc., Canoga Park, Calif.

**The synthesis of automatic controls for rocket engine systems requires information concerning the open loop frequency and transient response of such systems. This paper is concerned with the formulation of a mathematical model of a rocket engine system and the simulation of this model on an analog computer. Perturbation equations and computer circuit are developed for a pump-fed bipropellant system with turbine throttle valve area as the input variable. The frequency response of a typical system and the use of the computer model for estimating the effects of variations in the dimensions of interacting components on the frequency response are discussed.**

## Introduction

THE synthesis of automatic controls for rocket engine systems requires information concerning the open loop frequency and transient response of such systems. Simulation of rocket engine system dynamics on an analog computer economically aids the selection of control transfer functions and provides a theoretical framework which extends the scope of the usually limited test data available. The complex system consisting of a large number of relatively simple relations used to represent the rocket engine system can be explored adequately only with a model of the system made up of simple and reliable components such as provided by an electronic analog computer. The analysis of such a model is illustrated by a perturbation analysis of a bipropellant, pump-fed, gas turbine driven rocket engine system.

## Description of System

### *Rocket Engine System*

A typical liquid bipropellant rocket engine system is illustrated in Fig. 1. The thrust chamber is turbopump fed, with the fuel and oxidizer for the gas turbine combustor bled from the pump discharges. For the purposes of this analysis it is assumed that a control is to be designed to maintain the rocket engine at rated thrust conditions by sensing thrust chamber pressure and manipulating a turbine throttle valve. The variable representing the valve is the effective flow area through the valve.

The problem of this paper is, then, the calculation of the thrust chamber pressure variation due to turbine throttle valve variation.

The major assumptions made in setting up the mathematical model of the rocket engine system are:

1. The rocket engine system can be represented by a lumped parameter model.

2. The frequencies of interest ($\omega$) are low enough and the combustion time delays ($\delta$) are small enough that the phase shift ($\omega\delta$) so introduced can be neglected. (Consideration of the Laplace transform pair $f(t-\delta)$ and $e^{-s\delta}F(s)$ shows that for sinusoidal inputs $e^{-j\omega\delta}$ contributes a phase shift $\omega\delta$. See Equation [5] below.)

3. All flows except that through the turbine throttle valve are incompressible. The flow through the turbine throttle valve consists of an isentropic expansion followed by an increase in temperature at constant pressure to the inlet temperature.

4. All gases behave according to the equation of state for a perfect gas.

5. Average gas properties exist throughout the entire thrust chamber and turbine combustor volumes.

6. Thrust chamber temperature is constant.

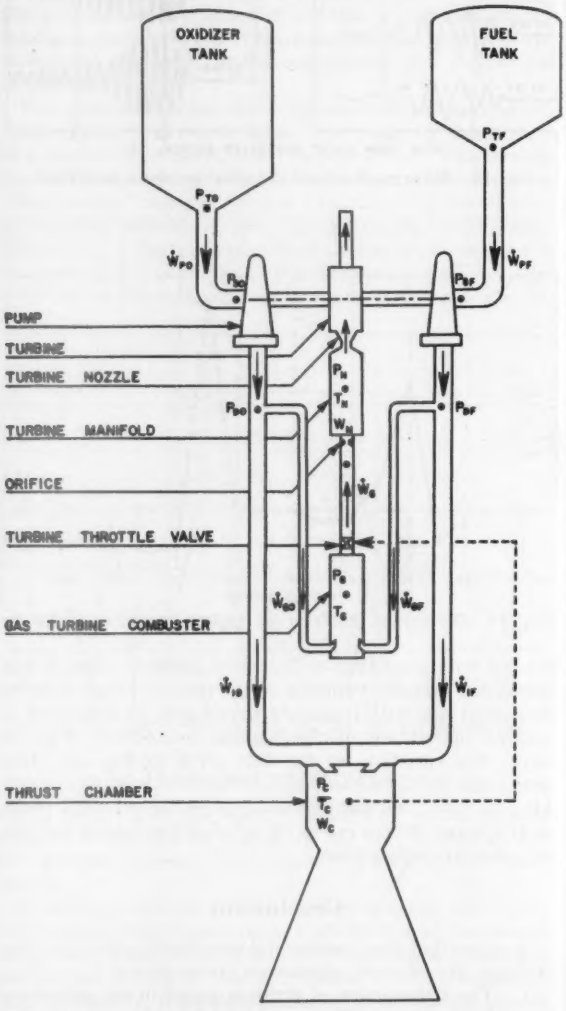


Fig. 1 Liquid bipropellant rocket engine system schematic

Presented at the ARS 25th Anniversary Fall Meeting, Chicago, Ill., Sept. 20, 1955.

[1] Supervisor, Dynamics, Rocketdyne Division.

7. Thrust chamber and turbine combustor injectors consist of single orifices for each propellant.
8. The variation of turbine pressure ratio is neglected.
9. Propellant tank outlet pressures are constant.
10. Changes of state in the turbine manifold are isentropic.
11. All mechanical components are inelastic.
12. The instantaneous values of all variables can be expressed as the algebraic sum of a time invariant portion and a perturbation which is a small percentage of the invariant portion.

The relations from which a mathematical model of the rocket engine system may be constructed are:

(A) Propellant line and orifice flow equations (see Table 1 for nomenclature)

$$P_1 - P_2 = K_{R1}\dot{W}^2 + K_{L1}\frac{d\dot{W}}{dt} \quad \ldots\ldots [1]$$

where $K_{R1}$ is the fluid resistance and $K_{L1}$, accounting for the effect of fluid inertia, is the summation of terms $l/Ag$ between points 1 and 2. ($l$ is the length of a section of fluid passage whose cross-sectional area is $A$. $g$ is gravitational acceleration.)

(B) Subsonic gas flow through an orifice or valve (neglecting the inertia of the gas in the line)

$$\dot{W} = \frac{K_2 P_2 A_v}{\sqrt{T_1}}\sqrt{\left(\frac{P_1}{P_2}\right)^{[(\gamma-1)/\gamma]}\left[\left(\frac{P_1}{P_2}\right)^{[(\gamma-1)/\gamma]} - 1\right]} \quad \ldots [2]$$

$$K_2 = C\sqrt{\left(\frac{2g}{R}\right)\left(\frac{\gamma}{\gamma-1}\right)}$$

where $C$ is a number such that $0 \leqq C \leqq 1$.

(C) Equation of state of a perfect gas

$$P = K_3 WT \quad \ldots\ldots [3]$$

where

$$K_3 = \frac{R}{V}$$

(D) Nozzle flow equation

$$\dot{W} = \frac{K_4 P_1}{\sqrt{T_1}} \quad \ldots\ldots [4]$$

where

$$K_4 = CA_N\left(\frac{2}{\gamma+1}\right)^{[\gamma/(\gamma-)]}\left[\frac{g\gamma(\gamma+1)}{2R}\right]^{1/2}$$

(E) Continuity equation

$$\frac{dW(t)}{dt} = \sum \dot{W}_i(t - \delta_i) - \sum \dot{W}_e(t) \quad \ldots\ldots [5]$$

If $\delta_i$ can be neglected

$$\frac{dW}{dt} = \sum \dot{W}_i - \sum \dot{W}_e$$

If the weight of fluid stored is negligible

$$\sum \dot{W}_i = \sum \dot{W}_e$$

(F) Gas temperature–mixture ratio relation

$$T = T\left(\frac{\dot{W}_0}{\dot{W}_F}\right)$$

which is approximated by drawing a tangent to the curve at the operating point so that

$$T = T_m\left(\frac{\dot{W}_0}{\dot{W}_F}\right) + T_b \quad \ldots\ldots [6]$$

(G) Turbine power equation

$$\dot{E}_t = \dot{W}_t h_t \eta_t,$$

which if

$$\dot{W}_t \propto \frac{P_N}{\sqrt{T_N}} \text{ and } h_t \propto T_N$$

$$\dot{E}_t = K_7 P_N \sqrt{T_N}\eta_t \quad \ldots\ldots [7]$$

where

$$K_7 = K_4\left(\frac{R}{J}\right)\left(\frac{\gamma}{\gamma-1}\right)\left[1 - \left(\frac{\bar{P}_e}{\bar{P}_N}\right)^{[(\gamma-1)/\gamma]}\right]$$

(H) Turbine efficiency, which is a function of the ratio of turbine wheel peripheral speed to jet speed and which can be approximated by

$$\eta_t = \eta_m K_8 \frac{N_t}{\sqrt{T_N}} + \eta_b \quad \ldots\ldots [8]$$

if wheel speed is $\propto N_t$ and jet speed is $\propto \sqrt{h_t} \propto \sqrt{T_N}$

$$K_8 = r_t \Big/ \sqrt{2gR\left(\frac{\gamma}{\gamma-1}\right)\left[1 - \left(\frac{\bar{P}_e}{\bar{P}_N}\right)^{[(\gamma-1)/\gamma]}\right]}$$

where $r_t$ is turbine wheel pitch radius.

(I), (J), (K), (L), and (M) Centrifugal pump head and power equations, which are conveniently expressed in terms of the dimensionless quantities $\Psi$, $\Phi$ (Ref. 7) and $X$ (Ref. 8) so that for pump head $\Psi = \Psi(\Phi)$. For a tangent to the curve at the operating point

$$\Psi = \Psi_m \Phi + \Psi_b \quad \ldots\ldots [9]$$

$$\Psi = K_{10}\left[\frac{P_D - P_S}{N_P^2}\right] \quad \ldots\ldots [10]$$

$$K_{10} = \frac{g}{\rho r_P^2}$$

and

$$\Phi = K_{11}\left[\frac{\dot{W}_P}{N_P}\right] \quad \ldots\ldots [11]$$

$$K_{11} = \frac{1}{A_P r_P \rho}$$

where $A_P$ is the pump impeller peripheral area.

For pump power

$$X = X(\Phi) \text{ and } X = X_m\Phi + X_b \quad \ldots\ldots [12]$$

where

$$X = K_{13}\left[\frac{\dot{E}_P}{N_P^3}\right] \quad \ldots\ldots [13]$$

$$K_{13} = \frac{1}{\rho A_P r_P^3}$$

$\Psi(\Phi)$ and $X(\Phi)$ are obtained empirically for a particular pump.

(N) Available power for accelerating the pumps

$$I_g N_P \frac{dN_P}{dt} = \eta_g \dot{E}_t - \dot{E}_P \quad \ldots\ldots [14]$$

(O) Isentropic change of state of gas stored in turbine manifold volume

$$T = K_{15} P^{[(\gamma-1)/\gamma]} \quad \ldots\ldots [15]$$

### *Linearization of Model*

A direct analysis of the nonlinear mathematical model outlined is possible by an extension of the computing techniques described below. However, in this paper a "small motion" (perturbation) analysis is used which, although theoretically valid only for infinitesimal motions, yields information of practical value for changes of appreciable magnitude in the vicinity of steady-state conditions.

The linearization is accomplished by taking differentials of all equations and assuming that the differentials in the resulting equations are the variables. A further modification of the equations may be made during the linearization procedure which aids the numerical computations. The variables may be nondimensionalized with respect to their steady-state values. Thus, if $dX$ is a variable obtained as a result of the linearization procedure, the nondimensional form is $dX/\overline{X} = x$. $x$ is the variation in $X$ expressed as a percentage of $X$.

Applying the linearization procedure to Equation [1]

$$dP_1 - dP_2 = 2K_{R1}\dot{W}d\dot{W} + K_{L1}d\left(\frac{d\dot{W}}{dt}\right)$$

The first term on the right-hand side of this equation results from

$$d(K_{R1}\dot{W}^2) = \frac{\partial(K_{R1}\dot{W}^2)}{\partial\dot{W}}\,d\dot{W}$$

where the partial derivative is evaluated at steady state so that $\dot{W} = \dot{W}$.

The second term results from

$$d\left(K_{L1}\frac{d\dot{W}}{dt}\right) = \frac{\partial[K_{L1}(d\dot{W}/dt)]}{\partial(d\dot{W}/dt)}\,d(d\dot{W}/dt)$$

Then

$$[\overline{P}_1]\frac{dP_1}{\overline{P}_1} - [\overline{P}_2]\frac{dP_2}{\overline{P}_2} = [2K_{R1}\dot{W}^2]\frac{d\dot{W}}{\dot{W}} + [K_{L1}\dot{W}]\frac{d(d\dot{W}/dt)}{\dot{W}}$$

and

$$p_1 - \left[\frac{\overline{P}_2}{\overline{P}_1}\right]p_2 = \left[\frac{2K_{R1}\dot{W}^2}{\overline{P}_1}\right]\dot{w} + \left[\frac{K_{L1}\dot{W}}{\overline{P}_1}\right]\frac{d\dot{w}}{dt}$$

Or since

$$\left[\frac{2K_{R1}\dot{W}^2}{\overline{P}_1}\right] \equiv 2\left[1 - \frac{\overline{P}_2}{\overline{P}_1}\right]$$

$$p_1 - \left[\frac{\overline{P}_2}{\overline{P}_1}\right]p_2 = 2\left[1 - \frac{\overline{P}_2}{\overline{P}_1}\right]\dot{w} + \left[\frac{K_{L1}\dot{W}}{\overline{P}_1}\right]\frac{d\dot{w}}{dt} \quad \text{[1a]}$$

Similarly we have

$$\dot{w} = a_v - \frac{1}{2}\theta_1 + \left\{\left(\frac{\gamma-1}{\gamma}\right)\left[\frac{(\overline{P}_1/\overline{P}_2)^{[(\gamma-1)/\gamma]} - \frac{1}{2}}{(\overline{P}_1/P_2)^{[(\gamma-1)/\gamma]} - 1}\right]\right\}p_1 - \left\{\left(\frac{\gamma-1}{\gamma}\right)\left[\frac{(\overline{P}_1/\overline{P}_2)^{[(\gamma-1)/\gamma]} - \frac{1}{2}}{(\overline{P}_1/P_2)^{[(\gamma-1)/\gamma]} - 1}\right] - 1\right\}p_2 \quad \text{[2a]}$$

$$p = w + \theta \quad \text{[3a]}$$

$$\dot{w} = p_1 - \tfrac{1}{2}\theta_1 \quad \text{[4a]}$$

$$\frac{dw}{dt} = \Sigma\left[\frac{\dot{W}_i}{\dot{W}}\right]\dot{w}_i - \Sigma\left[\frac{\dot{W}_e}{\dot{W}}\right]\dot{w}_e \quad \text{[5a]}$$

$$\theta = \left[1 - \frac{T_b}{\overline{T}}\right][\dot{w}_O - \dot{w}_F] \quad \text{[6a]}$$

$$\dot{e}_t = p_N + \tfrac{1}{2}\theta_N + \epsilon_t \quad \text{[7a]}$$

$$\epsilon_t = \left[1 - \frac{\eta_b}{\overline{\eta}}\right][n_t = \tfrac{1}{2}\theta_N] \quad \text{[8a]}$$

$$\psi = \left[1 - \frac{\Psi_b}{\overline{\Psi}}\right]\phi \quad \text{[9a]}$$

$$\psi = \left[\frac{1}{1 - (\overline{P}_S/\overline{P}_D)}\right]p_D - \left[\frac{\overline{P}_S/\overline{P}_D}{1 - (\overline{P}_S/\overline{P}_D)}\right]p_S - 2n_P \quad \text{[10a]}$$

$$\phi = \dot{w}_P - n_P \quad \text{[11a]}$$

$$\chi = \left[1 - \frac{X_b}{\overline{X}}\right]\phi \quad \text{[12a]}$$

$$\chi = \dot{e}_P - 3n_P \quad \text{[13a]}$$

$$\frac{dn_P}{dt} = \left[\frac{\dot{E}_P}{I_p\overline{N}_P}\right][\dot{e}_t - \dot{e}_P] \quad \text{[14a]}$$

$$\theta = \left[\frac{\gamma-1}{\gamma}\right]p \quad \text{[15a]}$$

### *Analog Computer Circuit*

The completed mathematical model of the rocket engine system of Fig. 1 consists of an array of linear algebraic and differential equations with constant coefficients assembled from the types of equations listed above. An analog computer presents a practical means of solving the array for the dynamics of the system.

The simultaneous solution of the system equations is accomplished by first expressing the array of equations symbolically in a block diagram and then interpreting the block diagram as a circuit schematic of an electronic model of the equations (and hence an electronic model of the system). References (1) and (2) provide an exposition of the details of analog computer circuitization.

Temporarily ignoring the existence of the coefficients in the linear equations and adopting the conventions of Fig. 2, a complete block diagram for the rocket engine of Fig. 1 can be constructed, Fig. 3, which implies all the functional relationships found on examining the equations. Locate, for example, the rate of change of line flow variation $\dot{w}_{GO} \equiv d\dot{w}_{GO}/dt$ in Fig. 3. It is evident that $w_{GO}$ is formed by $-[-p_{DO} + p_G + \dot{w}_{GO}]$, which is readily checked by reference to Fig. 1 for the physical location of the relation and Equation [1a] which can be rewritten

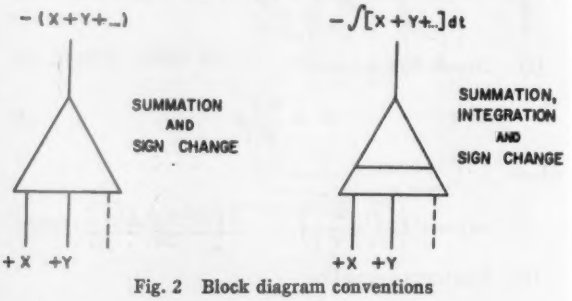


Fig. 2 Block diagram conventions

$$\dot{w} = \frac{\overline{P}_1}{K_{L1}\dot{W}}\int\left\{p_1 - \left[\frac{\overline{P}_2}{\overline{P}_1}\right]p_2 - 2\left[1 - \frac{\overline{P}_2}{\overline{P}_1}\right]\dot{w}\right\}dt$$

An interesting feature of the block diagram of Fig. 3 is the correspondence between sections of the diagram and sections of the system schematic (Fig. 1). Note, for example, the location of the oxidizer system in the two figures.

## Discussion

An analog computer wired per the circuit schematic of Fig. 3 represents a physical model of the rocket engine system of

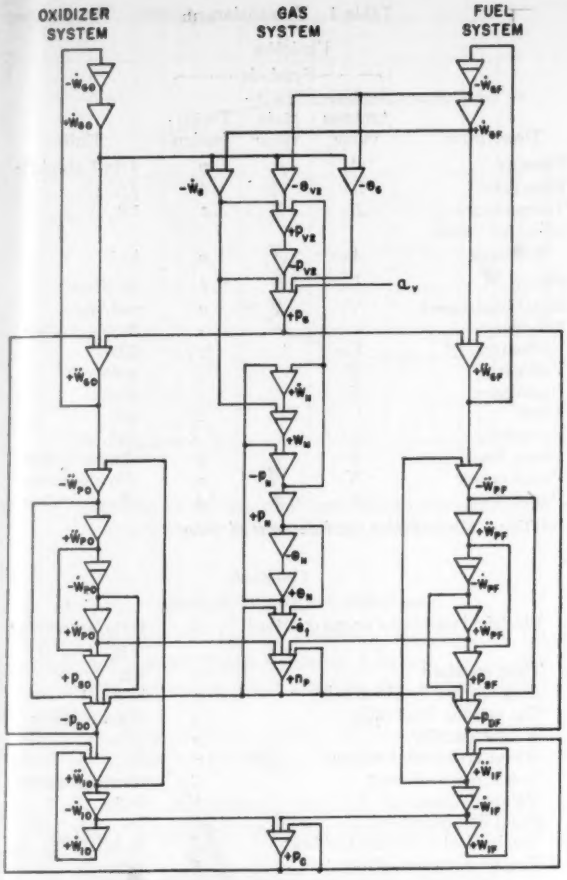


Fig. 3 Block diagram and computer circuit schematic

Fig. 1. The computer model will behave more or less like the actual rocket engine system depending on the extent to which the mathematical approximation presents a true picture of that system and the extent to which the computer can perform the mathematical operations indicated. Experience with this problem has shown that an analog computer can be made to perform the operations indicated with an accuracy at least as great as that consistent with (*a*) the basic data given, (*b*) the detail with which the problem can be outlined

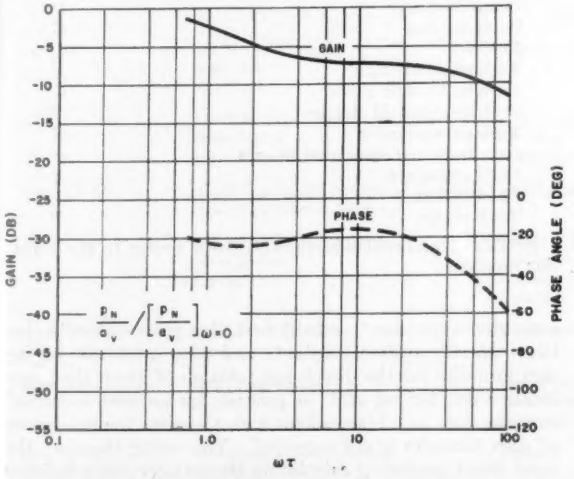


Fig. 5a Response of turbine inlet pressure to sinusoidal perturbations in turbine throttle valve area

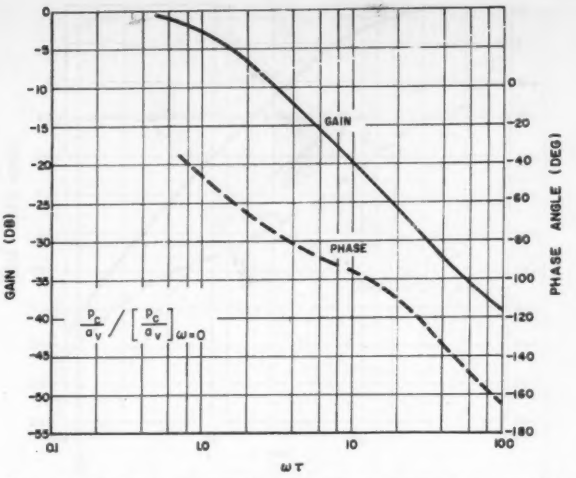


Fig. 4a Response of thrust chamber pressure to sinusoidal perturbations in turbine throttle valve area

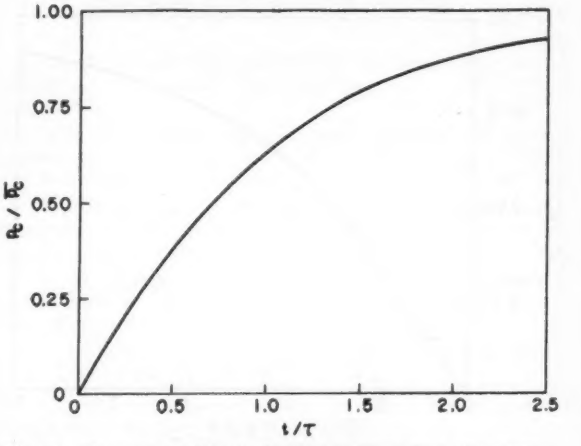


Fig. 4b Response of thrust chamber pressure to a step perturbation in turbine throttle valve area

analytically; and (*c*) preliminary control function design.

The attenuation and phase shift of the thrust chamber pressure variations with respect to sinusoidal turbine throttle valve area variations are presented in Fig. 4a. The transient

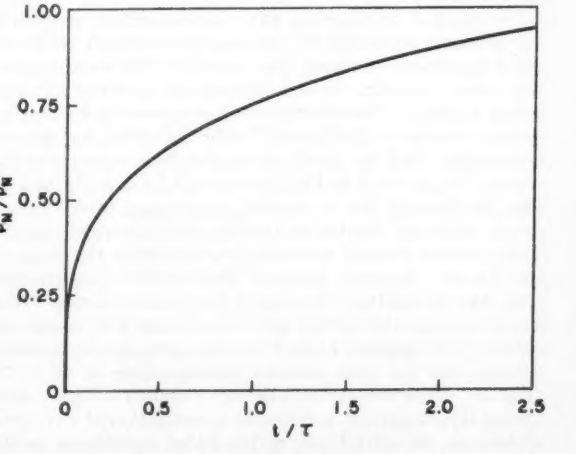


Fig. 5b Response of turbine inlet pressure to a step perturbation in turbine throttle valve area

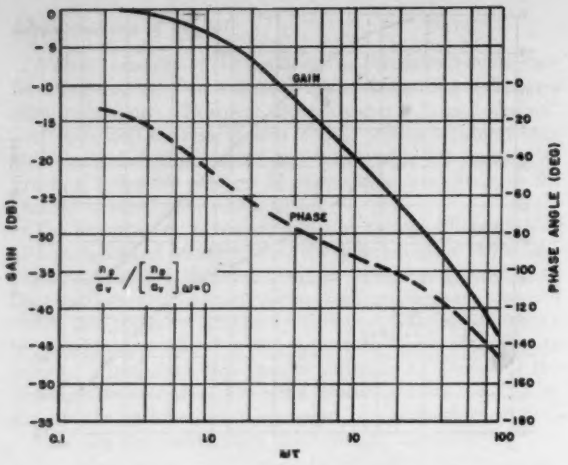


**Fig. 6a Response of pump speed to sinusoidal perturbations in turbine throttle valve area**

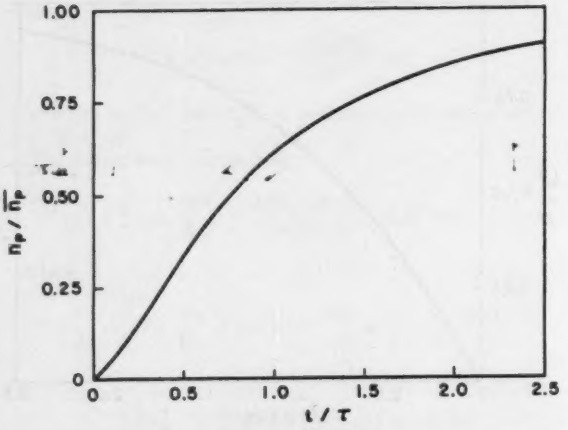


**Fig. 6b Response of pump speed to a step perturbation in turbine throttle valve area**

response of thrust chamber pressure to a step perturbation in turbine throttle valve area is plotted in Fig. 4b. These transfer characteristics of the rocket engine system were measured from a computer model for the synthesis of the required thrust control function.

The effect of variations in any system constant on system response may be studied by varying the coefficient ($s$) in the set of equations containing this constant. On the computer this means recording model response for a series of coefficient settings. The investigation of several rocket engine systems similar to the system under discussion has shown, for example, that the maximum lagging time constant in the system (i.e., $\omega\tau = 1$ in Figs. 4a through 7a and $t/\tau = 1$ in Figs. 4b through 7b) is directly proportional to the turbopump rotational inertia for turbine throttle valve inputs. This fact was checked by noting the change in the shape of the thrust chamber pressure attenuation characteristic (Fig. 4a) for arbitrary settings of turbopump inertia. In a similar manner the turbine manifold volume was varied and successive attenuation plots of turbine inlet pressure variation showed that the time constant corresponding to $\omega\tau = 77$ (Fig. 5a) varies directly with turbine manifold volume. Following this procedure, a complete investigation of any given system can be carried out, giving added significance to the selection of system dimensions.

In conclusion it must be pointed out that while the above computer experiments established the proportionality between specific system constants and time constants, no design formulas for the direct computation of given time constants were derived and, in general, for an interconnected complex such as a bipropellant rocket engine, the emergence of such formulas is not expected. This being the case, the most direct method of calculating the transfer characteristics of rocket engine systems is by means of analog computer models of such systems.

**Table 1 Nomenclature**

*Variables*

| Description | Symbols: Instantaneous value | Symbols: Steady-state value | Symbols: Perturbation | Units |
|---|---|---|---|---|
| Pressure | $P$ | $\bar{P}$ | $p$ | #/in.² absolute |
| Flow rate | $W$ | $\bar{W}$ | $w$ | #/sec |
| Temperature | $T$ | $\bar{T}$ | $\theta$ | °R |
| Effective value flow area | $A_v$ | $\overline{A_v}$ | $a_v$ | in.² |
| Power | $\dot{E}$ | $\bar{\dot{E}}$ | $\dot{e}$ | in. #/sec |
| Rotational speed | $N$ | $\bar{N}$ | $n$ | rad/sec |
| Efficiency | $\eta$ | $\bar{\eta}$ | $\epsilon$ | dimensionless |
| Enthalpy | $h$ | .. | .. | Btu/# |
| Voltage | $E$ | .. | .. | volts |
| Impedance | $Z$ | .. | .. | ohms |
| Time | $t$ | .. | .. | sec |
| Frequency | $\omega$ | .. | .. | rad/sec |
| Pump head | $\Psi$ | $\bar{\Psi}$ | $\psi$ | dimensionless |
| Pump power | $X$ | $\bar{X}$ | $\chi$ | dimensionless |
| Pump flow | $\Phi$ | $\bar{\Phi}$ | $\phi$ | dimensionless |

NOTE: All variables are functions of time.

*Constants*

| Description | Symbols | Units |
|---|---|---|
| Electrical resistance or gas constant | $R$ | volts/ampere or in.-#/#-°R |
| Time constant | $\tau$ | sec |
| Acce'eration due to gravity | $g$ | in./sec² |
| Gas specific heat ratio | $\gamma$ | dimensionless |
| Weight density | $\rho$ | #/in.³ |
| Wheel or impeller radius | $r$ | in. |
| Discharge coefficient | $C$ | dimensionless |
| Volume of gas | $V$ | in.³ |
| Fluid line length | $l$ | in. |
| Mechanical equivalent of heat | $J$ | ft-#/Btu |
| Combustion time delay | $\delta$ | sec |

*Subscripts*

| Description | Symbol |
|---|---|
| Upstream or one | 1 |
| Downstream or two | 2 |
| Oxidizer | $O$ |
| Fuel | $F$ |
| Inlet | $i$ |
| Exit | $e$ |
| Slope | $m$ |
| Intercept | $b$ |
| Thrust chamber | $C$ |
| Injector | $I$ |
| Pump | $P$ |
| Pump discharge | $D$ |
| Pump suction | $S$ |
| Turbine | $t$ |
| Turbine nozzle inlet | $N$ |
| Turbine throttle valve | $v$ |
| Turbine manifold storage | $M$ |
| Turbine combustor | $G$ |
| Gear train and associated masses | $g$ |
| Fluid resistance | $R$ |
| Fluid inertia | $L$ |
| Tank outlet | $T$ |

NOTE: Numbered subscripts on the $K$'s refer to the Equation number.

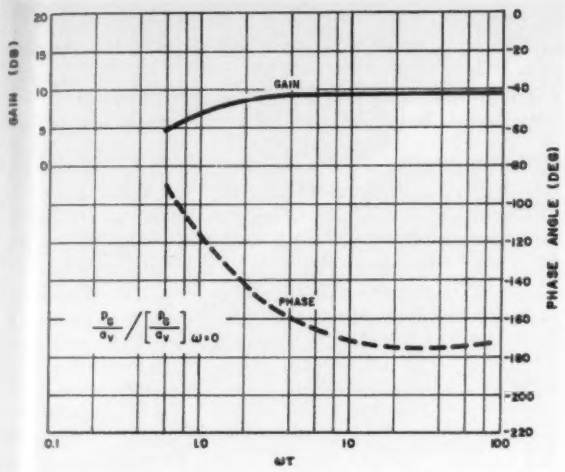


Fig. 7a Response of turbine combustor pressure to sinusoidal perturbations in turbine throttle valve area

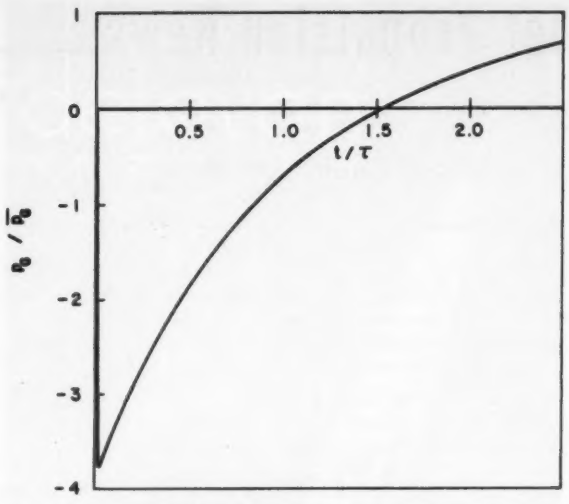


Fig. 7b Response of turbine combustor pressure to a step perturbation in turbine throttle valve area


## Acknowledgments

Acknowledgment is due the following members of the Rocketdyne Division, North American Aviation, Inc., whose aid in several capacities made possible the preparation of this paper:

M. C. Ek, Group Leader, Applied Mechanics, and G. P. Sutton, Group Leader, Preliminary Analysis, for their advice and encouragement

N. E. Wood, R. K. Seferian, and R. J. Bartholomew, Research Engineers in the Dynamics Unit for their valuable suggestions.

P. W. Hellwig, Barbara Morris, and Nora Lee Brown for their aid in the preparation of the manuscript.


## References


1 G. A. Korn and T. M. Korn, "Electronic Analog Computers," 1st ed., McGraw-Hill Book Company, Inc., New York, N. Y., 1952.

2 W. W. Soroka, "Analog Methods in Computation and Simulation," McGraw-Hill Book Company, Inc., New York, N. Y., 1954.

3 A. C. Hall, "Application of Frequency-Analysis Techniques to Hydraulic Control Systems," *Transactions of the ASME*, vol. 76, November 1954, p. 1245.

4 H. Chestnut and R. W. Mayer, "Servomechanisms and Regulations System Design," vol. I, John Wiley & Sons, Inc., New York, N. Y., 1951.

5 W. R. Ahrendt and J. F. Taplin, "Automatic Feedback Control," 1st ed., McGraw-Hill Book Company, Inc., New York, N. Y., 1951.

6 L. C. Lichty, "Thermodynamics," 2nd ed., McGraw-Hill Book Company, Inc., New York, N. Y., 1948.

7 A. J. Stepanoff, "Centrifugal and Axial Flow Pumps," John Wiley & Sons, Inc., New York, N. Y., 1948.

8 H. K. Georgius, Development of dimensionless pump power coefficient, North American Aviation, Inc., Unpublished Reports.


## ARS Meetings Calendar

| | | ARS Sessions | Technical Events Chairman | Abstracts Due |
|---|---|---|---|---|
| Jan. 24 | IAS Annual<br>Hotel Astor<br>New York | (see p. 51) | D. F. Ferris<br>Reaction Motors, Inc.<br>Denville, N. J. | .....<br>.....<br>..... |
| Mar. 14–16 | ASME Aviation Conference<br>Hotel Statler<br>Los Angeles | High temperatures<br>Rockets<br>Instrumentation | David Shonerd<br>Aerophysics Development Corp.<br>Box 949, Santa Monica, Calif. | ..... |
| May 23–25 | ASME-Engineering Institute of Canada<br>Mount Royal Hotel, Montreal | Guided missiles | ..... | Jan. 1, 1956 |
| June 17–21 | ARS-ASME Semi-Annual Meeting<br>Hotel Statler<br>Cleveland | Liquid rockets<br>Solid rockets<br>Ramjets<br>Satellites | Henry C. Burlage<br>Case Institute of Technology<br>10900 Euclid Avenue<br>Cleveland 6, Ohio | Jan. 15, 1956 |
| Sept. 17–21 | Seventh IAF Congress<br>Rome | Astronautics | ..... | Feb. 15, 1956 |
| Sept. 24–26 | ARS Fall Meeting<br>Buffalo | Propellants<br>Combustion<br>Telemetering | Harry Ferullo<br>Bell Aircraft Corp.<br>P. O. Box 1, Buffalo 5, N. Y. | Feb. 15, 1956 |
| Nov. 25–30 | ARS-ASME Annual Meeting<br>New York | General | ..... | May 15, 1956 |

# Jet Propulsion News

**Alfred J. Zaehringer**, American Rocket Company, *Associate Editor*
**Norman L. Baker**, Indiana Technical College, *Contributor*

## Rockets and Guided Missiles

VANGUARD is the name of the U. S. earth satellite project. The project, a joint Army-Navy-Air Force venture under Navy command, has awarded contracts to General Electric Co. for the propulsion system and to Glenn L. Martin Co. for the vehicle. The minimum program calls for launching 10 instrumented satellites—the size and configuration of which have not yet been announced.

● RV-A-10 is the General Electric large solid propellant missile (photo). A series of the missiles was launched from U.S.A.F. Long Range Proving Ground, Florida. The tests were successful and helped demonstrate the advantages of solid propellants over liquid propellants for certain missile applications. No other data were given, but it was stated that the RV-A-10 is one of the world's largest solid propellant rocket.

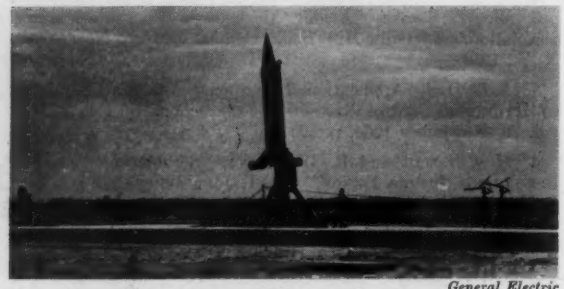

*General Electric*

**RV-A-10**

● The Army is currently seeking sites for construction of housing for NIKE missile crews. Priority in the program will be given to isolated NIKE sites and in those areas where reasonable rental housing is not available. Since NIKE crews must be readily available in emergencies, the housing units will be constructed in the immediate vicinity of the guided missile installations. It was recently revealed that NIKE solid propellant booster cases have been successfully fabricated from reinforced plastics (probably epoxy or polyester resins). The new cases exhibit unusually high strength-to-weight ratios, ease in fabrication, do not need critical materials, and may be made frangible to minimize booster drop-off damage in built-up areas. One limiting factor is now cost.

● Ground handling and price are two good economic parameters in selecting rocket propellants. H. R. Biederman and H. M. Kindsvater of Lockheed Missile Systems Division compared a rocket system using liquid oxygen (LOX) and IRFNA (inhibited red fuming nitric acid) as oxidants with JP-4 as fuel. Total systems cost was twice as great for LOX on a small scale while about the same for larger scale applications. In deciding whether to purchase LOX or to generate it on base, the breakeven point was over four years. Propellants were less than 15% of the system cost. Largest investment was due to installation.

● Another operational missile, the Air Force TM-61 Matador, is to see increased use. The 17th Tactical Missile Squadron has been placed into operation at Orlando AFB, Fla. A second Matador squadron is now in training there. Two other Matador squadrons are now deployed in Germany.

● Concrete was the warhead carried by the HONEST JOHN 3-ton rocket when it fired 6 miles over the lower slope of Mt. Fuji. The firing was the first test firing in Japan. SERGEANT is going to be a big brother to HONEST JOHN. SERGEANT, with a solid propellant motor, may have range capabilities placing it in the CORPORAL class.

● At the recent ARS Los Angeles meeting, two interesting facets of missile range operation were brought to light. In 1947 at White Sands, two missiles wandered off range and resulted in establishment of improved safety practices. The flight of wild missiles can now be terminated before they can become a threat to life or property. Missile capabilities are determined and safety provisions are made. During the last 5 years of missile testing at WSPG, the safety group has instrumented 275 missiles with no failures of electronic equipment and only one failure of associated equipment. Instrumenting rocket ranges is getting complex according to scientists at the U. S. Naval Ordnance Test Station, China Lake, Calif. Photography of missile flight is still not completely suitable. Cameras used are the Askania tracking camera and the Bowen fixed camera in conjunction with timing and control systems. Electronics is helping out, though, with the use of radars and telemetry. Accuracies of 1 part in $10^5$ are being asked for; 0.1 mil is now commonplace.

● At a recent demonstration at Fort Belvoir, Va., a 25,500 lb DC-3 took off with one engine completely throttled and windmilling and cleared a 50-ft obstacle in 3000 ft of runway. The plane (photo) was equipped with two Aerojet-General 15KS-1000-A1 smokeless rocket engines. Normal requirement under same conditions would have been 5000 ft of runway. Rocket installations are now planned for some 25 business aircraft and some will feature integral mounts.

*Aerojet-General*

**DC-3 makes take-off with two 15KS-1000 rockets**

● Guided missiles are fast bolstering our naval strength. TERRIER missile, which now has beam rider guidance, may be developed into a homing missile for low altitude antiaircraft. TERRIER, a two-stage rocket, now has a range of about 20 miles and a speed of about Mach 2.5. Booster of TERRIER is a solid propellant rocket by Allegany Ballistics Lab. Sustainer rocket is by the M. W. Kellogg Co. TERRIER is the result of a program begun by the Applied Physics Laboratory late in World War II to develop an antiaircraft weapon for shipboard use. Production of the missile was taken over by Convair at Pomona, Calif., in 1953. The *USS Boston*(CAG-1), will soon join the Atlantic Fleet as the Navy's first guided missile ship. Previous firings were made from the *USS Mississippi* (photo) late in 1954. The *Boston* carries a crew of 1635 men and is a sister ship to the *USS Canberra*. *Boston's* armament is two batteries of TERRIER's (two missiles per battery) with additional missiles being stored below decks. The batteries are mounted

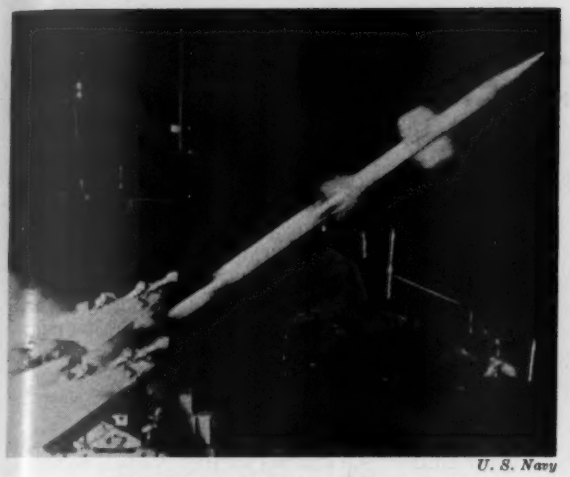

*U. S. Navy*

**TERRIER is fired from *USS Mississippi***

on the aft deck and operate in conjunction with guidance radar systems. The radar systems were built by the Reeves Instrument Corp. TRITON is another naval missile of unannounced characteristics that was developed under the BUMBLEBEE program which also developed the TERRIER and TALOS. The TALOS missile, ramjet-propelled, will be used to arm another light cruiser soon to join the fleet. Two submarines—the *USS Tunny* and the *USS Barbero*—are new guided missile launching submarines. The converted subs will be used to launch the REGULUS.

● Reliability of components is now the limiting factor in today's missiles, explains the Guided Missiles Committee of the Aircraft Industries Association. Efforts are being made by major designers and missile producers to improve the over-all reliability of missile systems. Improved reliability may be one of the factors in the FALCON step-up program at the Hughes Tucson, Ariz., plant. Production rate is now estimated at over 100 per month. Estimates as to present costs place the GAR-98 cost at between $25,000 to $50,000 each with an eventual large-scale production cost of $10,000 to $15,000 each.

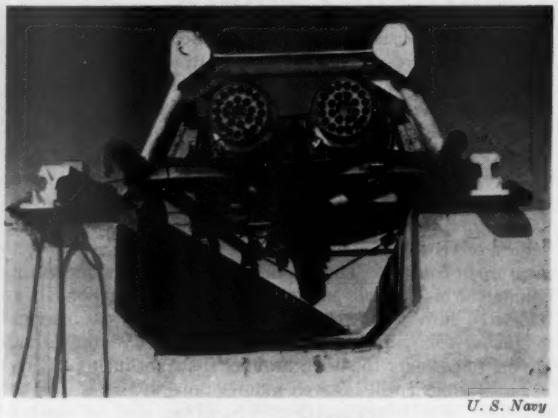

*U. S. Navy*

**Business end of SNORT**

● The SNORT rocket track at the Naval Ordnance Test Station has established a speed of 1280 mph. The photo shows the sturdy track construction with propelling rockets mounted on the sled. The "Y" water brake plow is seen projecting underneath.

CORRECTION: In the November 1955 issue it was erroneously reported that the AEROBEE had established a high altitude record of 180 miles.

# Space Flight Notes

**Kurt R. Stehling**, Naval Research Laboratory, Washington, D. C., *Contributor*

TWO sessions of the 25th Anniversary Annual Meeting of the AMERICAN ROCKET SOCIETY were devoted to the subjects of High Altitude Research and Space Flight. Because of the interest these papers attracted, they deserve analysis and comment in this column.

The first paper was entitled "On Applications of the Satellite Vehicle," by R. P. Haviland, General Electric Company, Schenectady, N. Y.

Mr. Haviland discussed the general utility of a satellite vehicle and listed the fields of potential usefulness: Mapping and Geodesy; Communications; Weather Charting and Forecasting; Research; Development of Space Flight.

The various fields of vision are listed for the satellite at various altitudes and flight paths. For instance, at 57 miles, 8 per cent of the earth is visible, while at 257 miles, 17 per cent is visible (approximately the whole of the United States). At 22,300 miles, 50 per cent is visible. However this field is reduced considerably (perhaps by $^3/_4$) for useful vision because of the grazing angle of incidence near the observed horizon and the subsequent atmospheric distortion.

*Mapping and Geodesy* is the first application covered in detail. It is suggested that the satellite could be used for triangulation surveys, tying together normal surveys on separate continents; also, a determination of the absolute value of "g" would be possible.

The resolving powers of various lenses are listed and it is shown that an 8-in. focal length camera with 5-in. film would completely photograph the earth in daylight with 900 photographs, with the vehicle in a polar orbit. Since recovery of the vehicle "would be quite a problem," the possibility of a video or facsimile transmission system is considered. The author states that the 400 line resolution of television would reduce the effective resolving power to $^1/_8$ with the 8-in. lens, with no reduction for the facsimile system with its effective 1000 lines per in. resolution.

*Communications.* Haviland outlines two justifications for the use of a satellite in the field of communications. The first would be as a relay station to permit long-range transmission of electromagnetic radiation normally limited to "line-of-sight." Extensive use of these newly available microwave channels would reduce the congestion which exists at present in useful long-range communication channels. The second use would be as a broadcasting station which would transmit FM and Video emissions to regions of the earth not normally accessible to ground station transmissions.

*Weather Charting and Forecasting.* The third listed major application of the orbital missile is that of weather survey and reconnaissance. The vehicle would have scanning equipment which would view the earth's atmosphere and show the location of clouds and weather fronts, precipitation and thunderstorm areas. With the satellite established as a reliable meteorological station, some of the present services such as Weather Ships, the Iceberg patrol, and Hurricane Hunter Flights could be suspended.

This review paper describes in a general way the commercial uses of an orbital vehicle. Certainly the layman finds these applications more conventional and easier to justify dollarwise than such enterprises as cosmic ray or magnetic field strength measurements. However, the latter fundamental scientific studies no longer need apologies and their necessity will undoubtedly provide the basis for small satellite utility.

Of the three discussed applications, Mapping, Communications, and Meteorology, the last seems the most feasible—at least within the near future. It is difficult to see how an orbital vehicle, even in a fixed position 22,000 miles above the earth's surface, can yield a much more accurate reference point for geodetic surveys than such existing bodies as the sun. These measurements have already approached accuracies approaching $^1/_{100}$ of 1 per cent and are reaching the point where instrument limitations and actual latitude variations, because of fluidity of the earth's crust, prevent greater refinements. Also, haze and dust in the atmosphere are already limiting the photogrammetric efforts of reconnaissance aircraft, except under unusual circumstances of dry, clear air or at low altitudes.

A paper entitled "Sun Follower for High Altitude Sounding Rocket," by D. D. Terwilliger and G. J. Granros, Aircraft Armaments Inc., Cockeysville, Maryland, describes a device built for the Naval Research Laboratory; its purpose is the tracking or following of the sun so that sunlight is constantly focused on the entrance pupil of a spectrograph located in the nose of a high altitude research rocket. Since high altitude vehicles, especially after engine shutoff, rarely have the goodness to maintain a constant attitude, it is necessary to devise instrumentation which will nullify the pitching and rolling of the vehicle. This is necessary, however, only when a recording instrument, such as a spectrograph, must be pointed continuously in one direction, in this case toward the sun.

The described instrument consists, in essence, of two pairs of photoelectric sun-detecting "eyes" for the control of the elevation and azimuth axes of the spectrograph. These eyes or photoelectric cells are mounted on rotating and tilting axes to compensate for rotation of the vehicle about two axes. A coarse eye searches for the sun, locks on, and brings the sun follower approximately in line with the sun. A vernier eye then keeps the follower accurately on the sun to within plus or minus 0.25 degrees.

The electrical outputs of the photoelectric eyes are passed through suitable resistor mixing networks into a servo amplifier and feedback system. When no sunlight falls on the eyes a servo loop is unbalanced and the amount of the unbalance is translated into an electric current which drives an elevation servo motor and an azimuth motor.

Three of these sun followers have been sent aloft in high altitude test vehicles; the first two in Aerobee rockets and the third in a Viking. The best results were obtained with the Viking; for 80 seconds of the flight path above 30 miles altitude, usable spectrographic data were obtained even though the vehicle rolled almost 180 rpm, 120 sec after take-off.

The appropriate attitude of an instrument in a rocket test vehicle or that of the vehicle itself is a difficult parameter to measure or control. There is no point in including measuring equipment in a vehicle payload if the instruments point in an undesired direction. It is difficult enough to interpret magnetic, solar, and cosmic ray telemetered data without having to consider the orientation of the transducing devices.

This problem will be even more serious in the case of the satellite. Sun followers, flywheels, gyros, and jet controls can all serve to orient a vehicle, either by reference to some external body or force, or responding to home-based command. However, these elements are not light and, if desired for inclusion in the vehicle, must share a large fraction of the payload.

Since sunlight is a readily available high energy (i.e., high light intensity) source, always available for a pole-to-pole orbiting vehicle, it can form a ready reference source; therefore some type of simple sun follower could possibly be used as an orientation control or indicator.

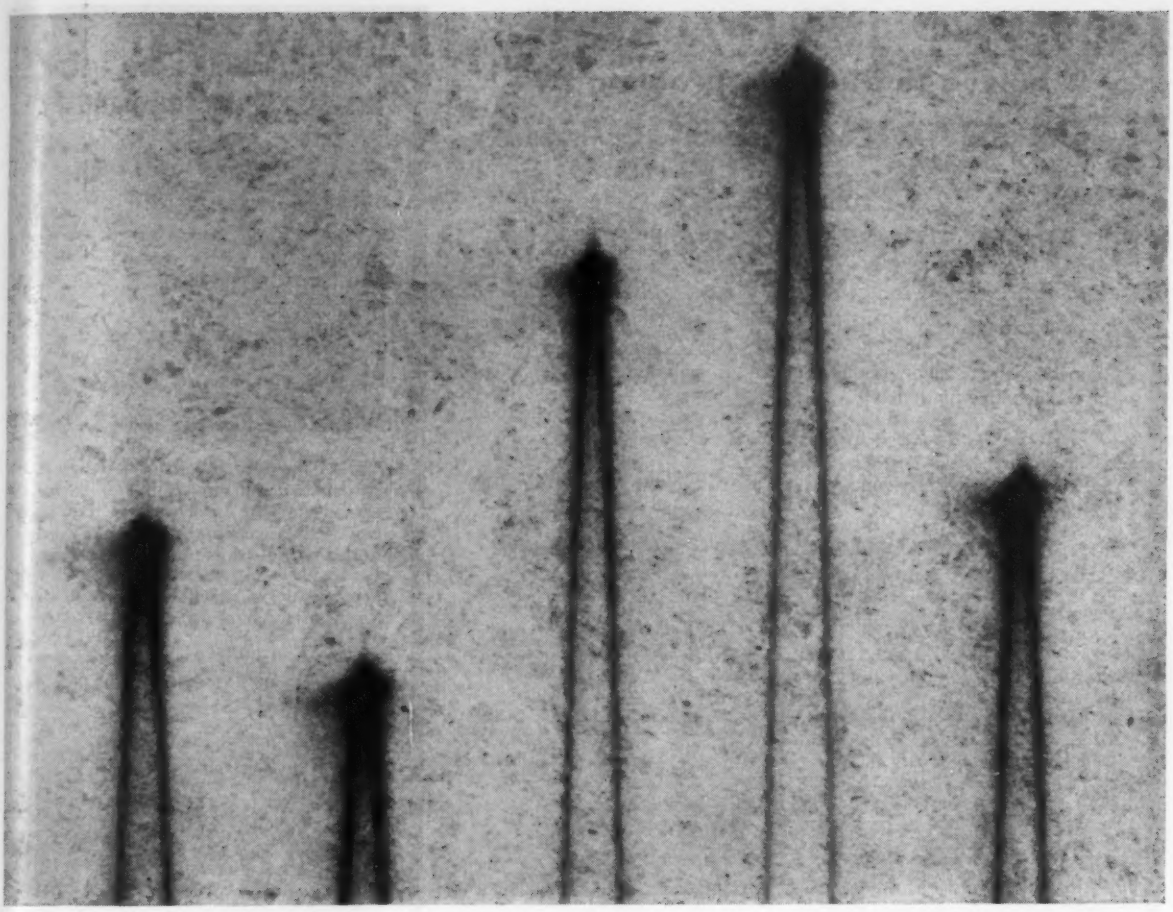

20× photomicrograph of high-spot-velocity trace on Kodak Linagraph 1344 Paper.

# Kodak Linagraph 1344 Paper is new

## *. . . you'll want to try it*

***It's a high speed paper:*** You can run it at variable paper speeds up to 400 in./sec., with galvanometer speeds up to 2,000 cycles/sec., with spot velocities up to 1,000 in./sec. and still get good, readable traces.

***It's thin:*** *Kodak Linagraph 1344 Paper* has a new ultra-thin base. No other paper gives more footage to a given roll diameter. High-strength stock, too, with no splices in any roll less than 1,000 feet long. There's a special toothing agent in the emulsion that makes it easy to write on with ink or pencil.

***It doesn't stain:*** After stabilization processing, the paper is still a clean white without a hint of the brownish-pink stain characteristic of high speed papers. It's easy to read by visual inspection and on data reduction equipment. It makes good, sharp duplicates on diazo-type equipment.

But, suppose you're running at slow paper speeds, say 10 in./sec. Then you don't want the extreme sensitivity of *Linagraph 1344 Paper.* So you use *Kodak Linagraph 483 Paper* which comes on the same ultra-thin base, has a wide exposure latitude, and can be processed at temperatures up to 120 F. Clean, white background—black, black traces. From your Kodak Graphic Reproduction dealer.

**EASTMAN KODAK COMPANY,** Rochester 4, N. Y.

Kodak
TRADE MARK

## Elected to ARS Posts • • •

Noah S. Davis, President

R. C. Truax, Vice-President

H. W. Ritchey, Director

S. K. Hoffman, Director

H. S. Seifert, Director

K. R. Stehling, Director

## Davis Assumes Board Chairmanship; Names Haley, Rosen, Stehling to Executive Committee

NOAH S. DAVIS, elected to succeed Richard W. Porter as president of ARS, has announced his intention to serve also as chairman of the Board of Directors during the ensuing year.

Dr. Davis, the twenty-first man to hold the office of president, has appointed the following committees:

*Executive Committee*
Noah S. Davis, *chairman*
Martin Summerfield (*ex-officio*)
Andrew G. Haley
Milton Rosen
Kurt Stehling
Robert M. Lawrence
A. C. Slade
James J. Harford

*Policy Committee*
R. C. Truax, *chairman*
Noah S. Davis
Andrew G. Haley
James J. Harford
H. S. Seifert
Martin Summerfield

*Awards Committee*
J. B. Cowen, *chairman*
S. K. Hoffman
H. W. Ritchey
Kurt Stehling

*Finance Committee*
H. W. Ritchey, *chairman*
Robert M. Lawrence
Milton Rosen
Martin Summerfield

*Membership Committee*
George P. Sutton, *chairman*
(members to be named)

*Program Committee*
Andrew G. Haley, *chairman*
H. S. Seifert
Kurt Stehling
Martin Summerfield

*Space Flight Committee*
S. K. Hoffman, *chairman*
J. B. Cowen
Milton Rosen
Wernher von Braun

## First JATO: "Ammonium Nitrate, Cornstarch, Black Powder, and Glue"

*In 1941, there was $10,000 available for solid propellant research at the Guggenheim Aeronautical Laboratory of the California Institute of Technology—the GALCIT project. This sum had to pay for three salaries, propellant materials, metal parts, equipment, and facilities.*

*Fred Miller of Aerojet-General Corp. recalled this in accepting the C. N. Hickman Award at the ARS 25th Anniversary Meeting at Chicago. He made several other remarks which invoked considerable nostalgia among ARS veterans:*

Our efforts were primitive by contemporary standards. The formulation of the propellant used in the first jet-assisted airplane take-offs in the United States consisted of ammonium nitrate, cornstarch, black powder, and—recollection tells me—Lepage's all-purpose glue. And this goop was discovered only after more than 40 other formulations had been tried.

Our units were scientifically tested, too. We used a small hydraulic thrust jack, recording thrust, and chamber pressure on Bourdon gages, which were then photographed at the rate of 1 to 4 frames per sec. But there was one difficulty: most tests lasted less than a tenth of a second. On film, the result was a state of absolute nothingness, with the film showing zero on both thrust and chamber pressure. Or else the needle was a blur covering the whole dial. Our control room was separated from the test stand by a wall of used railroad ties—the cheapest building material available at the time.

But despite the lack of MIL specs—or maybe because of it—we were able to provide the solid propellant for the first rocket-assisted take-off conducted in the United States. The pilot—brave man!—was Army Captain Homer A. Boushey (now Colonel Boushey of the U. S. Air Force) of Wright Air Development Center.

The place was March Field, Calif.—the date July 1941. The ship used was an Ercoupe monoplane. Colonel Boushey used six of our rockets for take-off, with a boost from his propeller in the first series of tests. Each unit produced 25 lb of thrust for 15 sec, and carried about 3 lb of propellant.

In the final test, *only* JATO power was used—this time twelve of 'em. The take-off was a thing of beauty—but I don't think the Colonel will ever forget the bump on landing. In fact, even recently I understand he's been heard to mutter about "those birds who got me to fly an airplane without a prop!"

## Ferris to Chair ARS Session at IAS Meeting

D. F. FERRIS, Chief, Preliminary Design, of Reaction Motors, Inc., Denville, New Jersey, will be the chairman of an ARS session on Rocket Propulsion at this year's annual meeting of the Institute of the Aeronautical Sciences. The session will take place at 2 p.m. on Jan. 24, second day of the three-day IAS program.

The following papers are slated: "Demonstration of Reliability in Liquid Propellant Rocket Engines," by Albert G. Thatcher, Chief, Projects Operations Dept., and H. A. Barton, Asst. Project Engineer, Reaction Motors; "Ballistic Missile Performance," by J. William Reece, R. David Joseph, and Dorothy Shaffer, Cornell Aero. Lab; "Improved On-Off Missile Stabilization," by Robert W. Bass, Research Asst., Dept. of Mathematics, Princeton University.

Other sessions being held include Aerodynamics, VTOL Aircraft, Thermal Stress Analysis, Structures, Hypersonics, Aeroelasticity, Internal Flow in Jet Engines, Helicopter Dynamics, Earth Satellites, Electronics, and Instruments.

Speaker at a Jan. 24 luncheon will be ARS Fellow Theodore von Karman.

## University of Michigan Forms ARS Group

THE charter for a **University of Michigan** Group of ARS was presented to J. B. Bullock, vice-president of the organization, by James J. Harford, Executive Secretary, at a Dec. 8 meeting at the Ann Arbor campus.

Bullock accepted the charter for Richard Signor, president, who was ill. The group plans meetings throughout the university year and will operate within the **Detroit** Section under the faculty guidance of Section Director Richard B. Morrison, a professor in Michigan's Aeronautical Engineering Department.

Dr. Morrison, chairman of the meeting, introduced Fred Klemach, section president. Klemach presented Dean of Engineering, G. B. Brown, who talked on future sources of energy.

## New England Section to Stage Panel Discussion on Ion Rocket

THE "ion rocket," so-called because it is premised on the development of propulsive power through the release of electrically charged particles, will be the subject of a panel discussion being arranged by the **New England** Section for February 14.

The leading proponent of the ion rocket theory, Ernst Stuhlinger, of the Guided Missile Development Division at Redstone Arsenal, will debate the subject with three outstanding New England scientists. They are: John Gale, Chief, Development Div., High Voltage Engineering Corp.; Bruce Billings, Director of Research at Baird Associates; and M. L. Vidale of the Operations Research Group at Arthur D. Little, Inc.

The meeting will be held at 7:30 p.m. at the Faculty Club of the Massachusetts Institute of Technology, Cambridge. It will be presided over by Joseph Kelley of Allied Research Associates, new president of the Section. Richard L. Bolin, ADL, and Ray Minichiello, General Electric, are in charge of the program.

## 600 Hear Summerfield, Van Allen on Satellite

A JOINT audience of ARS, AIEE, and IRE members from the metropolitan New York area got a briefing on the earth satellite vehicle on Dec. 7 at the Engineering Societies Building in New York.

**New York** Section president C. W. Chillson, introduced Martin Summerfield, Editor-in-Chief of JET PROPULSION to the audience of some 600. Dr. Summerfield outlined the principles that have to be considered in launching an ESV—choice of orbits, staging of vehicle, etc.—and compared the performance of a hypothetical three-stage ESV with that of Viking 11. His calculations produced a 15,000 lb gross weight first stage (lox-alcohol), 2400 lb second stage (lox-hydrazine), and a 200 lb solid propellant third stage. He noted the improvements necessary in various design and performance parameters before such a vehicle could be developed.

A. C. Beck, IRE Metropolitan Section chairman, then introduced James Van Allen of the State University of Iowa and member of the IGY's Technical Panel on the Earth Satellite.

Van Allen corrected some popular misconceptions about the ESV's: they're liable to be varishaped, they won't produce any "shocking" revelations, but will add significant knowledge about outer atmospheric phenomena which have been observed by much less effective means for years—cosmic ray intensity, the aurorae, air density, etc.

Dr. Van Allen also stated that the major problem anticipated in connection with the ESV program was in coordinating the observation effort.

He said that the bird would be likely to be 2 to 3 ft in diameter and weigh 20 to 30 lb.


*For want of a nail the shoe is lost,*
*for want of a shoe the horse is lost,*
*for want of a horse the rider is lost.*

George Herbert's statement applies to electronics today as it did to riders three centuries ago. The point may be illustrated by considering a vital electronic unit made up of thousands of components. If the least of these components fails, the whole unit may fail—and with it a strategic military mission.

The problem of *reliability* is becoming increasingly important as the science of electronics advances. "Black boxes" are hard pressed to perform more complicated tasks with increasing efficiency. And at the same time, the requirements call for smaller dimensions. Notwithstanding environmental extremes of an order hitherto unknown, every resistor, capacitor and relay *must* perform *reliably*. Each "nail" is critical.

That is why RCA is continuing its vigorous search for ways and means to increase the reliability of every component in an electronic unit. This program never ceases. It follows through from design to field evaluation. Everything learned is immediately applied to current development and production.

In seeking a degree of electronic perfection never before attained, RCA joins hands with others in this field. This matter of *reliability* is an industry challenge to be met by ingenuity, brain power and engineering knowledge wherever it is found.

**DEFENSE ELECTRONIC PRODUCTS**
**RADIO CORPORATION of AMERICA**
**CAMDEN, N.J.**

# New Equipment and Processes

## Equipment

**Avgas & JP Filters.** Handles 225 gpm. Retains 99% of solids and all water. Purolator Products, Inc., Rahway, N. J.

**Missile Gyro.** Model 45,000, Type DG 101 directional gyro performs in 10 G accelerations up to 2000 cps. Low drift rate over wide temperature range. Gyromechanisms, Inc., Halesite, N. Y.

**Small Rate Gyro.** Model 10RG weighs 1.25 oz and only occupies a 1 in. cube. Floating gimbal construction. Shock and vibration resistant. Hermetically sealed, uses 3 watts at 400 cps. Damping rate of 0.7 ±0.4 over critical. Operates at −55 to +75 C.

**Small Differential Pressure Transducer.** Model P-134 is designed for line pressures of 250 psig. High natural frequency. Insensitive to acceleration. Unbonded strain gage is temperature compensated. Ranges of ±2½ to ±25 psid and 0–5 to 0.150 psid. Statham Laboratories, 12401 W. Olympic Blvd., Los Angeles 64, Calif.

**Midget Crystal Accelerometer.** Type M-191 covers 0.001–1000 G at frequency of 10 cycles to 30 kc. Measures 1 1/16 in. long × 3/8 in. diam. Weight: 1 oz. Mass Laboratories, Inc., 5 Fottler Road, Hingham, Mass.

**Flowmeter.** Measures 0.07 to 0.7 gpm, produces a-c signal directly proportional to flow. Operates at −300 F to +450 F. Potter Aeronautical Co., Route 22, Union, N. J.

**Mixers.** Bulletin R-1701-B1 tells what to consider when buying a mixer. Describes mixing action, batch uniformity, maintenance, and repair costs as well as capacities, dimensions, etc. Worthington Corp., Harrison, N. J.

**Automatic Altitude Chamber.** Built for Douglas Aircraft (Tulsa), it measures 24 ft in diam. Temperatures of −65 F and altitudes of sea level to 60,000 ft. Tests up to 120,000 ft can be simulated, also. Fischer & Porter Co., Hatboro, Pa.

**New Accelerometer.** Model GLO is available in ranges from ±0.1 G to ±5 G or up to ±30 G with reduced damping. Case is oil filled to damp vibrations. Frequency: 6 cps to 10 cps; 1% linearity. Temperature range: −65 F to +180 F. Size: 3 1/4 in. diam × 3 7/16 in. Weight: 2 3/4 lb. Genisco, Inc., 2233 Federal Ave., Los Angeles 64, Calif.

## Materials

**Sheet Insulation.** Teflon-filled glass fiber withstands 500 F and can be made as thin as split mica. Has dielectric constant of 2.1 and can handle 1750 volts/mil. American Machine & Foundry Co., New York, N. Y.

**Bakelite Fluorthane Resin Coatings.** 4 mils thick, will resist fuming nitric acid, hydrazine. Features high tensile strength (25,000 psi), high dielectric strength, and resists heat. W. S. Shamban & Co., Culver City, Calif.

**Foam Resin Insulation.** Nafil polyurethane foam is produced by trapped carbon dioxide in 15 minutes. Produces expanded material which has good adhesion to metal, wood, masonry, stone, or glass. Cast or sprayed. Provides structural strength and is used for insulation and soundproofing. Chase Chemical Corp., 3527 Smallman St., Pittsburgh 1, Pa.

**Teflon Tubing.** For Class H service, is noncombustible, inert to chemicals and solvents. Tensile of 1500 psi, minimum breakdown voltage of 5000. Remains flexible to −90 C. Available ID's of 0.014-0.112 in.; wall thickness of 0.008 to 0.012 in. Hitemp Wires, 26 Windsor Ave., Mineola, N. Y.

**Silicone Lubricants.** Versilube F-50 and G-300 for jet aircraft operating at temperature ranges of −100 F to +400 F. Silicone Products Dept., General Electric Co., Waterford, N. Y.

**Epoxy Resins.** Resin selector chart for casting, impregnating, insulation, and potting. Furane Plastics, Inc., 4516 Brazil St., Los Angeles 39, Calif.

**Plastic Tooling.** Chart tells amount of plastic to use for a given job. Covers casting and foaming phenolics, laminating, die surface, metallic casting, and flexible casting epoxides. Rezolin, Inc., 5736 W. 96th St., Los Angeles 45, Calif.

**High Purity Nickel Powder.** 99.87% nickel, 0.1% cobalt. Sheritt-Gordon, Fort Saskatchewan, Alberta, Canada.

**Porcelain Enamel Coatings.** For turbojet tailcones, etc. Good adhesion to stainless and cold rolled steel, iron; poor to nonferrous. Coatings are 5–30 mils thick, while stainless steel coatings are 1–1.5 mil thick. Resists thermal and mechanical impact. Barrows Porcelain Enamel Co., Cincinnati, Ohio.

**Stainless Steel Porous Metal.** Has tensiles up to 85,000 psi. Porosity can be varied for applications such as jet engine wall cooling, boundary layer control, or high pressure filtration. Available in sheets (0.015–0.125 in. thick) up to 24 × 56 in. sizes or seamless tubing with diameters of up to 18 in. Poroloy Equipment, Inc., Pacoima, Calif.

## Product Literature

*Available free to those who request them on company letterhead.*

**Beryllium Product Directory.** Beryllium copper, nickel, and aluminum alloys. Cast and forged alloys and safety tools. Beryllium Corp., Reading, Pa.

**Couplings Catalog.** Leak-proof, quick-seal hose couplings. Titeflex, Inc., 10 Hendee St., Springfield 4, Mass.

**Thermocouple Bulletins.** 1601: "Design and Selection of Thermocouples"; 1602: "Liquid Temperature Thermocouples"; 1603: "Gas Temperature Thermocouples"; 1604: "Surface Temperature Thermocouples." Revere Corp. of America, Wallingford, Conn.

**High Strength Steel.** 76-page book of nickel alloy steels with tensiles up to 300,000 psi. International Nickel Co., 67 Wall St., New York 5, N. Y.

**Silicone Rubber.** Four-page book on Silastic details performance with regard to temperature extremes, weather, compression, chemicals, and dielectric strength. Dow Corning Corp., Midland, Mich.

(*Continued on page 61*)

# New Patents

**George F. McLaughlin,** *Contributor*

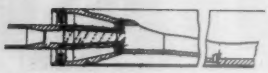

2,721,444

**Series type multiple ramjet propulsion system (2,721,444).** Horace James Johnson, Grosse Pointe, Mich.

Multistage power plant with first and second thrust generating ramjet units, each unit having input combustion and output portions, the second unit having a pressure-increasing diffuser section interposed between the input portion and the combustion chamber.

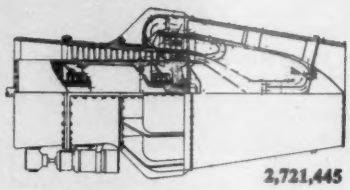

2,721,445

**Aircraft propulsion plant of the propeller-jet turbine type (2,721,445).** James V. Gilliberty, W. Hempstead, N. Y.

A flow-reversing jacketed combustion chamber adjacent to the final compressor stage and the first turbine stage. A portion of the compressor air is circulated around the jacket of the chamber, exhaust duct, and cone.

**Means for eliminating shock reflection in confined supersonic flow (2,721,476).** Michael Pindzola and Russell W. Gamage, St. Louis, Mo., assignors to United Aircraft Corp.

A body spaced from a fluid control surface over which a supersonic stream flows, and so located in the stream that a shock wave emanates. The upstream end of the surface moves about a pivot into the stream away from the surface to vary the mass flow from the stream to the low pressure area.

**Flush inlet (2,721,715).** Henry H. Hoadley, Manchester, Conn., assignor to Chance Vought Aircraft, Inc.

Boundary layer flow is sucked into a slot, eliminating fluid separation during air movement over concave and convex portions of an inboard opening on a jet aircraft.

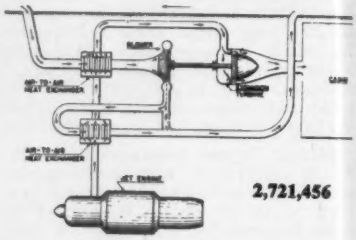

2,721,456

**Aircraft air conditioning system (2,721,456).** Vernon L. Whitney, Jr., Hicksville, N. Y., and John L. Weiler, Freeport, N. Y., assignors to Fairchild Engine and Airplane Corp.

Heat exchanger supplied with cooling air for precooling the cabin air prior to admission to the turbine. A second heat exchanger is interposed between the spent cooling air discharge and the outlet from the blower.

**2,724,237**

**Rocket projectile having discrete flight initiating and sustaining chambers (2,724,237).** Clarence N. Hickman, Jackson Heights, N. Y., assignor to the Secretary of War.

Valves for sealing a main chamber from the gas pressure generated in an auxiliary combustion chamber during combustion of the flight initiating propellant. Means for igniting the sustained flight propellant a predetermined time after ignition of the flight initiating propellant.

**Fuel systems for gas turbine engines or the like with main and pilot fuel injectors (2,722,800).** A. Jubb, Buttershaw, Bradford, and Wm. R. C. Ivens, Derby, England, assignors to Rolls Royce, Ltd.

Means for increasing the area of a jet nozzle on sensing temperature rise due to burning of fuel delivered by the pilot injector.

**Exhaust ducting arrangement for gas turbine engines (2,722,801).** A. A. Lombard, Allestree, Derby, England, assignor to Rolls-Royce, Ltd.

An exhaust ducting arrangement composed of an outer tubular structure supported from the engine and the external structure. Leakage of exhaust gas into the annular passage is prevented by a gas seal between the tubular member and the outer tubular structure.

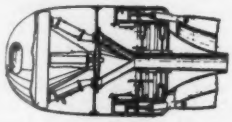

**2,724,238**

**Jet propulsive devices (2,724,238).** Tresham D. Gregg, New York, N. Y.

Gas turbine engine combined with an aerofoil ring thrust augmentor. A streamlined body in front of the ring has a plane surface presented toward the leading edge of the ring, and a nozzle is positioned at the aerodynamic center of the ring.

**Axial flow turbojet engines having independently rotating high and low pressure systems (2,722,802).** B. D. Blackwell and B. A. Peaster, Bristol, England, assignors to The Bristol Aeroplane Co.

Turbojet engines in which the ratio of tip diameter of the low pressure turbine to that of the first row of moving blades of the low pressure compressor is between 1 and 1.1; ratio between power absorbed by the high pressure compressor and that absorbed by the low pressure compressor is between 2 and 2.5.

**Simulated cabin pressurizing system for training aircraft personnel (2,724,192).** Robert G. Stern, Caldwell, and Thomas C. Wakefield, Denville, N. J., assignors to Curtiss-Wright Corp.

A deriving means responsive to variations in altitude, a second deriving means representing a pressure decreasing schedule of cabin altitude in relation to aircraft altitude, and means for modifying the decrement control quantities for representing cabin pressure leak.

# Book Reviews

A. B. Čambel, Northwestern University, *Associate Editor*

**Physical Meteorology** by J. C. Johnson, The Technology Press of the Massachusetts Institute of Technology and John Wiley & Sons, Inc., New York, 1954, 393 pp. $7.50.

Reviewed by Clyde D. Martin
Aerophysics Laboratory
North American Aviation, Inc.

The author's preface defines physical meteorology as a study of those meteorological phenomena, not directly concerned with the circulation of the atmosphere, which link meteorology with other branches of science. The preface further indicates that the text was designed to serve the dual purpose of a textbook for students in meteorology or physics, and a source of information for research workers in the fields in which the atmosphere plays a significant role.

In the first three chapters, Dr. Johnson presents a general treatment of the theories of refraction, scattering, and visibility in the atmosphere, and then proceeds, in chapters 4 and 5, to a discussion of radiation processes and the heat budget of the earth. Chapter 6 returns to a discussion of refraction and diffraction by atmospheric suspensoids. These six chapters, constituting the first half of the book, present a summary of the principles of meteorological optics and radiation that will leave little to be desired by the student, teacher, or research worker.

In the remainder of the book the author devotes two chapters to the subject of cloud physics, and one chapter each to the subjects of atmospheric electricity, the ionosphere and ozonosphere, and atmospheric properties of the upper atmosphere. The chapters on cloud physics contain a well-organized and up-to-date summary of conditions attending the formation, growth, collection efficiency, and evaporation of rain drops as well as a discussion of artificially stimulated precipitation, icing of aircraft, and radar meteorology.

The chapters on atmospheric electricity, and the ionosphere and ozonosphere adequately cover these fields for the undergraduate student and are most excellently presented. The chapter on temperature, density, pressure, and humidity of the upper atmosphere, however, seems to have been slighted when one considers the very great research effort expended in recent years on investigations of these atmospheric properties. An adequate discussion of general instrumentation problems and techniques is presented, but very little actual data and few results of this research have been included. The NACA Standard Atmosphere, which presents temperatures and pressures to 120 kilometers, has been shown to be considerably in error above 30 kilometers by rocket measurements, and subsequent to the publication of "Physical Meteorology," a new standard was adopted by the NACA.

In not including a discussion of the general circulation of the atmosphere, Dr. Johnson's book has deviated considerably from earlier textbooks on physical meteorology which have concentrated as much as 20 per cent of their content on this phase. Whatever criticism may be due for this deletion, however, is overcome by the extraordinarily complete treatment and excellent development of the principles that govern the transmission, attenuation, polarization, and dispersion of electromagnetic energy through the atmosphere.

Aside from content, Johnson has presented a most complete and up-to-date list of references with each chapter, and the instructor is certain to be pleased with an innovation for textbooks on Physical Meteorology—an excellent group of problems for each chapter. The index, on the other hand, might well have been more extensive, particularly since the book is intended to meet the needs of research workers in other fields who may not be familiar with common meteorological terms.

In summary, Dr. Johnson has presented a most excellent, comprehensive, and needed book which admirably accomplishes the objective of serving textbook requirements. Meteorologists and investigators from other fields will also find the book useful as a source of reference material.

## *Book Notices*

**Mathematical Foundations of Quantum Mechanics,** by John Von Neumann, translated from German edition by Robert T. Beyer, Princeton University Press, Princeton, N. J., 1955, 443 pp., $6. This translation follows closely the text of the original German edition. Close cooperation between the author and translator made possible the rendering of the ideas of the original volume into a translation which conveys the same meaning.

**Cycles and Performance Estimation (Gas-Turbine Series, Vol. I),** by James Hodge, Academic Press, Inc. New York, 1955, 329 pp., $9. The first volume in a new series on current gas-turbine practice presents the basic principles for analyzing gas-turbine cycles and predicting performance. A large portion of the book is devoted to the presentation of idealized cycles and performance data of actual cycles in graphic form. The field of gas-turbine application covers such installations as shaft power generating plants, blast furnace blowing, and aircraft engines.

**Directory of Commercial and College Testing Laboratories,** American Society of Testing Materials, Philadelphia, Pennsylvania, 1955, 39 pp., $1. This booklet lists 278 commercial and 86 college laboratories which will test commodities in accordance with standard specifications.

**Gas Turbine Principles and Practice,** edited by Sir Harold Roxbee Cox, D. Van Nostrand Co., Inc., New York, 1955, $12.50. A most comprehensive survey of thermodynamic principles, operating characteristics, and construction features of important types of gas turbines. Twenty-four specialists prepared the thirty sections dealing with such subjects as compressors, axial and radial turbines, materials, fuels, heat exchangers, and special problems.

# Technical Literature Digest

M. H. Smith, *Associate Editor*, and M. H. Fisher, *Contributor*
The James Forrestal Research Center, Princeton University

## Jet Propulsion Engines

**Noise Study of Turbojet Engines,** by M. Kobrynski, *Recherche Aéron.*, no. 46, July-Aug. 1955, pp. 57–59 (in French).

**Power Plants for Supersonic Flight,** by Eric S. Moult, *Inst. Aeron. Sci., Prepr.* 553, June 1955, 37 pp.

**Low Combustion Turbine Engines,** by A. A. Lombard, *Inst. Aeron. Sci., Prepr.* 560, June 1955, 26 pp.

**Relative Size of Turbojet Engine Components,** by D. Willens, *J. Aeron. Sci.*, vol. 22, Sept. 1955, pp. 652–653.

**Rolls-Royce Dart,** *Aircr. Production*, vol. 17, Sept. 1955, pp. 340–350.

**A Polar-Coordinate Survey Method for Determining Jet-Engine Combustion-Chamber Performance,** by Robert Friedman and Edward R. Carlson, *NACA TN* 3566, Sept. 1955, 29 pp.

**Slow Speed Thrust in Ram Jets,** by George A. Cicolani, *Inst. Aeron. Sci. Student Branch Competition, First Award Papers*, 1954, pp. 5–9.

**Design and Operating Characteristics of a Rotating Combustion Chamber Engine,** by Kelly W. Thurston, *Inst. Aeron. Sci. Student Branch Competition, First Award Papers*, 1954, pp. 63–67.

## Rocket Propulsion Engines

**Rocket Propulsion in Helicopters,** by Leon M. Slawecki, *J. Space Flight*, vol. 7, Sept. 1955, pp. 5–7.

**Rocket, Test Analysis, Performance, Design Calculations With Equilibrium Gas Composition, Using Mollier Charts,** by Frederick R. Weymouth, *Bell Aircraft Corp. Rep.* 59-982-003, April 1954, 108 pp.

**Determining the Minimum Combustion Chamber Volume by Nomogram,** by Ray Novotny, *Aero Digest*, vol. 71, Sept. 1955, pp. 27–29.

**The De Havilland Super Sprite,** *De Havilland Gazette*, no. 88, Aug. 1955, pp. 93–95.

**The Rocket Conceptions of K. Siemienowicz, 1650,** by M. Subotowicz, *J. Brit. Interplan. Soc.*, vol. 14, Sept.-Oct. 1955, pp. 245–248.

## Heat Transfer and Fluid Flow

**Inlet Duct-Engine Flow Compatibility,** by J. S. Alford, *Inst. Aeron. Sci., Prepr.* 566, June 1955, 20 pp.

**Visualization Study of Secondary Flows in Turbine Rotor Tips Regions,** by Hubert W. Allen and Milton G. Kofskey, *NACA TN* no. 3519, Sept. 1955, 33 pp.

**Secondary Flow in Axial Compressors,** by Robert C. Dean, Jr., *M.I.T. Gas Turb. Lab.*, May 1954, 110 pp.

**Correlation of Experimental Data on the Disintegration of Liquid Jets,** by C. C. Miesse, *Indust. Engng. Chem.*, vol. 47, Sept. 1955, Pt. 1, pp. 1690–1701.

**Pressure Distribution Measurements on Rotating Turbine Blades,** by Werner Fister, *VDI-Forschungsheft* 448, 1955, 32 pp. (in German).

**Some Factors in the Design of Subsonic Turbojet Ducts,** by LeRoy Fuss, Jr., *Inst. Aeron. Sci. Student Branch Competition, First Award Papers*, 1954, pp. 18–27.

**Criterions for Prediction and Control of Ram-Jet Flow Pulsations,** by William H. Sterbentz and John C. Evvard, *NACA TN* no. 3506, Aug. 1955, 60 pp.

## Combustion

**Ideal Temperature Rise Due to Constant-Pressure Combustion of a JP-4 Fuel,** by S. C. Huntley, *NACA RM* E55G27a, Sept. 1955, 53 pp.

**Combustion for Aircraft Engines,** by Walter T. Olson, *Inst. Aeron. Sci. Prepr.* 561, June 1955, 35 pp.

**The Fast and Slow Reactions of Hydrogen-Oxygen-Propane Mixtures,** by Arthur Levy, *Wright Air Dev. Center, TR* no. 54–137, Feb. 1954, 19 pp.

**Burning Rates of Deuterated Nitrate Esters,** by Rudolf Steinberg, Charles A. Orlick and Vincent P. Schaaf, *J. Amer. Chem. Soc.*, vol. 77, Sept. 20, 1955, pp. 4748–4750.

**Contribution to the Theory of Fast Reaction Rates,** by R. De Vogelaere and M. Boudart, *J. Chem. Phys.*, vol. 23, July 1955, pp. 1236–1244.

**Vibrational Relaxation Times of Diatomic Molecules and Rocket Performance,** by H. C. Penny and Henry Aroeste, *J. Chem. Phys.*, vol. 23, July 1955, pp. 1281–1283.

## Fuels, Propellants, and Materials

**How Commercial Titanium and Zirconium Were Born,** by W. J. Kroll, *J. Franklin Inst.*, vol. 260, Sept. 1955, pp. 169–192.

**Reactions Between Liquid Fuels and Oxidants,** by Martin Kilpatrick, Arthur G. Keenan, Louis Baker, Jr., and Ann Palm, *Ill. Inst. Tech. Dept. Chem.*, June 1955, 19 pp.

**Research on the Properties of Ozone, 1950–1955, Linde Air Products Co. Final Rept.,** May 1955, 75 pp.

**Values of Thermodynamic Functions to 12,000°K for Several Substances,** by W. Fickett and Robert D. Cowan, *Los Alamos Sci. Lab. Rept.* LA-1727, Sept. 1954, 21 pp.

**Kinetics of Fast Reactions; a Technical Report,** by S. H. Bauer, M. Blander, A. Shepp, J. J. Klein, C. C. Peterson, and Eliza Pollard, *Cornell Univ. Dept. Chem.*, July 1955.

**High Temperature Power Plant Materials,** by A. Levy, *Aircr. Engng.*, fol. 27, Sept. 1955, pp. 292–298.

**Reaction Rates of Ammonium Nitrate in Detonation,** by Melvin A. Cook, Earle B. Mayfield, and William S. Partridge, *J. Phys. Chem.*, vol. 59, Aug. 1955, pp. 675–682.

## New Equipment and Processes

(*Continued from page 55*)

**Detonator-Safe Initiators.** Leaflet D8I-555 details units for guided missile use. Used to provide firing safety. Specs on electrical needs and sizes. Beckman & Whitley, Inc., 1092 E. San Carlos Ave., San Carlos, Calif.

**Problems of the Thermal Barrier.** 12-page booklet surveys nine technical papers presented at ASME symposium. Office of Information Services, New York University, University Heights, New York 53, N. Y.

**Thermocouple Protectors.** Bulletin 11-13 of standard protectors. Claud S. Gordon Co., 3000 S. Wallace St., Chicago 16, Ill.

**Tool Steel.** Booklet written for non-metallurgist covers basic classifications of tool steel, gives properties and applications. Crucible Steel Co. of America, Box 88, Pittsburgh 30, Pa.

**Lathe Turning Calculator.** Selects lathe feed and spindle speed for fast and economical production. Cincinnati Lathe & Tool Co., Cincinnati 9, Ohio.

**Plastics Fact File.** Lists line of plastics: styrene, vinyl chloride, polyethylene, melamine, resorcinol, phenolics, etc., for laminating, bonding, coatings. Monsanto Chemical Co., Plastics Div., Springfield 2, Mass.

**Moly for High Temperatures.** 72-page book on arc cast molybdenum. Climax Molybdenum Co., 500 Fifth Avenue, New York 36, N. Y.

**Boron Handbook.** 16-page book on boron materials for use in atomic energy. Norton Co., Worcester 6, Mass.

**Titanium Progress Report.** How to handle titanium. E. I. duPont de Nemours & Co., Wilmington 98, Del.

**Elastomers.** Reprint discusses cross-linking and tensile strength, experimental data on natural rubber, styrenated GR-S, polybutadienes. Mellon Institute, 4400 Fifth Ave., Pittsburgh 13, Pa.

**Infrared.** Reprint surveys infrared spectroscopy in research and development. Applications given. Beckman Div., Beckman Instruments, Inc., Fullerton, Calif.

**Testing Instruments.** Catalog of burst strength testers, mercury vacuum and pressure gages, speed indicators, thickness gages, pressure gages, tensile testers, etc. Anchor Testing Instrument Co., 45 Van Sinderen Ave., Brooklyn 7, N. Y.

**Tailor-Made Metals.** Describes made-to-order metals in experimental quantities available to metallurgical industries. 16-page booklet is called "Precision Metals Services." Allied Products Div., Hamilton Watch Co., Lancaster, Pa.

**Heat Transfer.** Properties, applications of polyalkalene glycols for heat transfer. Folder F-7490 C. Carbide and Carbon Chemicals Co., 30 E. 42nd St., New York 17, N. Y.

**Sandwich Cores.** "Development of a Heat Resistant Foamed-in-Place, Low Density Silicone Resin Core Material," Report PB 111558, $3. OTS, U. S. Dept. of Commerce, Washington 25, D. C.

## Index to Advertisers

LSION